EUROPEAN ORGANIZATION FOR NUCLEAR RESEARCH

CERN-EP-2000-016
January 21, 2000

A Combination of Preliminary Electroweak Measurements and Constraints on the Standard Model

The LEP Collaborations* ALEPH, DELPHI, L3, OPAL, the LEP Electroweak Working Group† and the SLD Heavy Flavour and Electroweak Groups‡

Prepared from Contributions of the LEP and SLD experiments to the 1999 Summer conferences.

Abstract

This note presents a combination of published and preliminary electroweak results from the four LEP collaborations and the SLD collaboration which were prepared for the 1999 summer conferences. Averages are derived for hadronic and leptonic cross sections, the leptonic forward-backward asymmetries, the τ polarisation asymmetries, the $b\overline{b}$ and $c\overline{c}$ partial widths and forward-backward asymmetries and the $q\overline{q}$ charge asymmetry. The major changes with respect to results presented in summer 1998 are updates to the lineshape, W mass and triple-gauge-boson couplings from LEP, and $\mathcal{A}_b$ and $\mathcal{A}_c$ from SLD. The results are compared with precise electroweak measurements from other experiments. A significant update here are new W mass measurements from CDF and DØ. The parameters of the Standard Model are evaluated, first using the combined LEP electroweak measurements, and then using the full set of electroweak results.

*The LEP Collaborations each take responsibility for the preliminary data of their own experiment.

†D. Abbaneo, J. Alcaraz, P. Antilogus, P. Bambade, A. Barczyk, T. Behnke, G. Bella, A. Blondel, S. Blyth, D. Bourilkov, D.G. Charlton, R. Clare, P. de Jong, G. Duckeck, M. Elsing, F. Filthaut, D. Glenzinski, M.W. Grünewald, A. Gurtu, J.B. Hansen, R. Hawkings, J. Holt, R.W.L. Jones, T. Kawamoto, R.G. Kellogg, N. Kjaer, M. Kobel, E. Lançon, W. Lohmann, A. Macchiolo, C. Mariotti, M. Martinez, G. Martinez, C. Matteuzzi, M.N. Minard, J. Mnich, K. Mönig, P. Molnar, S. Olshevski, U. Parzefall, Ch. Paus, M. Pepe-Altarelli, B. Pietrzyk, G. Quast, D. Reid, P. Renton, H. Rick, J.M. Roney, E. Sanchez, C. Sbarra, R. Sekulin, D. Strom, R. Tenchini, F. Teubert, M.A. Thomson, J. Timmermans, M. Verzocchi, H. Wahlen, C.P. Ward, N.K. Watson, P.S. Wells.

‡J. Brau, N. de Groot, P.C. Rowson, M.Swartz, D. Su.

1 Introduction

The four LEP experiments have previously presented [1] parameters derived from the Z resonance using published and preliminary results based on data recorded until the end of 1995. Since then additional results have become available. To allow a quick assessment, a box highlighting the updates is given at the beginning of each section. Since 1996 LEP has run at energies above the W-pair production threshold. In 1998 the delivered luminosity was significantly higher than in previous years, and thus the knowledge of the properties of the W boson, especially its mass, has been significantly improved. These results are denoted as LEP-II results.

The LEP-I data (1990-1995) consist of the hadronic and leptonic cross sections, the leptonic forward-backward asymmetries, the τ polarisation asymmetries, the $\mathrm{b\overline{b}}$ and $\mathrm{c\overline{c}}$ partial widths and forward-backward asymmetries and the $\mathrm{q\overline{q}}$ charge asymmetry. The measurements of the $\mathrm{b\overline{b}}$ and $\mathrm{c\overline{c}}$ partial widths and left-right-forward-backward asymmetries for b and c quarks from SLD are treated consistently with the LEP data. Many technical aspects of their combination have already been described in References 2, 3 and references therein.

This note is organised as follows:

Section 2 Z line shape and leptonic forward-backward asymmetries;

Section 3 $\mathrm{f\overline{f}}$ production at energies above the Z;

Section 4 τ polarisation;

Section 5 A_{LR} measurement at SLD;

Section 6 Heavy flavour analyses;

Section 7 Inclusive hadronic charge asymmetry;

Section 8 W boson properties, including m_{W}, branching ratios, WW production cross sections and triple-gauge-boson couplings;

Section 9 ZZ production cross sections;

Section 10 Interpretation of the results, including the combination of results from LEP, SLD, neutrino interaction experiments and from CDF and DØ;

Section 11 Prospects for the future.

2 Z Lineshape and Lepton Forward-Backward Asymmetries

Updates with respect to last summer:
All experiments have updated their results. ALEPH have presented final values. Many recent theoretical developments have been included in the results and fits.

2.1 Results from the Z Peak Data

The results presented here are based on the full LEP-I data set. This includes the data taken during the energy scans in 1990 and 1991 in the range[1] $|\sqrt{s} - m_{\mathrm{Z}}| < 3$ GeV, the data collected at the Z peak in 1992 and preliminary analyses of the energy scans in 1993 and 1995 ($|\sqrt{s} - m_{\mathrm{Z}}| < 1.8$ GeV) and the peak running in 1994. The total statistics and the systematic errors on the individual analyses of the four LEP collaborations are given in Tables 1 and 2. Details of the individual analyses can be found in References 4–7.

		ALEPH	DELPHI	L3	OPAL	LEP
$\mathrm{q\overline{q}}$	'90-'91	433	357	416	454	1660
	'92	633	697	678	733	2741
	'93 prel.	630	682	646	642	2600
	'94 prel.	1640	1310	1359	1585	5894
	'95 prel.	735	659	526	652	2572
	total	4071	3705	3625	4066	15467
$\ell^+\ell^-$	'90-'91	53	36	40	58	187
	'92	77	70	58	88	293
	'93 prel.	78	75	64	79	296
	'94 prel.	202	137	127	191	657
	'95 prel.	90	66	54	81	291
	total	500	384	343	497	1724

Table 1: LEP statistics in units of 10^3 events used for the analysis of the Z line shape and lepton forward-backward asymmetries.

For the averaging of results the LEP experiments provide a standard set of 9 parameters describing the information contained in hadronic and leptonic cross sections and leptonic forward-backward asymmetries [2, 10]. These parameters are convenient for fitting and averaging since they have small correlations. They are:

- The mass and total width of the Z boson, where the definition is based on the Breit-Wigner denominator ($s - m_{\mathrm{Z}}^2 + is\Gamma_{\mathrm{Z}}/m_{\mathrm{Z}}$) ($s$-dependent width) [11].
- The hadronic pole cross section of Z exchange:

$$\sigma_{\mathrm{h}}^0 \equiv \frac{12\pi}{m_{\mathrm{Z}}^2} \frac{\Gamma_{\mathrm{ee}}\Gamma_{\mathrm{had}}}{\Gamma_{\mathrm{Z}}^2} \,. \tag{1}$$

Here Γ_{ee} and Γ_{had} are the partial widths of the Z for decays into electrons and hadrons.

[1] In this note $\hbar = c = 1$.

	ALEPH			DELPHI			L3			OPAL		
	'93	'94	'95	'93 prel.	'94 prel.	'95 prel.	'93 prel.	'94 prel.	'95 prel.	'93 prel.	'94 prel.	'95 prel.
$\mathcal{L}^{\text{exp. }(a)}$	0.067%	0.073%	0.080%	0.24%	0.09%	0.09%	0.086%	0.064%	0.068%	0.033%	0.033%	0.034%
σ_{had}	0.069%	0.072%	0.073%	0.10%	0.11%	0.10%	0.042%	0.041%	0.042%	0.073%	0.073%	0.082%
σ_{e}	0.18%	0.16%	0.18%	0.46%	0.52%	0.52%	0.24%	0.17%	0.28%	0.17%	0.14%	0.16
σ_{μ}	0.11%	0.09%	0.11%	0.28%	0.26%	0.28%	0.32%	0.31%	0.40%	0.16%	0.10%	0.12
σ_{τ}	0.26%	0.18%	0.25%	0.60%	0.60%	0.60%	0.68%	0.65%	0.76%	0.49%	0.42%	0.48
A_{FB}^{e}	0.0012	0.0012	0.0012	0.0026	0.0021	0.0020	0.0025	0.0025	0.0025	0.001	0.001	0.001
A_{FB}^{μ}	0.0005	0.0005	0.0005	0.0009	0.0005	0.0010	0.0008	0.0008	0.0015	0.0004	0.0003	0.0004
A_{FB}^{τ}	0.0009	0.0007	0.0009	0.0020	0.0020	0.0020	0.0032	0.0032	0.0032	0.0012	0.0012	0.0012

Table 2: Experimental systematic errors for the analysis of the Z line shape and lepton forward-backward asymmetries at the Z peak. The errors quoted do not include the common uncertainty due to the LEP energy calibration. The treatment of correlations between the errors for different years is described in References 4–7.
$^{(a)}$In addition, there is a theoretical error for the calculation of the small angle Bhabha cross section of 0.054% [8] for OPAL and a common 0.06% for the other three experiments [9]; the OPAL error has been treated as a fully correlated component of the common 0.06% error.

- The ratios:
$$R_{\text{e}} \equiv \Gamma_{\text{had}}/\Gamma_{\text{ee}}, \quad R_{\mu} \equiv \Gamma_{\text{had}}/\Gamma_{\mu\mu} \text{ and } R_{\tau} \equiv \Gamma_{\text{had}}/\Gamma_{\tau\tau}. \tag{2}$$
Here $\Gamma_{\mu\mu}$ and $\Gamma_{\tau\tau}$ are the partial widths of the Z for the decays $\text{Z} \to \mu^+\mu^-$ and $\text{Z} \to \tau^+\tau^-$. Due to the large mass of the τ lepton, a small difference of 0.2% is expected between the values for R_{e} and R_{μ}, and the value for R_{τ}, even under the assumption of lepton universality [12].

- The pole asymmetries, $A_{\text{FB}}^{0,\text{e}}$, $A_{\text{FB}}^{0,\mu}$ and $A_{\text{FB}}^{0,\tau}$, for the processes $\text{e}^+\text{e}^- \to \text{e}^+\text{e}^-$, $\text{e}^+\text{e}^- \to \mu^+\mu^-$ and $\text{e}^+\text{e}^- \to \tau^+\tau^-$. In terms of the real parts of the effective vector and axial-vector neutral current couplings of fermions, $g_{V\text{f}}$ and $g_{A\text{f}}$, the pole asymmetries are expressed as
$$A_{\text{FB}}^{0,\text{f}} \equiv \frac{3}{4}\mathcal{A}_{\text{e}}\mathcal{A}_{\text{f}} \tag{3}$$
with
$$\mathcal{A}_{\text{f}} \equiv \frac{2g_{V\text{f}}g_{A\text{f}}}{g_{V\text{f}}^2 + g_{A\text{f}}^2}\,. \tag{4}$$

The imaginary parts of the vector and axial-vector coupling constants as well as real and imaginary parts of the photon vacuum polarisation are taken into account explicitly in the fitting formulae and are fixed to their Standard Model values. The fitting procedure takes into account effects of initial-state radiation [11] to $\mathcal{O}(\alpha^3)$ [13–15], as well as t-channel and s-t interference contributions in the case of e^+e^- final states.

The set of 9 parameters does not describe hadron and lepton-pair production completely, because it does not include the interference of the s-channel Z exchange with the s-channel γ exchange. For the results presented in this section and used in the rest of the note, the γ-exchange contributions and the hadronic γZ interference terms are fixed to their Standard Model values. The leptonic γZ interference terms are expressed in terms of the effective couplings.

The four sets of 9 parameters provided by the LEP experiments are presented in Table 3. The covariance matrix of these parameters is constructed [10, 16] from the covariance matrices of the individual LEP experiments and common systematic errors [16]. The common systematic errors include theoretical errors as well as errors arising from the uncertainty in the LEP beam energy. The beam energy contributes 1.7 MeV to m_{Z} and 1.2 MeV to Γ_{Z} [17]. In addition, the uncertainty in the

centre-of-mass energy spread of about 1 MeV [18] contributes 0.2 MeV to Γ_Z. The theoretical error on calculations of the small-angle Bhabha cross section is 0.054% [8] for OPAL and 0.06% [9] for all other experiments, and results in the largest systematic uncertainty on σ_h^0. QED radiation, dominated by photon radiation from the initial state electrons, contributes an estimated common uncertainty of $\pm 0.02\%$ on σ_h^0 and of ± 0.5 MeV on m_Z and Γ_Z, where the latter one is dominated by the uncertainty in fermion pair radiation. The contribution of t-channel diagrams and the s-t interference in $Z \to e^+e^-$ leads to an additional theoretical uncertainty estimated to be $\pm 0.11\%$ on R_e and to ± 0.0013 on $A_{FB}^{0,e}$, which are -100% correlated. Uncertainties from the model-independent parameterisation of the energy dependence of the cross section are almost negligible, if the definitions of Reference [19] are applied. Through unavoidable Standard Model remnants, dominated by the need to fix the γ-Z interference contribution in the $q\overline{q}$ channel, there is some small dependence of ± 0.3 MeV of m_Z on the Higgs mass, m_H (in the range 95 GeV to 1000 GeV), or the value of the electromagnetic coupling constant. Such "parametric" errors are negligible for the other pseudo-observables. The combined parameter set and its correlation matrix are given in Tables 4 and 5.

	ALEPH	DELPHI	L3	OPAL
m_Z(GeV)	91.1886±0.0031	91.1864±0.0029	91.1893±0.0030	91.1852±0.0029
Γ_Z(GeV)	2.4952±0.0043	2.4870±0.0041	2.5017±0.0041	2.4941±0.0041
σ_h^0(nb)	41.558±0.057	41.580±0.069	41.536±0.055	41.508±0.055
R_e	20.683±0.075	20.88±0.12	20.814±0.089	20.905±0.085
R_μ	20.800±0.056	20.650±0.076	20.860±0.097	20.813±0.058
R_τ	20.707±0.062	20.84±0.13	20.79±0.14	20.834±0.091
$A_{FB}^{0,e}$	0.0184±0.0034	0.0173±0.0049	0.0106±0.0058	0.0090±0.0044
$A_{FB}^{0,\mu}$	0.0171±0.0024	0.0165±0.0025	0.0188±0.0033	0.0154±0.0023
$A_{FB}^{0,\tau}$	0.0170±0.0028	0.0241±0.0037	0.0260±0.0047	0.0145±0.0030
χ^2/d.o.f.	169/176	179/168	159/166	157/202

Table 3: Line shape and asymmetry parameters from 9-parameter fits to the data of the four LEP experiments.

Parameter	Average Value
m_Z(GeV)	91.1872±0.0021
Γ_Z(GeV)	2.4944±0.0024
σ_h^0(nb)	41.544±0.037
R_e	20.803±0.049
R_μ	20.786±0.033
R_τ	20.764±0.045
$A_{FB}^{0,e}$	0.0145±0.0024
$A_{FB}^{0,\mu}$	0.0167±0.0013
$A_{FB}^{0,\tau}$	0.0188±0.0017

Table 4: Average line shape and asymmetry parameters from the data of the four LEP experiments given in Table 3, without the assumption of lepton universality. The χ^2/d.o.f. of the average is 32/27.

If lepton universality is assumed, the set of 9 parameters given above is reduced to a set of 5 parameters. R_ℓ is defined as $R_\ell \equiv \Gamma_{had}/\Gamma_{\ell\ell}$, where $\Gamma_{\ell\ell}$ refers to the partial Z width for the decay into a pair of massless charged leptons. The data of each of the four LEP experiments are consistent with lepton universality (the difference in χ^2 over the difference in d.o.f. with and without the assumption of lepton universality is 4/4, 5/4, 5/4 and 2/4 for ALEPH, DELPHI, L3 and OPAL, respectively).

Table 6 gives the five parameters $m_{\rm Z}$, $\Gamma_{\rm Z}$, $\sigma^0_{\rm h}$, R_ℓ and $A^{0,\ell}_{\rm FB}$ for the individual LEP experiments, assuming lepton universality. Tables 7 and 8 give the combined result and the corresponding correlation matrix. Figure 1 shows, for each lepton species and for the combination assuming lepton universality, the resulting 68% probability contours in the R_ℓ-$A^{0,\ell}_{\rm FB}$ plane. For completeness the partial decay widths of the Z boson are listed in Table 9, although it should be noted that they are more correlated than the ratios given in Tables 4 and 5.

	$m_{\rm Z}$	$\Gamma_{\rm Z}$	$\sigma^0_{\rm h}$	$R_{\rm e}$	R_μ	R_τ	$A^{0,{\rm e}}_{\rm FB}$	$A^{0,\mu}_{\rm FB}$	$A^{0,\tau}_{\rm FB}$
$m_{\rm Z}$	1.000	−0.008	−0.050	0.073	0.001	0.002	−0.015	0.046	0.034
$\Gamma_{\rm Z}$	−0.008	1.000	−0.284	−0.006	0.008	0.000	−0.002	0.002	−0.003
$\sigma^0_{\rm h}$	−0.050	−0.284	1.000	0.109	0.137	0.100	0.008	0.001	0.007
$R_{\rm e}$	0.073	−0.006	0.109	1.000	0.070	0.044	−0.356	0.023	0.016
R_μ	0.001	0.008	0.137	0.070	1.000	0.072	0.005	0.006	0.004
R_τ	0.002	0.000	0.100	0.044	0.072	1.000	0.003	−0.003	0.010
$A^{0,{\rm e}}_{\rm FB}$	−0.015	−0.002	0.008	−0.356	0.005	0.003	1.000	−0.026	−0.020
$A^{0,\mu}_{\rm FB}$	0.046	0.002	0.001	0.023	0.006	−0.003	−0.026	1.000	0.045
$A^{0,\tau}_{\rm FB}$	0.034	−0.003	0.007	0.016	0.004	0.010	−0.020	0.045	1.000

Table 5: The correlation matrix for the set of parameters given in Table 4.

	ALEPH	DELPHI	L3	OPAL
$m_{\rm Z}$(GeV)	91.1888±0.0031	91.1862±0.0029	91.1890±0.0030	91.1847±0.0029
$\Gamma_{\rm Z}$(GeV)	2.4951±0.0043	2.4870±0.0041	2.5017±0.0041	2.4941±0.0040
$\sigma^0_{\rm h}$(nb)	41.558±0.057	41.580±0.069	41.536±0.054	41.508±0.054
R_ℓ	20.726±0.039	20.728±0.060	20.810±0.061	20.824±0.045
$A^{0,\ell}_{\rm FB}$	0.0172±0.0016	0.0186±0.0019	0.0192±0.0024	0.0142±0.0017
χ^2/d.o.f.	173/180	184/172	165/170	160/206

Table 6: Line shape and asymmetry parameters from 5-parameter fits to the data of the four LEP experiments, assuming lepton universality. R_ℓ is defined as $R_\ell \equiv \Gamma_{\rm had}/\Gamma_{\ell\ell}$, where $\Gamma_{\ell\ell}$ refers to the partial Z width for the decay into a pair of massless charged leptons.

Parameter	Average Value
$m_{\rm Z}$(GeV)	91.1871±0.0021
$\Gamma_{\rm Z}$(GeV)	2.4944±0.0024
$\sigma^0_{\rm h}$(nb)	41.544±0.037
R_ℓ	20.768±0.024
$A^{0,\ell}_{\rm FB}$	0.01701±0.00095

Table 7: Average line shape and asymmetry parameters assuming lepton universality. These results are derived from the LEP average given in Table 4.

	$m_{\rm Z}$	$\Gamma_{\rm Z}$	$\sigma^0_{\rm h}$	R_ℓ	$A^{0,\ell}_{\rm FB}$
$m_{\rm Z}$	1.000	−0.008	−0.051	0.031	0.053
$\Gamma_{\rm Z}$	−0.008	1.000	−0.284	0.002	−0.002
$\sigma^0_{\rm h}$	−0.051	−0.284	1.000	0.193	0.010
R_ℓ	0.031	0.002	0.193	1.000	−0.054
$A^{0,\ell}_{\rm FB}$	0.053	−0.002	0.010	−0.054	1.000

Table 8: The correlation matrix for the set of parameters given in Table 7.

Without Lepton Universality		
$\Gamma_{\rm ee}$	(MeV)	83.90±0.12
$\Gamma_{\mu\mu}$	(MeV)	83.96±0.18
$\Gamma_{\tau\tau}$	(MeV)	84.05±0.22
With Lepton Universality		
$\Gamma_{\ell\ell}$	(MeV)	83.959±0.089
$\Gamma_{\rm had}$	(MeV)	1743.9±2.0
$\Gamma_{\rm inv}$	(MeV)	498.8±1.5

Table 9: Partial decay widths of the Z boson, derived from the results of the 9-parameter (Tables 4 and 5) and the 5-parameter (Tables 7 and 8) fits. In the case of lepton universality, $\Gamma_{\ell\ell}$ refers to the partial Z width for the decay into a pair of massless charged leptons.

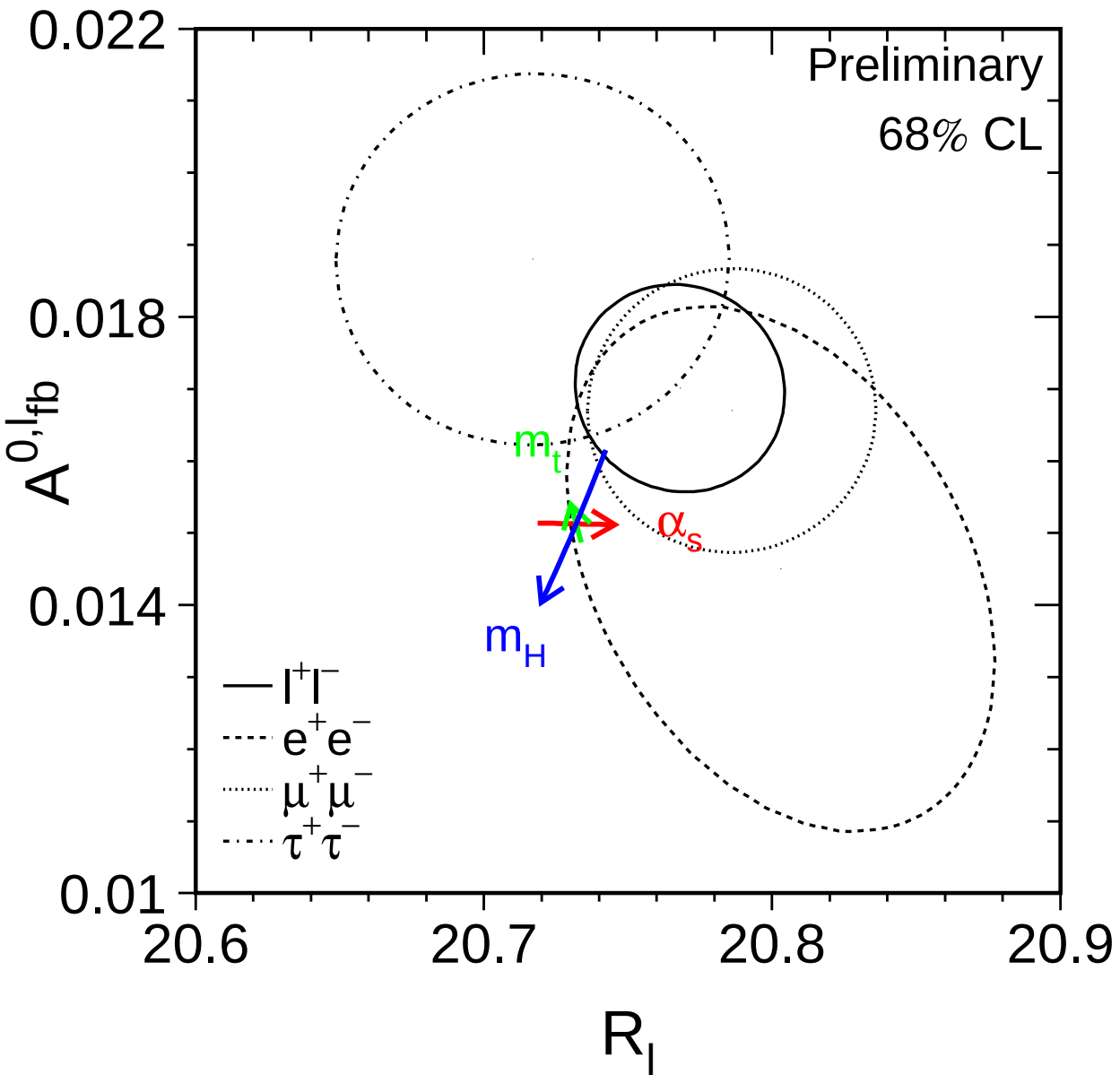

Figure 1: Contours of 68% probability in the R_ℓ-$A_{\rm FB}^{0,\,\ell}$ plane. For better comparison the results for the τ lepton are corrected to correspond to the massless case. The Standard Model prediction for $m_{\rm Z} = 91.1871$ GeV, $m_{\rm t} = 174.3$ GeV, $m_{\rm H} = 300$ GeV, and $\alpha_{\rm s}(m_{\rm Z}^2) = 0.119$ is also shown. The lines with arrows correspond to the variation of the Standard Model prediction when $m_{\rm t}$, $m_{\rm H}$ and $\alpha_{\rm s}(m_{\rm Z}^2)$ are varied in the intervals $m_{\rm t} = 174.3 \pm 5.1$ GeV, $m_{\rm H} = 300^{+700}_{-205}$ GeV, and $\alpha_{\rm s}(m_{\rm Z}^2) = 0.119 \pm 0.002$, respectively. The arrows point in the direction of increasing values of $m_{\rm t}$, $m_{\rm H}$ and $\alpha_{\rm s}$.

3 Fermion-pair production at LEP2 energies

Updates with respect to last summer:
This is a new section.

LEP has operated at energies well above the Z resonance since autumn 1995. During this time data have been collected at centre-of-mass energies of 130.2 and 136.2 GeV (in 1995 and 1997), 161.3 and 172.1 GeV (in 1996), 182.7 GeV (in 1997) and 188.6 GeV (in 1998). In this section the combination of the LEP results on $e^+e^- \to f\bar{f}$ for the data taken up to 1998 is considered.

The effect of initial state radiation is to reduce the effective center-of-mass energy $\sqrt{s'}$ of the final state fermion-pair. Because of the presence of the Z resonance, a large fraction of the events produced via an s=channel process will have $\sqrt{(}s') \approx m_Z$. For this reason, all experiments have divided their LEP-II samples into "radiative" and non-radiative samples, based on the the value of $\sqrt{(}s')$. The events with high effective center-of-mass energy are particularly interesting as they probe the hard-scattering processes at these high energies.

We combine directly the measured data in terms of cross sections (for $q\bar{q}$, $\mu^+\mu^-$ and $\tau^+\tau^-$ final states) and forward-backward asymmetries (for $\mu^+\mu^-$ and $\tau^+\tau^-$ final states). In this first attempt at such a combination, the e^+e^- final state is not considered, due to the complication of the t-channel effects. Nor are measurements for specific quark flavour final states combined. Only data corresponding to the non-radiative event samples are considered. Furthermore, the combination is made, so far, only for the 183 and 189 GeV datasets as these have the highest luminosities and centre-of-mass energies.

3.1 Definition of the $f\bar{f}$ Signal

There are differences between the LEP experiments in the methods used to determine $\sqrt{s'}$, the treatment of the ISR-FSR interference and the angular acceptance over which the results are presented. The definition of $\sqrt{s'}$ has some subtleties which are discussed in more detail in Reference 20. Therefore it was necessary to choose a common definition of the $f\bar{f}$ signal.

The averages presented here are obtained using two alternatives for the common signal definition:

- **Definition 1:** $\sqrt{s'}$ is taken to be the mass of the s-channel propagator, with the $f\bar{f}$ signal being defined by the cut $\sqrt{s'/s} > 0.85$. ISR-FSR photon interference is subtracted to render the propagator mass unambiguous.
- **Definition 2:** For dilepton events, $\sqrt{s'}$ is taken to be the bare invariant mass of outgoing difermion pair. For hadronic events, it is taken to be the mass of the s-channel propagator. In both cases, ISR-FSR photon interference is included and the signal is defined by the cut $\sqrt{s'/s} > 0.85$. When calculating the contribution to the hadronic cross section due to ISR-FSR interference, since the propagator mass is ill-defined, it is replaced by the bare $q\bar{q}$ mass.

For both definitions, results are presented inside the full 4π angular acceptance. Events containing additional fermion pairs from radiative processes are considered to be signal, providing that the primary pair passes the cut on $\sqrt{s'/s}$ and that the secondary pair has a mass below 70 GeV. The signal definitions used by the individual LEP experiments can be found in Reference 20. Definition 1 corresponds to that used by L3 and OPAL, whereas Definition 2 represents a compromise between those of ALEPH and DELPHI.

3.2 Input $f\bar{f}$ Data

In order to make the combination, each LEP experiment provided their measurements of the $q\bar{q}$, $\mu^+\mu^-$ and $\tau^+\tau^-$ cross sections and of the $\mu^+\mu^-$ and $\tau^+\tau^-$ asymmetries at 183 and 189 GeV according to their own signal definition. The results given by the experiments are based on numbers in their publications [21], although some applied small corrections to these.

The total uncertainty on each measurement is broken down into five subcomponents. For the results of final state X from experiment Y at a particular centre-of-mass energy, these are:

1) The statistical uncertainty plus uncorrelated systematic uncertainties, combined in quadrature.

2) The systematic uncertainty for the final state X which is fully correlated between energy points for that experiment.

3) The systematic uncertainty for experiment Y which is fully correlated between different final states for this energy point.

4) The systematic uncertainty for the final state X which is fully correlated between energy points and between different experiments.

5) The systematic uncertainty which is fully correlated between energy points and between different experiments for all final states.

Note that cross section measurements are always considered to be uncorrelated with asymmetry measurements.

It should be stressed that the breakdown of the errors in this form is a first attempt to do so and that, as such, it should be considered as preliminary.

3.3 Averaging Method for $f\bar{f}$

Before they are averaged, the measurements from each experiment are corrected to the common choice of signal definition by comparing Standard Model (SM) predictions for the measurements, according to the experiment's own signal definition, to predictions for the common definition.

The SM predictions are calculated using the semi-analytical program ZFITTER 6.04 [22]. The theoretical uncertainties on these predictions are assessed by comparison with the results of the semi-analytical program TOPAZ0 4.4 [23] and the Monte Carlo generator KK 4.02 [24]. More details on these, plus other generators used in $e^+e^- \to f\bar{f}$ analysis, can be found in the web pages of the LEP-II Monte Carlo Workshop [25]. The corrections applied to the data typically correspond to adding/removing ISR-FSR photon interference, changing the definition of $\sqrt{s'}$ between propagator and bare difermion mass, and altering the cuts on $\sqrt{s'}$ or on the polar angle acceptance. The maximum discrepancies seen between ZFITTER, TOPAZ0 and KK for the size of the corrections are 0.2% for the hadronic cross sections, 0.7% for dilepton cross sections and 0.003 for the leptonic asymmetries. These are taken as preliminary estimates of the theoretical uncertainty on the correction procedure [26]. A more exhaustive evaluation of the theoretical uncertainties is currently underway within the framework of the LEP-II Monte Carlo Workshop.

There are 40 input measurements, comprising 2 centre-of-mass energies times 4 experiments times 3 cross sections plus 2 asymmetries. The 40×40 error matrix E on these measurements is constructed, such that its element i, j is given by

$$E_{ij} = \sum_{k=1}^{5} C_{ij}^{k} \sigma_i^k \sigma_j^k,$$

where the sum extends over the five error contributions described in Section 3.2. σ_i^k represents the uncertainty on measurement i due to error source k ($1 \leq k \leq 5$). The factor C_{ij}^k is equal to 1 if error k correlates measurements i and j and equals zero if it does not.

The χ^2 which must be minimized to obtain the averages is then

$$\chi^2 = (\boldsymbol{V} - \boldsymbol{A})^T \; E^{-1} \; (\boldsymbol{V} - \boldsymbol{A}),$$

where $\boldsymbol{V}$ is a vector containing the 40 corrected input measurements, and $\boldsymbol{A}$ is a vector containing the desired averages corresponding to each of these measurements. The 40 elements of vector $\boldsymbol{A}$ consist of ten independent numbers (the averages) repeated four times.

3.4 Results of $f\bar{f}$ averages

In this section the results of the combination made for the 1999 Summer Conferences are presented. This information is also available on the web page [27].

Table 10 shows the preliminary combined results corresponding to the signal Definition 1, described in Section 3.1. Shown are the average cross sections and lepton forward-backward asymmetries at 183 and 189 GeV, together with the corresponding SM predictions obtained from ZFITTER 6.04. The quoted uncertainties on each result do not include the theoretical uncertainties arising from correcting the input data to a common signal definition, discussed in Section 3.3. Also shown is the difference between the results for Definition 1 and Definition 2. Due to the procedure of correcting the data, the same correction must be applied to the results and to the SM prediction.

The χ^2 per degree of freedom of the two sets of averages are identical at 24.6/30. The correlation matrix for the combination is also identical in both cases. It is given Table 11. The correlations are rather small, with the largest being 18% between the $q\overline{q}$ cross sections at 183 and 189 GeV. The combined errors are dominated by the statistical and uncorrelated experimental systematics. For example, for the 189 GeV hadronic cross section the part of the error arising from the correlated components is about one-third of the total error.

Figure 2 shows the LEP averaged cross sections and asymmetries, respectively, (based on Definition 1), as a function of centre-of-mass energy, together with the SM predictions.

There is good agreement between the SM expectations and the measurements of the individual experiments and the combined averages. There is no evidence in $e^+e^- \to f\bar{f}$ for physics beyond the SM.

3.5 Contact Interactions

The data can be used to put limits on various models of new physics beyond the SM. As an example of the sensitivity to physics beyond the Standard Model, the combined cross sections and asymmetries

cms energy	quantity	average value	SM prediction	$\Delta(2-1)$
182.7 GeV	$\sigma(q\overline{q})$	24.54 ± 0.43 pb	24.20 pb	-0.11 pb
	$\sigma(\mu^+\mu^-)$	3.44 ± 0.14 pb	3.45 pb	-0.14 pb
	$\sigma(\tau^+\tau^-)$	3.43 ± 0.18 pb	3.45 pb	-0.05 pb
	$A_{FB}(\mu^+\mu^-)$	0.547 ± 0.034	0.576	0.018
	$A_{FB}(\tau^+\tau^-)$	0.615 ± 0.044	0.576	0.018
188.6 GeV	$\sigma(q\overline{q})$	22.38 ± 0.25 pb	22.16 pb	-0.10 pb
	$\sigma(\mu^+\mu^-)$	3.193 ± 0.083 pb	3.207 pb	-0.131 pb
	$\sigma(\tau^+\tau^-)$	3.135 ± 0.102 pb	3.207 pb	-0.048 pb
	$A_{FB}(\mu^+\mu^-)$	0.562 ± 0.022	0.569	0.019
	$A_{FB}(\tau^+\tau^-)$	0.597 ± 0.027	0.569	0.018

Table 10: Preliminary combined 183 and 189 GeV LEP results for $e^+e^- \to f\overline{f}$. The results all correspond to the signal Definition 1 described in Section 3.1. The quoted uncertainties do not include the theoretical uncertainties discussed in Section 3.3. The last column shows the value that must be added to the result and the SM prediction to get the values corresponding to Definition 2.

cms energy	quantity										
183 GeV	$\sigma(q\overline{q})$	1.00	0.01	0.02	0.00	0.00	0.18	0.01	0.01	0.00	0.00
	$\sigma(\mu^+\mu^-)$	0.01	1.00	0.01	0.00	0.00	0.01	0.08	0.00	0.00	0.00
	$\sigma(\tau^+\tau^-)$	0.02	0.01	1.00	0.00	0.00	0.01	0.00	0.09	0.00	0.00
	$A_{FB}(\mu^+\mu^-)$	0.00	0.00	0.00	1.00	0.01	0.00	0.00	0.00	0.04	0.00
	$A_{FB}(\tau^+\tau^-)$	0.00	0.00	0.00	0.01	1.00	0.00	0.00	0.00	0.00	0.03
189 GeV	$\sigma(q\overline{q})$	0.18	0.01	0.01	0.00	0.00	1.00	0.01	0.01	0.00	0.00
	$\sigma(\mu^+\mu^-)$	0.01	0.08	0.00	0.00	0.00	0.01	1.00	0.00	0.00	0.00
	$\sigma(\tau^+\tau^-)$	0.01	0.00	0.09	0.00	0.00	0.01	0.00	1.00	0.00	0.00
	$A_{FB}(\mu^+\mu^-)$	0.00	0.00	0.00	0.04	0.00	0.00	0.00	0.00	1.00	0.04
	$A_{FB}(\tau^+\tau^-)$	0.00	0.00	0.00	0.00	0.03	0.00	0.00	0.00	0.04	1.00

Table 11: The correlation matrix of the averaged results.

for $e^+e^- \to \mu^+\mu^-$ and $e^+e^- \to \tau^+\tau^-$ have been used to place limits on contact interactions between leptons. Following reference [28] these interactions are parameterised by an effective Lagrangian $\mathcal{L}_{\text{eff}}$, added to the Standard Model Lagrangian of the form

$$\mathcal{L}_{\text{eff}} = \frac{g^2}{(1+\delta)\Lambda^2} \sum_{i,j=L,R} \eta_{ij} \overline{e}_i \gamma_\mu e_i \overline{f}_j \gamma^\mu f_j, \tag{5}$$

where $g^2/4\pi$ is taken to be 1 by convention, $\delta = 1$ (0) for $f = e$ ($f \neq e$), $\eta_{ij} = \pm 1$ or 0, Λ is the scale of the contact interactions, e_i and f_j are left or right-handed spinors. By assuming different helicity coupling between the initial state and final state currents and either constructive or destructive interference with the Standard Model (according to the choice of each η_{ij}) a basic set of 6 different models can be defined from this Lagrangian [29], with either constructive (+) or destructive (−) interference between the Standard Model process and the contact interactions. The models LL, RR, VV and AA are considered here since these models lead to large deviations in the $e^+e^- \to \mu^+\mu^-$ and $e^+e^- \to \tau^+\tau^-$ channels. The total hadronic cross section on its own is not particularly sensitive to contact interactions involving quarks. For the purpose of fitting contact interaction models to the data, a new parameter $\epsilon = 1/\Lambda^2$ is defined with $\epsilon = 0$ in the limit that there are no contact interactions. This parameter is allowed to take both positive and negative values in the fits. The

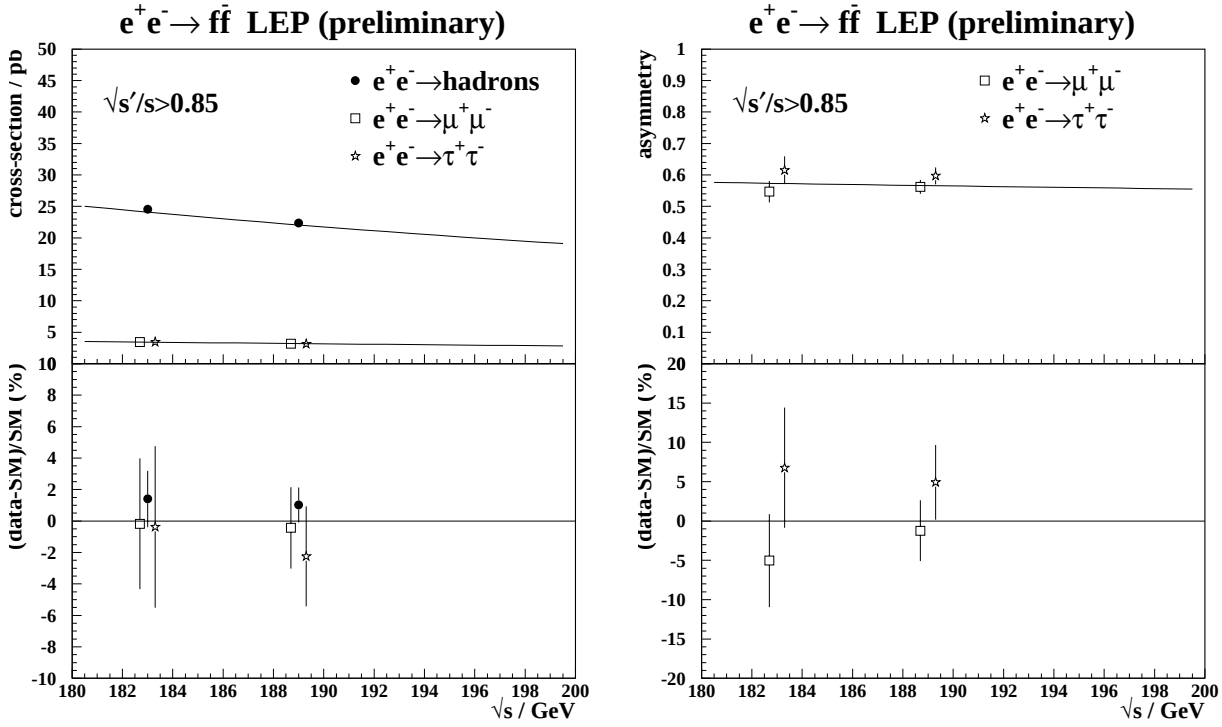

Figure 2: Preliminary combined LEP results on the cross sections and forward-backward asymmetries as a function of cms energy. The expectations of the SM are also shown. The lower plots show the differences between the data and the SM, divided by the SM prediction.

values of ϵ extracted for each model were all compatible with the Standard Model expectation $\epsilon = 0$, at the two standard deviation level. These errors on ϵ are typically a factor of two smaller than those obtained from a single LEP experiment with the same data set. The fitted values of ϵ were converted into 95% confidence level lower limits on Λ, and are shown in Table 12.

$e^+e^- \to \mu^+\mu^-$			
Model	ϵ (TeV^{-2})	Λ_+(TeV)	Λ_-(TeV)
LL	$-0.001^{+0.008}_{-0.008}$	8.8	8.4
RR	$-0.002^{+0.009}_{-0.009}$	8.4	8.0
VV	$0.000^{+0.003}_{-0.003}$	14.0	14.4
AA	$-0.002^{+0.004}_{-0.004}$	12.0	10.6

$e^+e^- \to \tau^+\tau^-$			
Model	ϵ (TeV^{-2})	Λ_+(TeV)	Λ_-(TeV)
LL	$-0.002^{+0.009}_{-0.010}$	7.9	7.3
RR	$-0.002^{+0.010}_{-0.011}$	7.5	7.0
VV	$-0.003^{+0.004}_{-0.004}$	12.7	10.3
AA	$0.004^{+0.005}_{-0.005}$	9.1	10.9

$e^+e^- \to \ell^+\ell^-$			
Model	ϵ (TeV^{-2})	Λ_+(TeV)	Λ_-(TeV)
LL	$-0.003^{+0.006}_{-0.006}$	10.0	8.8
RR	$-0.003^{+0.007}_{-0.007}$	9.5	8.4
VV	$-0.002^{+0.002}_{-0.002}$	16.2	14.0
AA	$0.000^{+0.003}_{-0.003}$	13.6	13.2

Table 12: Fitted values of ϵ and 95% confidence limits on the scale, Λ, for constructive (+) and destructive interference (−) with the Standard Model, for the contact interaction models discussed in the text. Results are given for $e^+e^- \to \mu^+\mu^-$, $e^+e^- \to \tau^+\tau^-$ and $e^+e^- \to \ell^+\ell^-$, assuming universality in the contact interactions between $e^+e^- \to \mu^+\mu^-$ and $e^+e^- \to \tau^+\tau^-$.

4 The τ Polarisation

Updates with respect to last summer:
DELPHI have updated their results.

The longitudinal τ polarisation $\mathcal{P}_\tau$ of τ pairs produced in Z decays is defined as

$$\mathcal{P}_\tau \equiv \frac{\sigma_{\mathrm{R}} - \sigma_{\mathrm{L}}}{\sigma_{\mathrm{R}} + \sigma_{\mathrm{L}}}, \tag{6}$$

where σ_{R} and σ_{L} are the τ-pair cross sections for the production of a right-handed and left-handed τ^-, respectively. The distribution of $\mathcal{P}_\tau$ as a function of the polar scattering angle θ between the e^- and the τ^-, at $\sqrt{s} = m_{\mathrm{Z}}$, is given by

$$\mathcal{P}_\tau(\cos\theta) = -\frac{\mathcal{A}_\tau(1+\cos^2\theta) + 2\mathcal{A}_{\mathrm{e}}\cos\theta}{1+\cos^2\theta + 2\mathcal{A}_\tau\mathcal{A}_{\mathrm{e}}\cos\theta}, \tag{7}$$

with $\mathcal{A}_{\mathrm{e}}$ and $\mathcal{A}_\tau$ as defined in Equation (4). Equation (7) is valid for pure Z exchange. The effects of γ exchange, γ-Z interference and electromagnetic radiative corrections for initial-state and final-state radiation are taken into account in the experimental analyses. In particular, these corrections account for the $\sqrt{s}$ dependence of the τ polarisation, which is important because the off-peak data are included in the event samples for all experiments. When averaged over all production angles $\mathcal{P}_\tau$ is a measurement of $\mathcal{A}_\tau$. As a function of $\cos\theta$, $\mathcal{P}_\tau(\cos\theta)$ provides nearly independent determinations of both $\mathcal{A}_\tau$ and $\mathcal{A}_{\mathrm{e}}$, thus allowing a test of the universality of the couplings of the Z to e and τ.

Each experiment makes separate $\mathcal{P}_\tau$ measurements using the five τ decay modes $\mathrm{e}\nu\overline{\nu}$, $\mu\nu\overline{\nu}$, $\pi\nu$, $\rho\nu$ and $a_1\nu$ [30–33]. The $\rho\nu$ and $\pi\nu$ are the most sensitive channels, contributing weights of about 40% each in the average. DELPHI and L3 have also used an inclusive hadronic analysis. The combination is made using the results from each experiment already averaged over the τ decay modes.

4.1 Results

Tables 13 and 14 show the most recent results for $\mathcal{A}_\tau$ and $\mathcal{A}_{\mathrm{e}}$ obtained by the four LEP collaborations [30–33] and their combination. Common systematic errors arise from uncertainties in the decay radiation in the $\pi\nu$ and $\rho\nu$ channels, and in the modelling of the a_1 decays [2]. These errors need further investigation and might need to be taken into account for the final results (see Reference 32). For the current combination the systematic errors on $\mathcal{A}_\tau$ and $\mathcal{A}_{\mathrm{e}}$ are treated as uncorrelated between the experiments. The statistical correlation between the extracted values of $\mathcal{A}_\tau$ and $\mathcal{A}_{\mathrm{e}}$ is small ($\leq$ 5%), and is neglected.

The average values for $\mathcal{A}_\tau$ and $\mathcal{A}_{\mathrm{e}}$:

$$\mathcal{A}_\tau = 0.1425 \pm 0.0044 \tag{8}$$

$$\mathcal{A}_{\mathrm{e}} = 0.1483 \pm 0.0051, \tag{9}$$

are compatible, in agreement with lepton universality. Assuming e-τ universality, the values for $\mathcal{A}_\tau$ and $\mathcal{A}_{\mathrm{e}}$ can be combined. This combination is performed neglecting any possible common systematic error between $\mathcal{A}_\tau$ and $\mathcal{A}_{\mathrm{e}}$ within a given experiment, as these errors are also estimated to be small. The combined result of $\mathcal{A}_\tau$ and $\mathcal{A}_{\mathrm{e}}$ is:

$$\mathcal{A}_\ell = 0.1450 \pm 0.0033. \tag{10}$$

Experiment		$\mathcal{A}_\tau$
ALEPH	(90 - 95), prel.	$0.1452 \pm 0.0052 \pm 0.0032$
DELPHI	(90 - 95), prel.	$0.1359 \pm 0.0079 \pm 0.0055$
L3	(90 - 95), final	$0.1476 \pm 0.0088 \pm 0.0062$
OPAL	(90 - 94), final	$0.134 \pm 0.009 \pm 0.010$
LEP Average		0.1425 ± 0.0044

Table 13: LEP results for $\mathcal{A}_\tau$. The χ^2/d.o.f. for the average is 1.3/3. The first error is statistical and the second systematic. In the LEP average, statistical and systematic errors are combined in quadrature. The systematic component of the error is ± 0.0026.

Experiment		$\mathcal{A}_{\mathrm{e}}$
ALEPH	(90 - 95), prel.	$0.1505 \pm 0.0069 \pm 0.0010$
DELPHI	(90 - 95), prel.	$0.1382 \pm 0.0116 \pm 0.0005$
L3	(90 - 95), final	$0.1678 \pm 0.0127 \pm 0.0030$
OPAL	(90 - 94), final	$0.129 \pm 0.014 \pm 0.005$
LEP Average		0.1483 ± 0.0051

Table 14: LEP results for $\mathcal{A}_{\mathrm{e}}$. The χ^2/d.o.f. for the average is 4.8/3. The first error is statistical and the second systematic. In the LEP average, statistical and systematic errors are combined in quadrature. The systematic component of the error is ± 0.0009.

5 Measurement of $A_{\rm LR}$ at SLC

Updates with respect to last summer:
SLD have updated the $A_{\rm LR}$ and the leptonic left-right forward-backward asymmetries.

The measurement of the left-right cross section asymmetry ($A_{\rm LR}$) by SLD [34] at the SLC provides a systematically precise, statistics dominated, determination of the coupling $\mathcal{A}_{\rm e}$, and is presently the most precise single measurement, with the smallest systematic error, of this quantity. In principle the analysis is straightforward: one counts the numbers of Z bosons produced by left and right longitudinally polarised electrons, forms an asymmetry, and then divides by the luminosity-weighted e^- beam polarisation magnitude (the e^+ beam is not polarised):

$$A_{\rm LR} = \frac{N_{\rm L} - N_{\rm R}}{N_{\rm L} + N_{\rm R}} \frac{1}{P_{\rm e}}. \tag{11}$$

Since the advent of high polarisation "strained lattice" GaAs photocathodes (1994), the average electron polarisation at the interaction point has been in the range 73% to 77%. The method requires no detailed final state event identification (e^+e^- final state events are removed, as are non-Z backgrounds) and is insensitive to all acceptance and efficiency effects. The small total systematic error of 0.65% relative is dominated by the 0.5% relative systematic error in the determination of the e^- polarisation. The present relative statistical error on $A_{\rm LR}$ is about 1.3%.

The precision Compton polarimeter detects beam electrons that have been scattered by photons from a circularly polarised laser. Two additional polarimeters that are sensitive to the Compton-scattered photons and which are operated in the absence of positron beam, have verified the precision polarimeter result to within their estimated errors of about 0.5%. In 1998, a dedicated experiment was performed in order to directly test the expectation that accidental polarisation of the positron beam was negligible; the e^+ polarisation was found to be consistent with zero ($-0.02 \pm 0.07\%$).

The $A_{\rm LR}$ analysis includes several very small corrections. The polarimeter result is corrected for higher order QED and accelerator related effects (a total of $-0.22 \pm 0.15\%$ for 1997/98 data), and the event asymmetry is corrected for backgrounds and accelerator asymmetries (a total of $+0.15 \pm 0.07\%$, for 1997/98 data).

The translation of the $A_{\rm LR}$ result to a "pole" value is a $-2.5 \pm 0.4\%$ effect, where the uncertainty arises from the precision of the centre-of-mass energy determination. This small error due to the beam energy measurement is slightly larger than seen previously (it was closer to 0.3%) and reflects the results of a scan of the Z peak used to calibrate the energy spectrometers to LEP data, which was performed for the first time during the most recent SLC run. The pole value, $A^0_{\rm LR}$, is equivalent to a measurement of $\mathcal{A}_{\rm e}$.

The 1999 result is included in a running average of all of the SLD $A_{\rm LR}$ measurements (1992, 1993, 1994/1995, 1996, 1997 and 1998). This updated result for $A^0_{\rm LR}$ ($\mathcal{A}_{\rm e}$) is 0.15108 ± 0.00218. In addition, the left-right forward-backward asymmetries for leptonic final states have been measured. From these, the parameters $\mathcal{A}_{\rm e}$, $\mathcal{A}_\mu$ and $\mathcal{A}_\tau$ can be determined. The preliminary results are $\mathcal{A}_{\rm e} = 0.1558 \pm 0.0064$, $\mathcal{A}_\mu = 0.137 \pm 0.016$ and $\mathcal{A}_\tau = 0.142 \pm 0.016$.

Assuming lepton universality, the $A_{\rm LR}$ result and the results on the leptonic left-right forward-backward asymmetries can be combined yielding

$$\mathcal{A}_\ell = 0.15121 \pm 0.00204. \tag{12}$$

6 Results from b and c Quarks

Updates with respect to last summer:
DELPHI has published their R_b and R_c measurements with the full LEP-I dataset, SLD has included data up to spring 1998 and L3 have updated their R_b result.
SLD have updated their R_c measurement with more data.
L3 has published their $A_{FB}^{b\bar{b}}$ with jet charge and $A_{FB}^{b\bar{b}}$ with lepton measurements. DELPHI has published $A_{FB}^{b\bar{b}}$ with jet charge and $A_{FB}^{b\bar{b}}$ and $A_{FB}^{c\bar{c}}$ with D mesons. ALEPH has presented new measurements of $A_{FB}^{b\bar{b}}$ and $A_{FB}^{c\bar{c}}$ with leptons at the peak.
SLD have updated most of their $\mathcal{A}_b$ and $\mathcal{A}_c$ analyses with new data.
DELPHI, L3 and OPAL have updated their BR($b \to \ell$) and BR($b \to c \to \bar{\ell}$) measurement.
BR($c \to \ell$) is now a fit parameter.

The relevant quantities in the heavy quark sector at LEP/SLD which are currently determined by the combination procedure are:

- The ratios of the b and c quark partial widths of the Z to its total hadronic partial width: $R_b^0 \equiv \Gamma_{b\bar{b}}/\Gamma_{had}$ and $R_c^0 \equiv \Gamma_{c\bar{c}}/\Gamma_{had}$.
- The forward-backward asymmetries, $A_{FB}^{b\bar{b}}$ and $A_{FB}^{c\bar{c}}$.
- The final state coupling parameters $\mathcal{A}_b$, $\mathcal{A}_c$ obtained from the left-right-forward-backward asymmetry at SLD.
- The semileptonic branching ratios, BR($b \to \ell$), BR($b \to c \to \bar{\ell}$) and BR($c \to \ell$), and the average time-integrated $B^0\overline{B^0}$ mixing parameter, $\overline{\chi}$. These are often determined at the same time or with similar methods as the asymmetries. Including them in the combination greatly reduces the errors. For example the measurements of $\overline{\chi}$ act as an effective measurement of the charge tagging efficiency, so that all errors coming from the mixture of different lepton sources in $b\overline{b}$ events cancel in the asymmetries.

  For the first time the branching ratio BR($c \to \ell$) is also taken from LEP measurements. Because of the large differences in semileptonic branching ratios of the different charmed hadrons the usage of the low energy number implied the assumption that the D-hadron mixture is energy independent. This assumption could be dropped with the new measurements of BR($c \to \ell$) at LEP. However, the LEP results are in excellent agreement with the old assumption.
- The probability that a c quark produces a D^+, D_s, D^{*+} meson[2] or a charmed baryon. The probability that a c quark fragments into a D^0 is calculated from the constraint that the probabilities for the weakly decaying charmed hadrons add up to one. These quantities (f_X) are determined now with good accuracy by the LEP experiments. The interpretation of the D^* rate in terms of R_c and the determination of the charm background in the lifetime tag R_b measurements can now be made without assumptions on the energy dependence of the D meson production rates.

A full description of the averaging procedure is published in [3]; the main motivations for the procedure are outlined here. Several analyses measure more than one parameter simultaneously, for example the asymmetry measurements with leptons or D mesons. Some of the measurements of electroweak parameters depend explicitly on the values of other parameters, for example R_b depends on R_c.

[2] Actually the product $P(c \to D^{*+}) \times BR(D^{*+} \to \pi^+ D^0)$ is fitted because this quantity is needed and measured by the LEP experiments.

The common tagging and analysis techniques lead to common sources of systematic uncertainty, in particular for the double-tag measurements of R_b. The starting point for the combination is to ensure that all the analyses use a common set of assumptions for input parameters which give rise to systematic uncertainties. The input parameters have been updated and extended [35] to accommodate new analyses and more recent measurements. The correlations and interdependences of the input measurements are then taken into account in a χ^2 minimisation which results in the combined electroweak parameters and their correlation matrix.

In a first fit the asymmetry measurements on peak, above peak and below peak are corrected to three common centre-of-mass energies and are then combined at each energy point. The results of this fit, including the SLD results, are given in Appendix A. The dependence of the average asymmetries on centre-of-mass energy agrees with the prediction of the Standard Model. A second fit is made to derive the pole asymmetries $A_{FB}^{0,q}$ from the measured quark asymmetries, in which all the off-peak asymmetry measurements are corrected to the peak energy before combining. This fit determines a total of 14 parameters: the two partial widths, two LEP asymmetries, two coupling parameters from SLD, three semileptonic branching ratios, the average mixing parameter and the probabilities for c quark to fragment into a D^+, a D_s, a D^{*+}, or a charmed baryon. If the SLD measurements are excluded from the fit there are 12 parameters to be determined.

6.1 Summary of Measurements and Averaging Procedure

All measurements are presented by the LEP and SLD collaborations in a consistent manner for the purpose of combination. The tables prepared by the experiments include a detailed breakdown of the systematic error of each measurement and its dependence on other electroweak parameters. Where necessary, the experiments apply small corrections to their results in order to use agreed values and ranges for the input parameters to calculate systematic errors. The measurements, corrected where necessary, are summarised in Appendix A in Tables 35–54, where the statistical and systematic errors are quoted separately. The correlated systematic entries are from sources shared with one or more other results in the table and are derived from the full breakdown of common systematic uncertainties. The uncorrelated systematic entries come from the remaining sources.

Recently the OPAL collaboration have published a new measurement of the gluon splitting probability into a $c\overline{c}$ pair [36]. Using this result instead of the old one and following the averaging procedure [35] for the gluon splitting rates to $b\overline{b}$ and $c\overline{c}$ yields for the rate of heavy quark pairs from gluon splitting in hadronic events:

$$g_{c\overline{c}} = (3.19 \pm 0.46)\% \quad (13)$$

$$g_{b\overline{b}} = (0.251 \pm 0.063)\% \quad (14)$$

These values are used consistently by all experiments.

In addition the QCD corrections to the forward-backward asymmetries have been updated. A summary of the new corrections can be found in section 6.1.3.

6.1.1 Averaging procedure

A χ^2 minimisation procedure is used to derive the values of the heavy-flavour electroweak parameters as published in Reference 3. The full statistical and systematic covariance matrix for all measurements

is calculated. This correlation matrix takes into account correlations between different measurements of one experiment and between different experiments. The explicit dependence of each measurement on the other parameters is also accounted for. The most important example is the dependence of the value of $R_{\rm b}$ on the assumed value of $R_{\rm c}$.

Since c-quark events form the main background in the $R_{\rm b}$ analyses, the value of $R_{\rm b}$ depends on the value of $R_{\rm c}$. If $R_{\rm b}$ and $R_{\rm c}$ are measured in the same analysis, this is reflected in the correlation matrix for the results. However the analyses do not determine $R_{\rm b}$ and $R_{\rm c}$ simultaneously but instead measure $R_{\rm b}$ for an assumed value of $R_{\rm c}$. In this case the dependence is parameterised as

$$R_{\rm b} \;=\; R_{\rm b}^{\rm meas} + a(R_{\rm c})\frac{(R_{\rm c} - R_{\rm c}^{\rm used})}{R_{\rm c}}. \tag{15}$$

In this expression, $R_{\rm b}^{\rm meas}$ is the result of the analysis assuming a value of $R_{\rm c} = R_{\rm c}^{\rm used}$. The values of $R_{\rm c}^{\rm used}$ and the coefficients $a(R_{\rm c})$ are given in Table 35 where appropriate. The dependence of all other measurements on other electroweak parameters is treated in the same way, with coefficients $a(x)$ describing the dependence on parameter x.

6.1.2 Partial width measurements

The measurements of $R_{\rm b}$ and $R_{\rm c}$ fall into two categories. In the first, called a single-tag measurement, a method to select b or c events is devised, and the number of tagged events is counted. This number must then be corrected for backgrounds from other flavours and for the tagging efficiency to calculate the true fraction of hadronic Z decays of that flavour. The dominant systematic errors come from understanding the branching ratios and detection efficiencies which give the overall tagging efficiency. For the second technique, called a double-tag measurement, the event is divided into two hemispheres. With N_t being the number of tagged hemispheres, N_{tt} the number of events with both hemispheres tagged and $N_{\rm had}$ the total number of hadronic Z decays one has

$$\frac{N_t}{2N_{\rm had}} \;=\; \varepsilon_{\rm b}R_{\rm b} + \varepsilon_{\rm c}R_{\rm c} + \varepsilon_{\rm uds}(1 - R_{\rm b} - R_{\rm c}), \tag{16}$$

$$\frac{N_{tt}}{N_{\rm had}} \;=\; \mathcal{C}_{\rm b}\varepsilon_{\rm b}^2R_{\rm b} + \mathcal{C}_{\rm c}\varepsilon_{\rm c}^2R_{\rm c} + \mathcal{C}_{\rm uds}\varepsilon_{\rm uds}^2(1 - R_{\rm b} - R_{\rm c}), \tag{17}$$

where $\varepsilon_{\rm b}$, $\varepsilon_{\rm c}$ and $\varepsilon_{\rm uds}$ are the tagging efficiencies per hemisphere for b, c and light-quark events, and $\mathcal{C}_{\rm q} \neq 1$ accounts for the fact that the tagging efficiencies between the hemispheres may be correlated. In the case of $R_{\rm b}$ one has $\varepsilon_{\rm b} \gg \varepsilon_{\rm c} \gg \varepsilon_{\rm uds}$, $\mathcal{C}_{\rm b} \approx 1$. The correlations for the other flavours can be neglected. These equations can be solved to give $R_{\rm b}$ and $\varepsilon_{\rm b}$. Neglecting the c and uds backgrounds and the correlations they are approximately given by

$$\varepsilon_{\rm b} \;\approx\; 2N_{tt}/N_t, \tag{18}$$

$$R_{\rm b} \;\approx\; N_t^2/(4N_{tt}N_{\rm had}). \tag{19}$$

The double-tagging method has the advantage that the b tagging efficiency is derived directly from the data, reducing the systematic error. The residual background of other flavours in the sample, and the evaluation of the correlation between the tagging efficiencies in the two hemispheres of the event are the main sources of systematic uncertainty in such an analysis.

This method can be enhanced by including more tags. All additional efficiencies can be determined from data, reducing the statistical uncertainties without adding new systematic uncertainties.

Small corrections must be applied to the results to obtain the partial width ratios R_b^0 and R_c^0 from the cross section ratios R_b and R_c. These corrections depend slightly on the invariant mass cutoff of the simulations used by the experiments, so that they are applied by the collaborations before the combination.

The partial width measurements included are:

- Lifetime (and lepton) double tag measurements for R_b from ALEPH [37], DELPHI [38], L3 [39], OPAL [40] and SLD [41]. These are the most precise determinations of R_b. Since they completely dominate the combined result, no other R_b measurements are used at present. The basic features of the double-tag technique were discussed above. In the ALEPH, DELPHI, OPAL and SLD measurements the charm rejection has been enhanced by using the invariant mass information. DELPHI also adds information from the energy of all particles at the secondary vertex and their rapidity. The ALEPH and DELPHI measurements make use of several different tags; this improves the statistical accuracy and reduces the systematic errors due to hemisphere correlations and charm contamination, compared with the simple single/double tag.

- Analyses with $D/D^{*\pm}$ mesons to measure R_c from ALEPH, DELPHI and OPAL. All measurements are constructed in such a way that no assumptions on the energy dependence of charm fragmentation are necessary. The available measurements can be divided into four groups:

  - inclusive/exclusive double tag (ALEPH [42], DELPHI [43, 44], OPAL [45]): In a first step $D^{*\pm}$ mesons are reconstructed in several decay channels and their production rate is measured, which depends on the product $R_c \times P(c \to D^{*+}) \times BR(D^{*+} \to \pi^+ D^0)$. This sample of $c\overline{c}$ (and $b\overline{b}$) events is then used to measure $P(c \to D^{*+}) \times BR(D^{*+} \to \pi^+ D^0)$ using a slow pion tag in the opposite hemisphere. In the ALEPH measurement R_c is unfolded internally in the analysis so that no explicit $P(c \to D^{*+}) \times BR(D^{*+} \to \pi^+ D^0)$ is available.
  - exclusive double tag (ALEPH [42]): This analysis uses exclusively reconstructed D^{*+}, D^0 and D^+ mesons in different decay channels. It has lower statistics but better purity than the inclusive analyses.
  - reconstruction of all weakly decaying charmed states (ALEPH [46], DELPHI [44], OPAL [47]): These analyses make the assumption that the production rates of D^0, D^+, D_s and Λ_c saturate the fragmentation of $c\overline{c}$ with small corrections applied for the unobserved baryonic states. This is a single tag measurement, relying only on knowing the decay branching ratios of the charm hadrons. These analyses are also used to measure the c hadron production ratios which are needed for the R_b analyses.

  Since DELPHI have presented their final results for the inclusive/exclusive R_c measurement, the old, preliminary, double inclusive result [48] is no longer used.

- A lifetime plus mass double tag from SLD to measure R_c [49]. This analysis uses the same tagging algorithm as the SLD R_b analysis, but requires that the mass of the secondary vertex be smaller than the D meson mass. Although the charm tag has a purity of about 67%, most of the background is from b which can be measured from the b/c mixed tag rate.

- A measurement of R_c using single leptons assuming $BR(c \to \ell)$ from ALEPH [42].

6.1.3 Asymmetry measurements

All b and c asymmetries given by the experiments are corrected to full acceptance.

The QCD corrections to the forward-backward asymmetries depend strongly on the experimental analyses. For this reason the numbers given by the collaborations are also corrected for QCD effects. A detailed description of the procedure can be found in Reference 50.

Recently an analytic calculation of the second order QCD corrections [51] gave a result not in agreement with the one used in Reference 50. This result had been confirmed by a numerical calculation [52]. This calculation also gives the second order result using the thrust axis, which is actually used in the experimental analyses. The calculation in Reference 52 is strictly massless and also neglects the so called 2-jet and 3-jet corrections in Reference 53 which come from triangle diagrams involving top quarks and thus depend on the top quark mass. The diagrams corresponding to the much larger 2-jet correction lead to two parton final states. The correction has thus to be identical for the quark and the thrust axis and can be safely added to the final result from Reference 52. The second order coefficients of the QCD corrections to the asymmetries which are used from now on are $c_2 = 5.93$ for $A_{\rm FB}^{\rm b}$ and $c_2 = 8.5$ for $A_{\rm FB}^{\rm c}$. Following the notation of Reference 50 the final QCD correction coefficients, including fragmentation effects, are then $C_{\rm QCD}^{\rm had,T} = 0.0354 \pm 0.0063$ for $A_{\rm FB}^{\rm b}$ and $C_{\rm QCD}^{\rm had,T} = 0.0413 \pm 0.0063$ for $A_{\rm FB}^{\rm c}$. The breakdown of the errors is given in Table 15.

Error source	$\rm b\overline{b}$	$\rm c\overline{c}$
higher orders [52]	0.0025	0.0046
mass effects [50]	0.0015	0.0008
higher order mass [52]	0.005	0.002
$\alpha_s(0.119 \pm 0.003)$	0.0012	0.0015
hadronisation [50]	0.0023	0.0035
total	0.0063	0.0063

Table 15: Error sources for the QCD corrections to the forward-backward asymmetries. The evaluation of the error follows exactly the quoted references.

For the 12- and 14-parameter fits described above, the LEP peak and off-peak asymmetries are corrected to $\sqrt{s} = 91.26$ GeV using the predicted dependence from ZFITTER [22]. The slope of the asymmetry around $m_{\rm Z}$ depends only on the axial coupling and the charge of the initial and final state fermions and is thus independent of the value of the asymmetry itself.

After calculating the overall averages, the quark pole asymmetries, $A_{\rm FB}^{0,\rm q}$, are derived by applying the corrections described below. To relate the pole asymmetries to the measured ones a few corrections that are summarised in Table 16 have to be applied. These corrections are due to the energy shift from 91.26 GeV to $m_{\rm Z}$, initial state radiation, γ exchange and γ-Z interference. A very small correction due to the nonzero value of the b quark mass is included in the correction called γ-Z interference. All corrections are calculated using ZFITTER.

Source	$\delta A_{\rm FB}^{\rm b}$	$\delta A_{\rm FB}^{\rm c}$
$\sqrt{s} = m_{\rm Z}$	-0.0013	-0.0034
QED corrections	$+0.0041$	$+0.0104$
γ, γ-Z, mass	-0.0003	-0.0008
Total	$+0.0025$	$+0.0062$

Table 16: Corrections to be applied to the quark asymmetries as $A_{\rm FB}^0 = A_{\rm FB}^{meas} + \delta A_{\rm FB}$.

The SLD left-right-forward-backward asymmetries are also corrected for all radiative effects and are directly presented in terms of $\mathcal{A}_{\rm b}$ and $\mathcal{A}_{\rm c}$.

The measurements used are:

- Measurements of $A_{\rm FB}^{\rm b\bar{b}}$ and $A_{\rm FB}^{\rm c\bar{c}}$ using leptons from ALEPH [54], DELPHI [55], L3 [56] and OPAL [57]. These analyses measure either $A_{\rm FB}^{\rm b\bar{b}}$ only from a high p_t lepton sample or they obtain $A_{\rm FB}^{\rm b\bar{b}}$ and $A_{\rm FB}^{\rm c\bar{c}}$ from a fit to the lepton spectra. In the case of OPAL the lepton information has been combined with hadronic variables in a neural net. Some asymmetry analyses also measure $\overline{\chi}$.

- Measurements of $A_{\rm FB}^{\rm b\bar{b}}$ based on lifetime tagged events with a hemisphere charge measurement from ALEPH [58], DELPHI [59], L3 [60] and OPAL [61]. These measurements contribute roughly the same weight to the combined result as the lepton fits.

- Analyses with D mesons to measure $A_{\rm FB}^{\rm c\bar{c}}$ from ALEPH [62] or $A_{\rm FB}^{\rm c\bar{c}}$ and $A_{\rm FB}^{\rm b\bar{b}}$ from DELPHI [63] and OPAL [64].

- Measurements of $\mathcal{A}_{\rm b}$ and $\mathcal{A}_{\rm c}$ from SLD. These results include measurements using lepton [65], D meson [65] and vertex mass plus hemisphere charge [66] tags, which have similar sources of systematic errors as the LEP asymmetry measurements. SLD also uses vertex mass for bottom or charm tags in conjunction with a kaon tag for an $\mathcal{A}_{\rm b}$ measurement [67], with a vertex charge and kaon tag for an $\mathcal{A}_{\rm c}$ measurement [68] and with vertex charge only for an $\mathcal{A}_{\rm b}$ measurement [69].

6.1.4 Other measurements

The measurements of the charmed hadron fractions $\mathrm{P(c \to D^{*+}) \times BR(D^{*+} \to \pi^+ D^0)}$, $f(\mathrm{D^+})$, $f(\mathrm{D_s})$ and $f(\mathrm{c_{baryon}})$ are included in the $R_{\rm c}$ measurements and are described there.

ALEPH [70], DELPHI [71], L3 [39, 72] and OPAL [73] measure $\mathrm{BR(b \to \ell)}$, $\mathrm{BR(b \to c \to \bar{\ell})}$ and $\overline{\chi}$ or a subset of them from a sample of leptons opposite to a b-tagged hemisphere and from a double lepton sample. DELPHI [43] and OPAL [74] measure $\mathrm{BR(c \to \ell)}$ from a sample opposite to a high energy $\mathrm{D^{*\pm}}$.

6.2 Results

6.2.1 Results of the 12-Parameter Fit to the LEP Data

Using the full averaging procedure gives the following combined results for the electroweak parameters:

$$\begin{aligned} R_{\rm b}^0 &= 0.21642 \pm 0.00075 \\ R_{\rm c}^0 &= 0.1675 \pm 0.0048 \\ A_{\rm FB}^{0,\,\rm b} &= 0.0988 \pm 0.0020 \\ A_{\rm FB}^{0,\,\rm c} &= 0.0689 \pm 0.0037\,, \end{aligned} \tag{20}$$

where all corrections to the asymmetries and partial widths have been applied. The χ^2/d.o.f. is $51/(87-12)$. The corresponding correlation matrix is given in Table 17.

	$R_{\rm b}^0$	$R_{\rm c}^0$	$A_{\rm FB}^{0,\,{\rm b}}$	$A_{\rm FB}^{0,\,{\rm c}}$
$R_{\rm b}^0$	1.00	−0.15	−0.03	0.01
$R_{\rm c}^0$	−0.15	1.00	0.07	−0.06
$A_{\rm FB}^{0,\,{\rm b}}$	−0.03	0.07	1.00	0.09
$A_{\rm FB}^{0,\,{\rm c}}$	0.01	−0.06	0.09	1.00

Table 17: The correlation matrix for the four electroweak parameters from the 12-parameter fit.

6.2.2 Results of the 14-Parameter Fit to LEP and SLD Data

Including the SLD results for $R_{\rm b}$, $\mathcal{A}_{\rm b}$ and $\mathcal{A}_{\rm c}$ into the fit the following results are obtained:

$$\begin{aligned} R_{\rm b}^0 &= 0.21642 \pm 0.00073 \\ R_{\rm c}^0 &= 0.1674 \pm 0.0038 \\ A_{\rm FB}^{0,\,{\rm b}} &= 0.0988 \pm 0.0020 \\ A_{\rm FB}^{0,\,{\rm c}} &= 0.0692 \pm 0.0037 \\ \mathcal{A}_{\rm b} &= 0.911 \pm 0.025 \\ \mathcal{A}_{\rm c} &= 0.630 \pm 0.026\,, \end{aligned} \tag{21}$$

with a χ^2/d.o.f. of $56/(96-14)$. The corresponding correlation matrix is given in Table 18 and the dominant errors for the electroweak parameters are listed in Table 19.

In deriving these results the parameters $\mathcal{A}_{\rm b}$ and $\mathcal{A}_{\rm c}$ have been treated as independent of the forward-backward asymmetries $A_{\rm FB}^{0,\,{\rm b}}$ and $A_{\rm FB}^{0,\,{\rm c}}$. In Figure 3 the results for $R_{\rm b}^0$ and $R_{\rm c}^0$ are shown compared with the Standard Model expectation.

	$R_{\rm b}^0$	$R_{\rm c}^0$	$A_{\rm FB}^{0,\,{\rm b}}$	$A_{\rm FB}^{0,\,{\rm c}}$	$\mathcal{A}_{\rm b}$	$\mathcal{A}_{\rm c}$
$R_{\rm b}^0$	1.00	−0.14	−0.03	0.01	−0.03	0.02
$R_{\rm c}^0$	−0.14	1.00	0.05	−0.05	0.02	−0.02
$A_{\rm FB}^{0,\,{\rm b}}$	−0.03	0.05	1.00	0.09	0.02	0.00
$A_{\rm FB}^{0,\,{\rm c}}$	0.01	−0.05	0.09	1.00	−0.01	0.03
$\mathcal{A}_{\rm b}$	−0.03	0.02	0.02	−0.01	1.00	0.15
$\mathcal{A}_{\rm c}$	0.02	−0.02	0.00	0.03	0.15	1.00

Table 18: The correlation matrix for the six electroweak parameters from the 14-parameter fit.

The 14 parameter fit yields the $\rm b \to \ell$ branching ratio:

$$\mathrm{BR}(\mathrm{b} \to \ell) \;=\; 0.1062 \pm 0.0017. \tag{22}$$

The dominant error sources on this quantity are the dependences on the semileptonic decay models $\rm b \to \ell$, $\rm c \to \ell$ with

$$\begin{aligned} \Delta\mathrm{BR}(\mathrm{b} \to \ell)(\mathrm{b} \to \ell\mathrm{model}) &= 0.0006, \\ \Delta\mathrm{BR}(\mathrm{b} \to \ell)(\mathrm{c} \to \ell\mathrm{model}) &= 0.0006. \end{aligned}$$

Extensive studies have been made to understand the size of these errors. If only the measurements of $\mathrm{BR}(\mathrm{b} \to \ell)$ are combined a consistent result is obtained with modelling errors of 0.0008 and 0.0007.

	R_b^0 (10^{-3})	R_c^0 (10^{-3})	$A_{FB}^{0,b}$ (10^{-3})	$A_{FB}^{0,c}$ (10^{-3})	$\mathcal{A}_b$ (10^{-2})	$\mathcal{A}_c$ (10^{-2})
statistics	0.46	2.6	1.8	3.2	1.8	2.0
internal systematics	0.32	2.3	0.8	1.5	1.7	1.6
QCD effects	0.21	0.2	0.2	0.1	0.5	0.2
BR(D $\rightarrow$ neut.)	0.17	0.1	0	0	0	0
D decay multiplicity	0.10	0.3	0	0	0	0
BR($D^+ \rightarrow K^-\pi^+\pi^+$)	0.11	0.4	0.1	0	0	0
BR($D_s \rightarrow \phi\pi^+$)	0.03	0.9	0.1	0	0	0
BR($\Lambda_c \rightarrow$p $K^-\pi^+$)	0.06	0.8	0	0.1	0	0
D lifetimes	0.07	0.2	0	0.1	0	0
gluon splitting	0.28	0.7	0	0.2	0.1	0.1
c fragmentation	0.08	0.4	0.1	0.1	0.1	0.1
light quarks	0.08	0.3	0.5	0.1	0	0
total	0.73	3.8	2.0	3.7	2.5	2.6

Table 19: The dominant error sources for the electroweak parameters from the 14-parameter fit.

The reduction of the modelling uncertainty is due to the inclusion of asymmetry measurements using different methods. Those using leptons depend on the semileptonic decay models while those using a lifetime tag and jet charge or D mesons do not. The mutual consistency of the asymmetry measurements effectively constrains the semileptonic decay models, and reduces the uncertainty in the semileptonic branching ratio.

The result of the full fit to the LEP+SLC results including the off-peak asymmetries and the non-electroweak parameters can be found in Appendix A. It should be noted that the results for the non-electroweak parameters are independent of the treatment of the off-peak asymmetries and the SLD data.

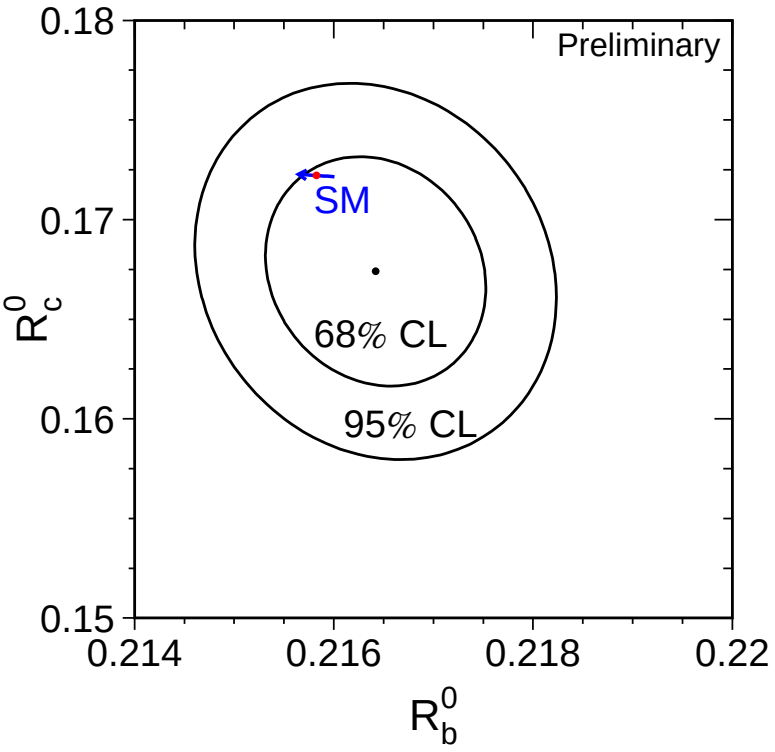

Figure 3: Contours in the R_b^0-R_c^0 plane derived from the LEP+SLD data, corresponding to 68% and 95% confidence levels assuming Gaussian systematic errors. The Standard Model prediction for $m_t = 174.3 \pm 5.1$ GeV is also shown. The arrow points in the direction of increasing values of m_t.

7 The Hadronic Charge Asymmetry $\langle Q_{\rm FB} \rangle$

Updates with respect to last summer:
L3 have published their result.

The LEP experiments ALEPH [75–77], DELPHI [78, 79], L3 [60] and OPAL [80, 81] have provided measurements of the hadronic charge asymmetry based on the mean difference in jet charges measured in the forward and backward event hemispheres, $\langle Q_{\rm FB} \rangle$. DELPHI have also provided a related measurement of the total charge asymmetry by making a charge assignment on an event-by-event basis and performing a likelihood fit [78]. The experimental values quoted for the average forward-backward charge difference, $\langle Q_{\rm FB} \rangle$, cannot be directly compared as some of them include detector dependent effects such as acceptances and efficiencies. Therefore the effective electroweak mixing angle, $\sin^2\theta^{\rm lept}_{\rm eff}$, as defined in Section 10.4, is used as a means of combining the experimental results summarised in Table 20.

Experiment		$\sin^2\theta^{\rm lept}_{\rm eff}$
ALEPH	(90-94), final	$0.2322 \pm 0.0008 \pm 0.0011$
DELPHI	(91-94), prel.	$0.2311 \pm 0.0010 \pm 0.0014$
L3	(91-95), final	$0.2327 \pm 0.0012 \pm 0.0013$
OPAL	(91-94), prel.	$0.2326 \pm 0.0012 \pm 0.0013$
LEP Average		0.2321 ± 0.0010

Table 20: Summary of the determination of $\sin^2\theta^{\rm lept}_{\rm eff}$ from inclusive hadronic charge asymmetries at LEP. For each experiment, the first error is statistical and the second systematic. The latter is dominated by fragmentation and decay modelling uncertainties.

The dominant source of systematic error arises from the modelling of the charge flow in the fragmentation process for each flavour. All experiments measure the required charge properties for $\mathrm{Z} \to \mathrm{b\overline{b}}$ events from the data. ALEPH also determines the charm charge properties from the data. The fragmentation model implemented in the JETSET Monte Carlo program [82] is used by all experiments as reference; the one of the HERWIG Monte Carlo program [83] is used for comparison. The JETSET fragmentation parameters are varied to estimate the systematic errors. The central values chosen by the experiments for these parameters are, however, not the same. The smaller of the two fragmentation errors in any pair of results is treated as common to both. The present average of $\sin^2\theta^{\rm lept}_{\rm eff}$ from $\langle Q_{\rm FB} \rangle$ and its associated error are not very sensitive to the treatment of common uncertainties. The ambiguities due to QCD corrections may cause changes in the derived value of $\sin^2\theta^{\rm lept}_{\rm eff}$. These are, however, well below the fragmentation uncertainties and experimental errors. The effect of fully correlating the estimated systematic uncertainties from this source between the experiments has a negligible effect upon the average and its error.

There is also some correlation between these results and those for $A^{\rm b\bar{b}}_{\rm FB}$ using jet charges. The dominant source of correlation is again through uncertainties in the fragmentation and decay models used. The typical correlation between the derived values of $\sin^2\theta^{\rm lept}_{\rm eff}$ from the $\langle Q_{\rm FB} \rangle$ and the $A^{\rm b\bar{b}}_{\rm FB}$ jet charge measurements has been estimated to be about 20% to 25%. This leads to only a small change in the relative weights for the $A^{\rm b\bar{b}}_{\rm FB}$ and $\langle Q_{\rm FB} \rangle$ results when averaging their $\sin^2\theta^{\rm lept}_{\rm eff}$ values (Section 10.4). Furthermore, the jet charge method contributes at most half of the weight of the $A^{\rm b\bar{b}}_{\rm FB}$ measurement. Thus, the correlation between $\langle Q_{\rm FB} \rangle$ and $A^{\rm b\bar{b}}_{\rm FB}$ from jet charge will have little impact on the overall Standard Model fit, and is neglected at present.

8 Measurement of W Boson Properties at LEP-II

Updates with respect to last summer:
There are new results on the WW cross section, the W mass and the Triple Gauge Boson couplings at 189 GeV. The W decay branching ratios have been updated.

In 1996 the energy of LEP was increased in two steps to 161 GeV and 172 GeV, allowing the production of W boson pairs. In 1997 and 1998, the energy was further increased to 183 and 189 GeV, respectively. The data recorded at 161 GeV, which is just above the pair production threshold, was used to determine the W mass by comparing the measured cross section with the predicted cross section. At higher energies, the mass is determined by directly reconstructing the decay products of the W bosons. In addition, the data at all energies have been used to determine other properties, such as the W decay branching ratios and the couplings of the W to other bosons.

In 1998, at an average centre-of-mass energy of 188.6 GeV [84], the average integrated luminosity collected per experiment is approximately 172 pb^{-1}.

All LEP experiments have final measurements of the WW cross section at 183 GeV [85–88] and preliminary results at 189 GeV [89–92].

All LEP experiments have final W mass results based on the combined 172 GeV and 183 GeV data [93–96]; in addition ALEPH has a preliminary update from an analysis of the fully leptonic channel [97]. All LEP experiments [98–101] have produced preliminary W mass results based on data collected at a centre-of-mass energy of 188.6 GeV in 1998.

8.1 WW cross sections

Table 21 summarises the W-pair cross section (CC03) values, assuming Standard Model decay branching ratios for the W decays, obtained by ALEPH, DELPHI, L3 and OPAL. The LEP average for the different centre-of-mass energies is also given in the table. In the averaging procedure, the QCD component of the systematic errors from each individual measurement has been taken as correlated between experiments. The average WW cross section at 182.67 GeV centre-of-mass energy [102] is 15.83 ± 0.36 pb, with a χ^2 per degree of freedom of 1.49/3; the common error amounts to 0.10 pb. At a preliminary mean centre-of-mass energy of 188.63 GeV [84], the averaged WW cross section is 16.05 ± 0.22 pb, with a χ^2 per degree of freedom of 2.94/3; the common error amounts to 0.08 pb. Figure 4 shows the evolution of the W-pair cross section with centre-of-mass energy.

From the cross sections for the individual W decay channels measured by the four experiments (at all centre-of-mass energies up to 189 GeV), the W decay branching ratios have been determined, with and without the assumption of lepton universality (Table 22). Correlated errors between the individual channels have been taken into account.

Due to cross-contaminations in the identification of W decays, BR($\mathrm{W} \to \tau\nu$) is 24% anti-correlated with each of the other two leptonic branching ratios, while BR($\mathrm{W} \to \mu\nu$) and BR($\mathrm{W} \to \mathrm{e}\nu$) are less than 1.0% correlated. Under the assumption of lepton universality, the measured hadronic W decay branching ratio is $67.96 \pm 0.41\%$ and the leptonic one is $10.68 \pm 0.13\%$.

Within the Standard Model the branching ratios of the W boson depend on the six elements of the Cabibbo-Kobayashi-Maskawa quark-mixing matrix (V_{CKM}) not involving the top quark and on

Experiment	$\sigma_{W^+W^-}$ (pb)		
	172.12 GeV (final)	182.67 GeV (final)	188.63 GeV (preliminary)
ALEPH	$11.7 \pm 1.2 \pm 0.3$	$15.57 \pm 0.62 \pm 0.29$	$15.69 \pm 0.34 \pm 0.17$
DELPHI	$11.58^{+1.4}_{-1.3} \pm 0.32$	$15.86 \pm 0.69 \pm 0.26$	$15.79 \pm 0.38 \pm 0.31$
L3	$12.27^{+1.4}_{-1.3} \pm 0.23$	$16.53 \pm 0.67 \pm 0.26$	$16.20 \pm 0.37 \pm 0.27$
OPAL	$12.3 \pm 1.3 \pm 0.3$	$15.43 \pm 0.61 \pm 0.26$	$16.55 \pm 0.35 \pm 0.20$
LEP Average	12.0 ± 0.7	15.83 ± 0.36	16.05 ± 0.22

Table 21: The measurements of the W-pair cross sections by the four LEP experiments from 172.12 to 188.63 GeV. The first error is statistical and the second is the total systematic error

Experiment	BR(W$\to$eν)	BR(W$\to \mu\nu$)	BR(W$\to \tau\nu$)	BR(W$\to$hadrons)
ALEPH	$11.34 \pm 0.46 \pm 0.17$	$11.29 \pm 0.44 \pm 0.15$	$10.48 \pm 0.56 \pm 0.22$	$66.89 \pm 0.67 \pm 0.31$
DELPHI	$10.11 \pm 0.53 \pm 0.28$	$10.86 \pm 0.48 \pm 0.22$	$11.14 \pm 0.72 \pm 0.36$	$67.96 \pm 0.73 \pm 0.58$
L3	$10.31 \pm 0.44 \pm 0.17$	$9.95 \pm 0.46 \pm 0.17$	$11.20 \pm 0.63 \pm 0.25$	$68.69 \pm 0.68 \pm 0.39$
OPAL	$10.52 \pm 0.42 \pm 0.15$	$10.47 \pm 0.40 \pm 0.13$	$10.69 \pm 0.51 \pm 0.22$	$68.34 \pm 0.61 \pm 0.31$
LEP Average	10.61 ± 0.25	10.65 ± 0.24	10.82 ± 0.32	67.96 ± 0.41

Table 22: Preliminary measurements of the W decay branching ratios in percent. The hadronic branching ratio is determined assuming lepton universality. There are large correlations between the individual leptonic branching ratios, which have been taken into account in determining the hadronic branching ratio. The first error is statistical and the second is the total systematic error.

α_s. Using the current world-average values and errors of the other matrix elements not assuming the unitarity of V_{CKM} [104], and from the world average value of $\alpha_s(m_W^2) = 0.121 \pm 0.002$ [104], a constraint on the least well measured CKM matrix element is obtained:

$$|V_{cs}| \quad = \quad 0.997 \pm 0.020. \tag{23}$$

The error includes the errors on α_s and the other V_{CKM} elements but is dominated by the statistical error (0.016) on the W branching fractions. The element V_{cs} is also determined by counting charm and strange jets in W decays; details are given in References 105–108.

8.2 W mass measurement

Examples of the invariant mass distributions of the reconstructed decay products of W bosons from the four experiments at 189 GeV are shown in Figure 5. The data have been analysed in terms of all W-pair final states, $q\bar{q}q\bar{q}$, $q\bar{q}\ell\nu$ and $\ell\nu\ell\nu$. The first is referred to as 4q and the latter two are collectively referred to as non-4q. Table 23 summarises the W mass values measured by each experiment [98–101] at this centre-of-mass energy.

A combined W mass measurement has been obtained from the results of the four LEP experiments in the 4q and non-4q decay channels at each individual centre of mass energy (172, 183 and 189 GeV; L3 combined 172 and 183 GeV). There are 22 measurements in total. Correlations of systematic errors between channels and between experiments have been taken into account in the averaging procedure. Five different sources of systematic errors have been considered:

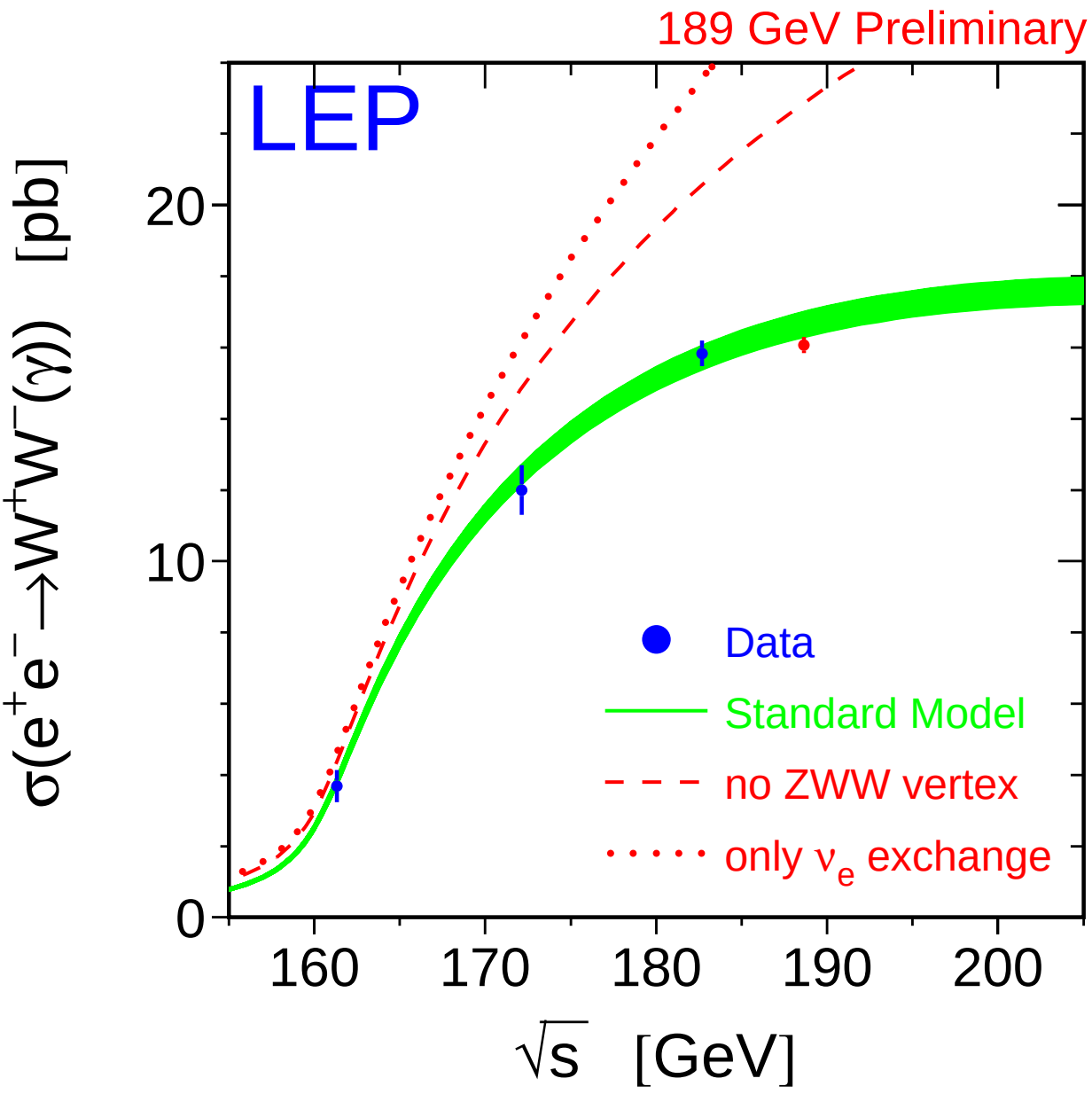

Figure 4: The W-pair cross section as a function of the centre-of-mass energy. The data points are the LEP averages. Also shown is the Standard Model prediction [103] (shaded area) with a possible theoretical uncertainty of ±2% on the calculations, and for comparison the cross section if the ZWW coupling did not exist (dashed line), or if only the t-channel ν_e exchange diagram existed (dotted line).

1. Systematic errors uncorrelated between channels and experiments,

2. Systematic errors correlated within an experiment between channels but uncorrelated with other experiments, such as detector calibration and simulation,

Experiment	m_W (GeV)		
	non-4q	4q	combined
ALEPH (prel.)	$80.406 \pm 0.114 \pm 0.033$	$80.561 \pm 0.116 \pm 0.077$	$80.472 \pm 0.081 \pm 0.050$
DELPHI (prel.)	$80.163 \pm 0.174 \pm 0.067$	$80.467 \pm 0.110 \pm 0.067$	$80.370 \pm 0.093 \pm 0.054$
L3 (prel.)	$80.133 \pm 0.140 \pm 0.080$	$80.610 \pm 0.126 \pm 0.118$	$80.353 \pm 0.093 \pm 0.082$
OPAL (prel.)	$80.366 \pm 0.111 \pm 0.055$	$80.315 \pm 0.112 \pm 0.094$	$80.345 \pm 0.080 \pm 0.055$

Table 23: The (preliminary) measurements of m_W at 189 GeV in the $q\bar{q}\ell\nu$, $q\bar{q}q\bar{q}$ and combined channels, for the four experiments and the LEP average. In this table, the first error is statistical and the second is the total systematic error which includes the LEP energy uncertainty.

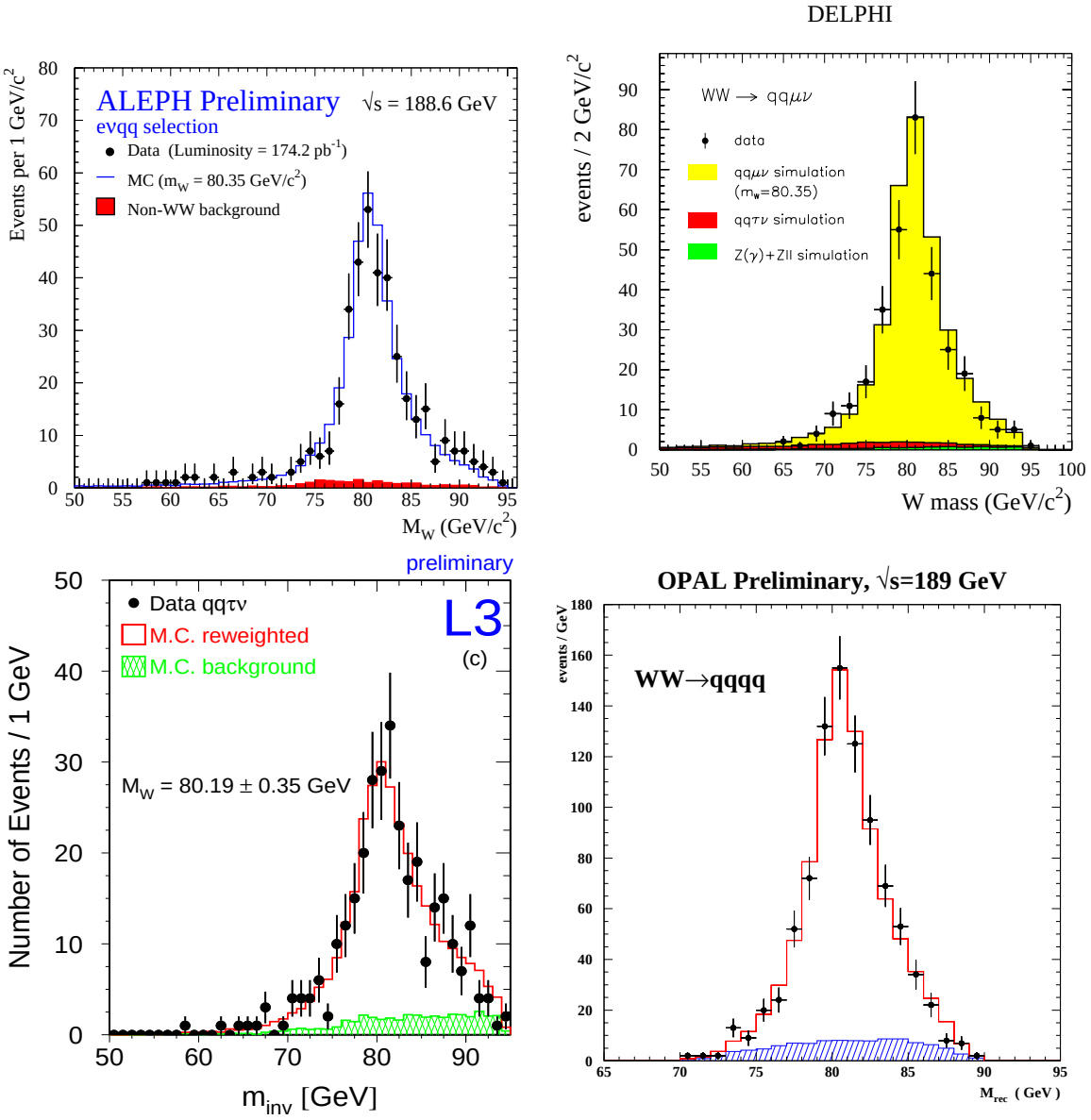

Figure 5: Examples of reconstructed W mass distributions from the four LEP experiments at 189 GeV.

3. Systematic uncertainties associated to Final State Interactions (Bose-Einstein and Colour Reconnection effects) which affect the 4q channel only,

4. Systematic uncertainties arising from ISR and fragmentation effects have been considered to be correlated between different channels and different experiments,

5. The LEP energy error [102] and its correlation between years have also been considered.

Using different models, all experiments have evaluated the uncertainty on the W mass from Final State Interactions. In table 24 are summarised the W mass measurements from direct reconstructiuon from the four LEP experiments in the non-4q and 4q channels.

Experiment	m_{W} (GeV)	
	non-4q	4q
ALEPH (prel.)	80.343 ± 0.098	80.561 ± 0.121
DELPHI (prel.)	80.297 ± 0.155	80.367 ± 0.115
L3 (prel.)	80.224 ± 0.135	80.656 ± 0.156
OPAL (prel.)	80.362 ± 0.105	80.345 ± 0.134
LEP Average	80.313 ± 0.063	80.429 ± 0.089

Table 24: Summary of W mass measurements by direct reconstruction (from 172 to 189 GeV) from the four LEP experiments in the non-4q and the 4q channels

The combined W mass measurement derived from the non-4q channels is

$$m_{\mathrm{W}}^{\text{non-4q}} = 80.313 \pm 0.052(\text{stat.}) \pm 0.032(\text{syst.}) \pm 0.017(\text{LEP}) \text{ GeV}. \tag{24}$$

The combined W mass measurement from the fully hadronic channel is

$$m_{\mathrm{W}}^{\text{4q}} = 80.429 \pm 0.049(\text{stat.}) \pm 0.043(\text{syst.}) \pm 0.058(\text{FSI}) \pm 0.017(\text{LEP}) \text{ GeV}. \tag{25}$$

The total errors of these two mass measurements are 25% correlated and the χ^2 per degree of freedom is 17.9/20.

The difference between the 4q and the non-4q masses has been determined to be $\Delta(m_{\mathrm{W}}^{\text{4q}} - m_{\mathrm{W}}^{\text{non-4q}}) = 152 \pm 74$ MeV, neglecting the FSI uncertainty which amounts to 58 MeV (the χ^2 per degree of freedom is 18.3/20). At the current level of accuracy there is no significant difference between the W mass determined from the two channels.

The combined mass value from all channels is

$$m_{\mathrm{W}}^{\text{4f}} = 80.347 \pm 0.036(\text{stat.}) \pm 0.036(\text{syst.}) \pm 0.020(\text{FSI}) \pm 0.017(\text{LEP}) \text{ GeV}; \tag{26}$$

the χ^2 per degree of freedom is 19.4/21.

The W mass measurement from direct reconstruction is combined with the W mass determination from the WW cross section at threshold ($80.400 \pm 0.220 \pm 0.025(\text{LEP})$ GeV [109]), yielding

$$m_{\mathrm{W}}^{\text{LEP}} = 80.350 \pm 0.056 \text{ GeV} \tag{27}$$

as the current LEP-II average W mass.

8.3 TGC

The W^+W^- production process involves the triple gauge boson vertices between the W^+W^- and the Z or photon. The four LEP experiments have already combined [110], together with DØ, preliminary and published [111–115] measurements of coupling parameters.

The parametrization of TGCs is described in References 116–121. Assuming electromagnetic gauge invariance and C and P conservation there are five free parameters. One common set is $\{g_1^z, \kappa_z, \kappa_\gamma, \lambda_z, \lambda_\gamma\}$ where $g_1^z = \kappa_z = \kappa_\gamma = 1$ and $\lambda_z = \lambda_\gamma = 0$ in the Standard Model.

The LEP collaborations agreed to express their results directly through the parameters Δg_1^z, $\Delta\kappa_\gamma$, λ_γ, imposing the constraints [121]

$$\Delta\kappa_z = -\Delta\kappa_\gamma \tan^2\theta_W + \Delta g_1^z, \quad (28)$$

$$\lambda_z = \lambda_\gamma \quad (29)$$

where Δ indicates the deviation of the respective quantity from its Standard Model value (and therefore are all zero in this context), and θ_W is the electroweak mixing angle.

Anomalous TGCs can affect both the total production cross section and the shape of the differential cross section as a function of the W^- production angle in W pair production. The relative contributions of each helicity state of the W bosons are also changed, which in turn affects the distributions of their decay products. Results from $e\nu W$ ("single W") and $\nu\bar{\nu}\gamma$ production have also been included. Single W production has a particular sensitivity to κ_γ and therefore provides complementary information to W pair production. The analyses presented by each experiment make use of different combinations of these quantities. The results presented here use measurements of all three parameters Δg_1^z, $\Delta\kappa_\gamma$ and λ_γ, by ALEPH, DELPHI, L3 and OPAL. In each case, the individual references should be consulted for details.

The method followed for the combination is the same as that used previously [110]. Single and double parameter fits are performed. In the first case, the values of all the parameters are set to their Standard Model values, except the one to be measured. The results from each experiment and the combined results are shown in Table 25. The combined results are also shown in Figure 6. The value of each TGC parameter given in the table is consistent with the expectation of the Standard Model.

The results of fits to data in which two parameters were allowed to vary are shown in Table 26 for each of the four LEP experiments and combined. The combinations of the two-dimensional likelihood distributions result in the 68% C.L. and 95% C.L. contours, as shown in Figure 7, for example. The 68% C.L. contours are obtained by requiring $\Delta \log \mathcal{L} = +1.15$, while for the 95% C.L. contours a value $\Delta \log \mathcal{L} = +3.0$ is required.

	Δg_1^z	$\Delta\kappa_\gamma$	λ_γ
ALEPH [111]	$0.00^{+0.06}_{-0.06}$	$-0.01^{+0.14}_{-0.11}$	$-0.05^{+0.07}_{-0.06}$
DELPHI [112]	$-0.02^{+0.07}_{-0.06}$	$0.23^{+0.16}_{-0.18}$	$0.02^{+0.08}_{-0.08}$
L3 [113]	$-0.02^{+0.07}_{-0.07}$	$-0.18^{+0.14}_{-0.13}$	$0.00^{+0.08}_{-0.07}$
OPAL [114]	$-0.01^{+0.08}_{-0.07}$	$0.00^{+0.27}_{-0.19}$	$-0.11^{+0.08}_{-0.07}$
68% C.L.	$-0.01^{+0.03}_{-0.03}$	$0.04^{+0.08}_{-0.08}$	$-0.04^{+0.04}_{-0.04}$
95% C.L. interval	$[-0.07, \quad 0.06]$	$[-0.11, \quad 0.20]$	$[-0.10, \quad 0.03]$

Table 25: The combined 68% C.L. errors and 95% confidence intervals obtained after combination (last two rows) of the results from the four LEP experiments.

	Δg_1^z $\Delta\kappa_\gamma$	$\Delta\kappa_\gamma$ λ_γ	Δg_1^z λ_γ
ALEPH [111]	$0.03^{+0.06}_{-0.06}$ $-0.05^{+0.13}_{-0.11}$	$0.07^{+0.12}_{-0.11}$ $-0.07^{+0.06}_{-0.06}$	$-0.02^{+0.07}_{-0.07}$ $-0.02^{+0.08}_{-0.07}$
DELPHI [112]	$-0.03^{+0.07}_{-0.06}$ $0.28^{+0.15}_{-0.16}$	$0.20^{+0.16}_{-0.15}$ $0.02^{+0.09}_{-0.08}$	$-0.03^{+0.09}_{-0.09}$ $0.04^{+0.11}_{-0.11}$
L3 [113]	$0.00^{+0.07}_{-0.07}$ $-0.13^{+0.17}_{-0.14}$	$-0.14^{+0.17}_{-0.14}$ $0.03^{+0.08}_{-0.08}$	$-0.05^{+0.11}_{-0.11}$ $0.04^{+0.12}_{-0.11}$
OPAL [114]	$-0.13^{+0.08}_{-0.06}$ $0.62^{+0.31}_{-0.33}$	$0.66^{+0.27}_{-0.72}$ $-0.20^{+0.08}_{-0.07}$	$0.14^{+0.10}_{-0.11}$ $-0.23^{+0.10}_{-0.09}$
68% C.L.	$0.00^{+0.04}_{-0.04}$ $0.04^{+0.10}_{-0.09}$	$0.09^{+0.09}_{-0.08}$ $-0.05^{+0.04}_{-0.04}$	$0.00^{+0.05}_{-0.05}$ $-0.03^{+0.05}_{-0.05}$
95% C.L. interval	$[-0.09, \quad 0.07]$ $[-0.12, \quad 0.24]$	$[-0.07, \quad 0.26]$ $[-0.12, \quad 0.03]$	$[-0.09, \quad 0.09]$ $[-0.13, \quad 0.07]$
Correlation	-0.49	-0.41	-0.71

Table 26: The combined 68% C.L. errors and 95% C.L. intervals obtained after combination (last two rows) of the results from the four LEP experiments. The two listed parameters are varied while the third one is fixed to its SM value. Both statistical and systematic errors are included.

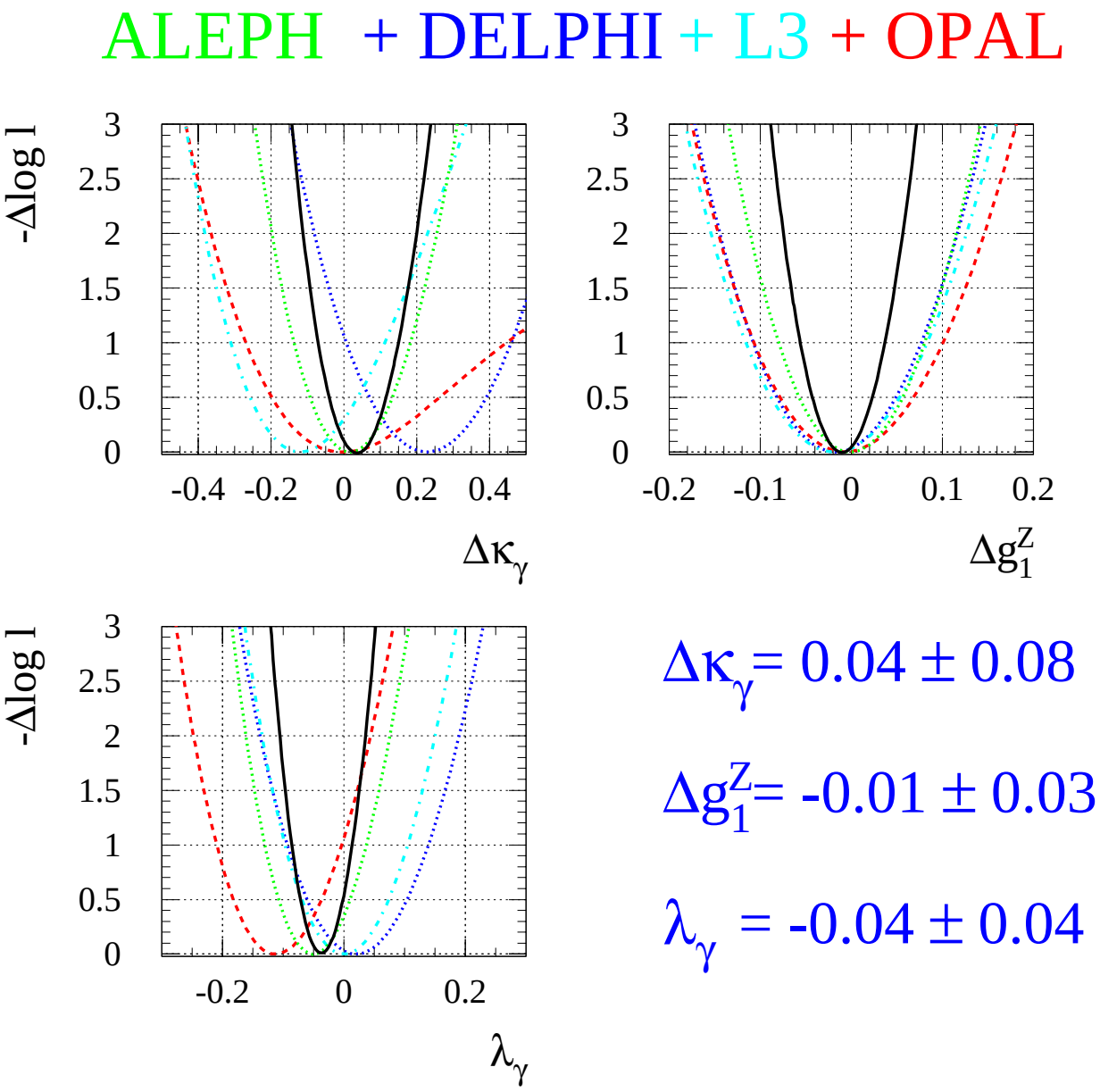

Figure 6: Results for the three couplings from the individual experiments (dashed lines) and the combination (solid lines).

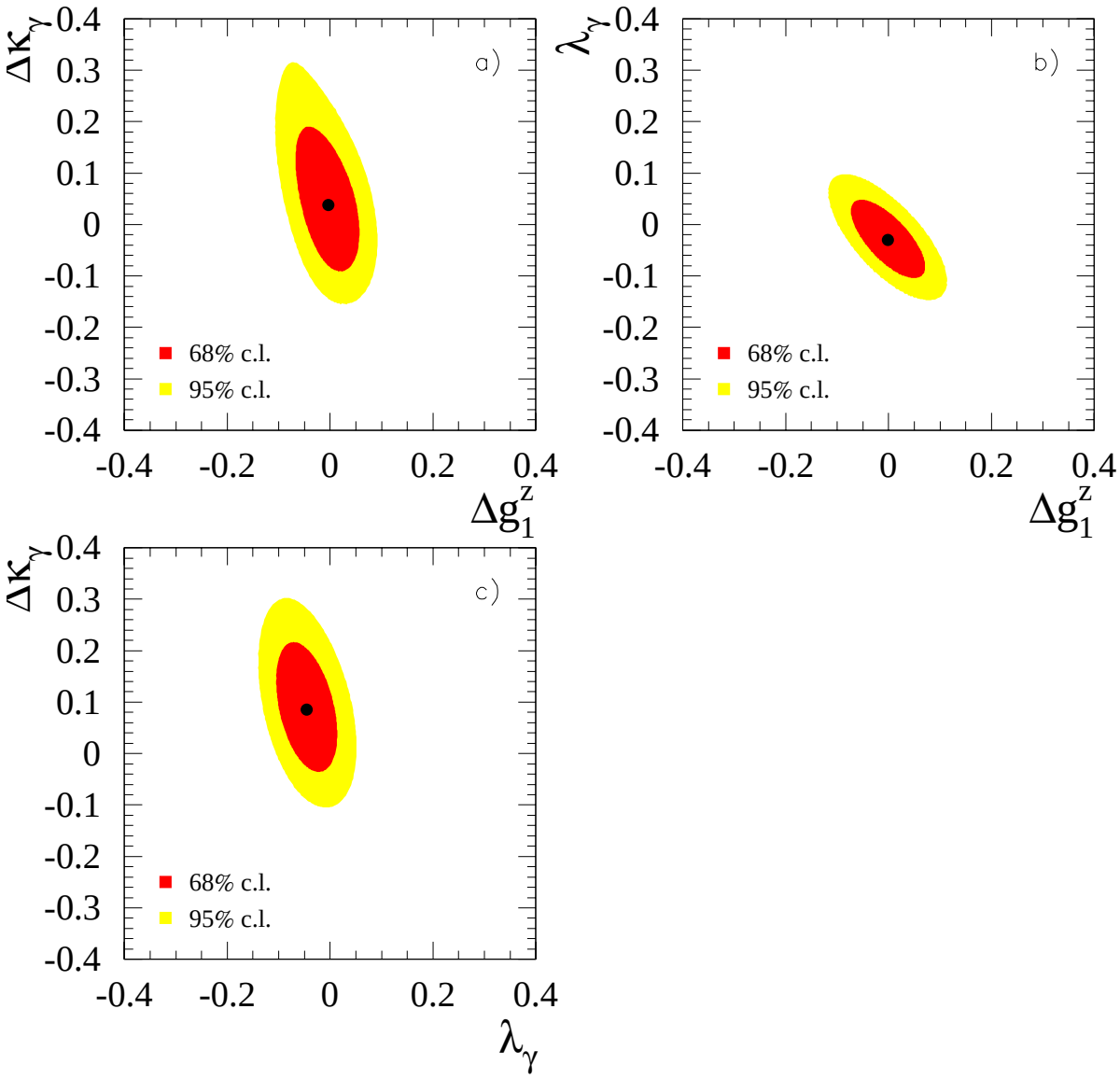

Figure 7: The 68% C.L. and 95% C.L. contours in the parameter spaces $\Delta\kappa_\gamma$-Δg_1^z, λ_γ-Δg_1^z, $\Delta\kappa_\gamma$-λ_γ obtained from the sum of the log-likelihood distributions from the individual experiments, plotting the contours at $\Delta \log \mathcal{L} = 1.15$ and $\Delta \log \mathcal{L} = 3.0$, respectively.

9 Measurement of the ZZ production cross section

Updates with respect to last summer:
This is a new section.

At center-of-mass energies above twice the Z boson mass, the production of pairs of Z bosons is possible. The Z boson pair production cross section has been measured at centre-of-mass energies of 183 [122] and 189 GeV [123–126]. Table 27 summarises the Z-pair cross section (NC02) values, assuming Standard Model decay branching ratios for the Z decays, obtained by ALEPH, DELPHI, L3 and OPAL. The LEP average for the different centre-of-mass energies is also given in the table. In the averaging procedure the following uncertainties have been taken as correlated between experiments: 5% on the QCD 4-jet rate, 2% on the WW rate. The average ZZ cross section at 183 GeV centre-of-mass energy is 0.17 ± 0.09 pb, with a χ^2 per degree of freedom of 0.83/2; the common error amounts to 0.01 pb. At 189 GeV the averaged ZZ cross section is 0.70 ± 0.08 pb, with a χ^2 per degree of freedom of 0.65/3; the common error amounts to 0.02 pb. Figure 8 shows the evolution of the Z-pair cross section with centre-of-mass energy.

Experiment	σ_{ZZ} (pb)	
	182.67 GeV (preliminary)	188.63 GeV (preliminary)
ALEPH	$0.11^{+0.16}_{-0.11} \pm 0.04$	$0.67 \pm 0.13 \pm 0.04$
DELPHI		$0.58 \pm 0.17 \pm 0.06$
L3	$0.31^{+0.16+0.07}_{-0.15-0.03}$	$0.75^{+0.15}_{-0.14} \pm 0.03$
OPAL	$0.12^{+0.20+0.03}_{-0.18-0.02}$	$0.76^{+0.14+0.06}_{-0.13-0.05}$
LEP Average	0.17 ± 0.09	0.70 ± 0.08

Table 27: The measurements of the Z-pair cross sections by the four LEP experiments from 183 to 189 GeV. The first error is statistical and the second is the total systematic error.

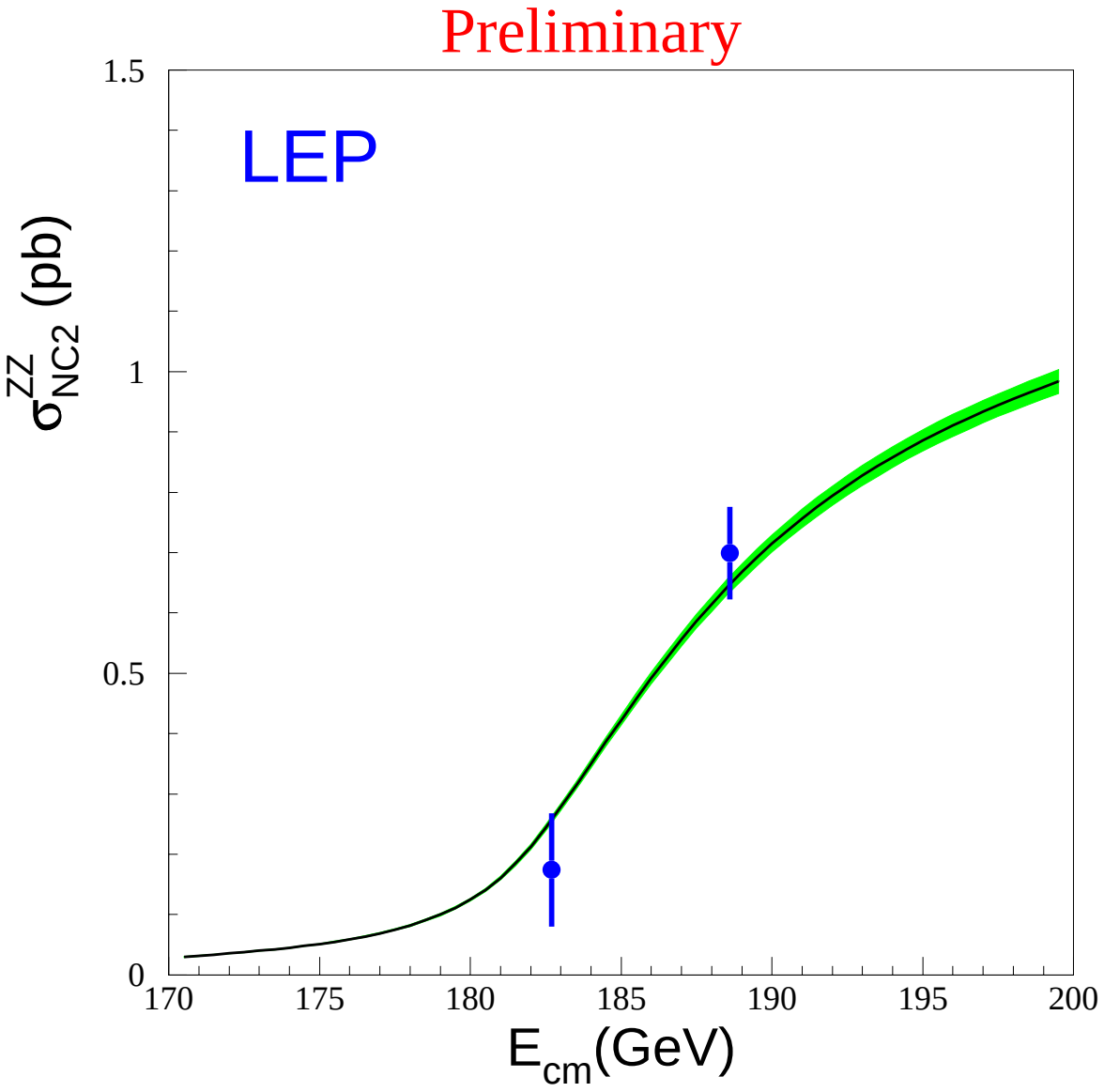

Figure 8: The Z-pair cross section as a function of the centre-of-mass energy. The data points are the LEP averages. Also shown is the Standard Model prediction [127] (shaded area) with a possible theoretical uncertainy of ±2% on the calculations.

10 Interpretation of Results

Updates with respect to last summer:
For the Standard Model fits, new versions of the analytical programs which incorporate higher-order corrections have been used.

10.1 Number of Neutrino Species

An important aspect of our measurement concerns the information related to Z decays into invisible channels. Using the results of Tables 7 and 8, the ratio of the Z decay width into invisible particles and the leptonic decay width is determined:

$$\Gamma_{\rm inv}/\Gamma_{\ell\ell} \quad = \quad 5.941 \pm 0.016\,. \tag{30}$$

The Standard Model value for the ratio of the partial widths to neutrinos and charged leptons is:

$$(\Gamma_{\nu\nu}/\Gamma_{\ell\ell})_{\rm SM} \quad = \quad 1.9912 \pm 0.0012\,. \tag{31}$$

The central value is evaluated for $m_{\rm Z} = 91.1869$ GeV and the error quoted accounts for a variation of $m_{\rm t}$ in the range $m_{\rm t} = 174.3 \pm 5.1$ GeV and a variation of $m_{\rm H}$ in the range 95 GeV $\leq m_{\rm H} \leq$ 1000 GeV. The number of light neutrino species is given by the ratio of the two expressions listed above:

$$N_\nu \quad = \quad 2.9835 \pm 0.0083, \tag{32}$$

which is 2 standard deviations below the expected value of 3.

Alternatively, one can assume 3 neutrino species and determine the width from additional invisible decays of the Z. This yields

$$\Delta\Gamma_{\rm inv} \quad = \quad -2.9 \pm 1.7 \text{ MeV}. \tag{33}$$

The negative additional width results from a measured total width that is below the Standard Model expectation. If a conservative approach is taken to limit the result to only positive values of $\Delta\Gamma_{\rm inv}$, then the 95% CL upper limit on additional invisible decays of the Z is

$$\Delta\Gamma_{\rm inv} \quad < \quad 2.0 \text{ MeV}. \tag{34}$$

The uncertainties on N_ν and $\Delta\Gamma_{\rm inv}$ are dominated by the theoretical error on the luminosity. These results have therefore improved due to the improved theoretical calculations on Bhabha scattering [9].

10.2 The Coupling Parameters $\mathcal{A}_{\rm f}$

The coupling parameters $\mathcal{A}_{\rm f}$ are defined in terms of the effective vector and axial-vector neutral current couplings of fermions (Equation (4)). The LEP measurements of the forward-backward asymmetries of charged leptons (Section 2) and b and c quarks (Section 6) determine the products $A_{\rm FB}^{0,\rm f} = \frac{3}{4}\mathcal{A}_{\rm e}\mathcal{A}_{\rm f}$ (Equation (3)). The LEP measurements of the τ polarisation (Section 4), $\mathcal{P}_\tau(\cos\theta)$, determine $\mathcal{A}_\tau$ and $\mathcal{A}_{\rm e}$ separately (Equation (7)).

Table 28 shows the results for the leptonic coupling parameter $\mathcal{A}_\ell$ from the LEP and SLD measurements, assuming lepton universality.

	$\mathcal{A}_\ell$	Cumulative Average	χ^2/d.o.f.
$A_{\rm FB}^{0,\ell}$	0.1506 ± 0.0042		
$\mathcal{P}_\tau(\cos\theta)$	0.1450 ± 0.0033	0.1471 ± 0.0026	1.1/1
$\mathcal{A}_\ell$ (SLD)	0.1512 ± 0.0020	0.1497 ± 0.0016	2.6/2

Table 28: Determination of the leptonic coupling parameter $\mathcal{A}_\ell$ assuming lepton universality. The second column lists the $\mathcal{A}_\ell$ values derived from the quantities listed in the first column. The third column contains the cumulative averages of these $\mathcal{A}_\ell$ results. The averages are derived assuming no correlations between the measurements. The χ^2 per degree of freedom for the cumulative averages is given in the last column.

	LEP ($\mathcal{A}_\ell = 0.1471 \pm 0.0026$)	SLD	LEP+SLD ($\mathcal{A}_\ell = 0.1497 \pm 0.0016$)
$\mathcal{A}_{\rm b}$	0.896 ± 0.024	0.911 ± 0.025	0.892 ± 0.016
$\mathcal{A}_{\rm c}$	0.625 ± 0.035	0.630 ± 0.026	0.625 ± 0.021

Table 29: Determination of the quark coupling parameters $\mathcal{A}_{\rm b}$ and $\mathcal{A}_{\rm c}$ from LEP data alone (using the LEP average for $\mathcal{A}_\ell$), from SLD data alone, and from LEP+SLD data (using the LEP+SLD average for $\mathcal{A}_\ell$) assuming lepton universality.

Using the measurements of $\mathcal{A}_\ell$ one can extract $\mathcal{A}_{\rm b}$ and $\mathcal{A}_{\rm c}$ from the LEP measurements of the b and c quark asymmetries. The SLD measurements of the left-right forward-backward asymmetries for b and c quarks are direct determinations of $\mathcal{A}_{\rm b}$ and $\mathcal{A}_{\rm c}$. Table 29 shows the results on the quark coupling parameters $\mathcal{A}_{\rm b}$ and $\mathcal{A}_{\rm c}$ derived from LEP or SLD measurements separately (Equations 20 and 21) and from the combination of LEP+SLD measurements (Equation 21). The LEP extracted values of $\mathcal{A}_{\rm b}$ and $\mathcal{A}_{\rm c}$ are in excellent agreement with the SLD measurements, and in reasonable agreement with the Standard Model predictions (0.935 and 0.668, respectively, essentially independent of $m_{\rm t}$ and $m_{\rm H}$) However, the combination of LEP and SLD of $\mathcal{A}_{\rm b}$ is 2.7 sigma below the Standard Model. This is due to three independent results: the SLD measurement of $\mathcal{A}_{\rm b}$ is low compared to the Standard Model, while the LEP measurement of $A_{\rm FB}^{0,{\rm b}}$ and the combined LEP+SLD measurement of $\mathcal{A}_\ell$ are respectively low and high compared with the Standard Model fit of Table 32. This can be seen in Figure 9.

10.3 The Effective Vector and Axial-Vector Coupling Constants

The partial widths of the Z into leptons and the lepton forward-backward asymmetries (Section 2), the τ polarisation and the τ polarisation asymmetry (Section 4) can be combined to determine the effective vector and axial-vector couplings for e, μ and τ. The asymmetries (Equations (3) and (7)) determine the ratio $g_{V\ell}/g_{A\ell}$ (Equation (4)), while the leptonic partial widths determine the sum of the squares of the couplings:

$$\Gamma_{\ell\ell} \;=\; \frac{G_{\rm F} m_{\rm Z}^3}{6\pi\sqrt{2}}(g_{V\ell}^2 + g_{A\ell}^2)(1+\delta_\ell^{QED})\,, \tag{35}$$

where $\delta_\ell^{QED} = 3q_\ell^2\alpha(m_{\rm Z}^2)/(4\pi)$ accounts for final state photonic corrections. Corrections due to lepton masses, neglected in Equation 35, are taken into account for the results presented below.

The averaged results for the effective lepton couplings are given in Table 30 for both the LEP data alone as well as for the LEP and SLD measurements. Figure 10 shows the 68% probability contours

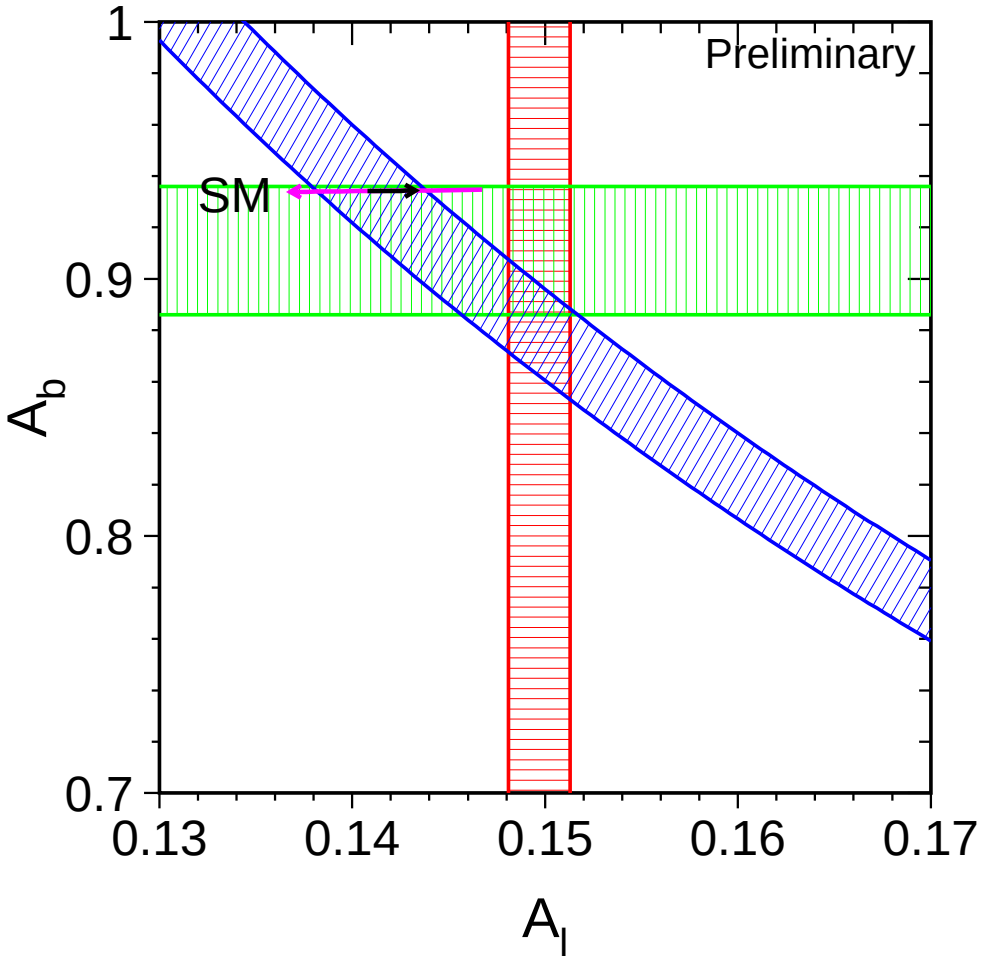

Figure 9: The measurements of the combined LEP+SLD $\mathcal{A}_\ell$ (vertical band), SLD $\mathcal{A}_\mathrm{b}$ (horizontal band) and LEP $A_\mathrm{FB}^{0,\mathrm{b}}$ (diagonal band), compared to the Standard Model expectations (arrows). The arrow pointing to the left shows the variation in the SM prediction for m_H in the range 300^{+700}_{-205} GeV, and the arrow pointing to the right for m_t in the range 174.3 ± 5.1 GeV. It should be noted that although the $A_\mathrm{FB}^{0,\mathrm{b}}$ measurements prefer a high Higgs mass, the Standard Model fit to the full set of measurements prefers a low Higgs mass because of the influence of $\mathcal{A}_\ell$.

in the $g_{A\ell}$-$g_{V\ell}$ plane for the individual lepton species from the LEP data. The signs of $g_{A\ell}$ and $g_{V\ell}$ are based on the convention $g_{A\mathrm{e}} < 0$. With this convention the signs of the couplings of all charged leptons follow from LEP data alone. For comparison, the $g_{V\ell}$-$g_{A\ell}$ relation following from the measurement of $\mathcal{A}_\ell$ from SLD [34] is indicated as a band in the $g_{A\ell}$-$g_{V\ell}$-plane of Figure 10. The measured ratios of the e, μ and τ couplings provide a test of lepton universality and are shown in Table 30. All values are consistent with lepton universality. The combined results assuming universality are also given in the Table and are shown as a solid contour in Figure 10.

The neutrino couplings to the Z can be derived from the measured value of the invisible width of the Z, Γ_inv (see Table 9), attributing it exclusively to the decay into three identical neutrino generations

($\Gamma_{\rm inv} = 3\Gamma_{\nu\nu}$) and assuming $g_{A\nu} \equiv g_{V\nu} \equiv g_\nu$. The relative sign of g_ν is chosen to be in agreement with neutrino scattering data [128], resulting in $g_\nu = +0.50058 \pm 0.00075$.

	Without Lepton Universality:	
	LEP	LEP+SLD
$g_{V\mathrm{e}}$	-0.0375 ± 0.0011	-0.03809 ± 0.00047
$g_{V\mu}$	-0.0374 ± 0.0032	-0.0360 ± 0.0024
$g_{V\tau}$	-0.0365 ± 0.0011	-0.0364 ± 0.0010
$g_{A\mathrm{e}}$	-0.50099 ± 0.00038	-0.50105 ± 0.00036
$g_{A\mu}$	-0.50081 ± 0.00058	-0.50117 ± 0.00054
$g_{A\tau}$	-0.50173 ± 0.00065	-0.50198 ± 0.00064
	Ratios of couplings:	
	LEP	LEP+SLD
$g_{V\mu}/g_{V\mathrm{e}}$	0.998 ± 0.099	0.946 ± 0.065
$g_{V\tau}/g_{V\mathrm{e}}$	0.972 ± 0.042	0.955 ± 0.030
$g_{A\mu}/g_{A\mathrm{e}}$	1.0000 ± 0.0014	1.0002 ± 0.0013
$g_{A\tau}/g_{A\mathrm{e}}$	1.0019 ± 0.0015	1.0019 ± 0.0015
	With Lepton Universality:	
	LEP	LEP+SLD
$g_{V\ell}$	-0.03707 ± 0.00067	-0.03772 ± 0.00041
$g_{A\ell}$	-0.50121 ± 0.00027	-0.50117 ± 0.00027
g_ν	$+0.50085 \pm 0.00075$	$+0.50085 \pm 0.00075$

Table 30: Results for the effective vector and axial-vector couplings derived from the combined LEP data without and with the assumption of lepton universality. For the right column the SLD measurements of $A^0_{\rm LR}$, $\mathcal{A}_\mathrm{e}$, $\mathcal{A}_\mu$ and $\mathcal{A}_\tau$ are also included.

10.4 The Effective Electroweak Mixing Angle $\sin^2\theta^{\rm lept}_{\rm eff}$

The asymmetry measurements from LEP can be combined into a single observable, the effective electroweak mixing angle, $\sin^2\theta^{\rm lept}_{\rm eff}$, defined as:

$$\sin^2\theta^{\rm lept}_{\rm eff} \equiv \frac{1}{4}\left(1 - \frac{g_{V\ell}}{g_{A\ell}}\right), \tag{36}$$

without making strong model-specific assumptions.

For a combined average of $\sin^2\theta^{\rm lept}_{\rm eff}$ from $A^{0,\ell}_{\rm FB}$, $\mathcal{A}_\tau$ and $\mathcal{A}_\mathrm{e}$ only the assumption of lepton universality, already inherent in the definition of $\sin^2\theta^{\rm lept}_{\rm eff}$, is needed. We can also include the hadronic forward-backward asymmetries if we assume the quark couplings to be given by the Standard Model. This is justified within the Standard Model as the hadronic asymmetries $A^{0,\mathrm{b}}_{\rm FB}$ and $A^{0,\mathrm{c}}_{\rm FB}$ have a reduced sensitivity to corrections particular to the quark vertex. The results of these determinations of $\sin^2\theta^{\rm lept}_{\rm eff}$ and their combination are shown in Table 31 and in Figure 11. Also the value derived from the measurements of $\mathcal{A}_\ell$ from SLD is given.

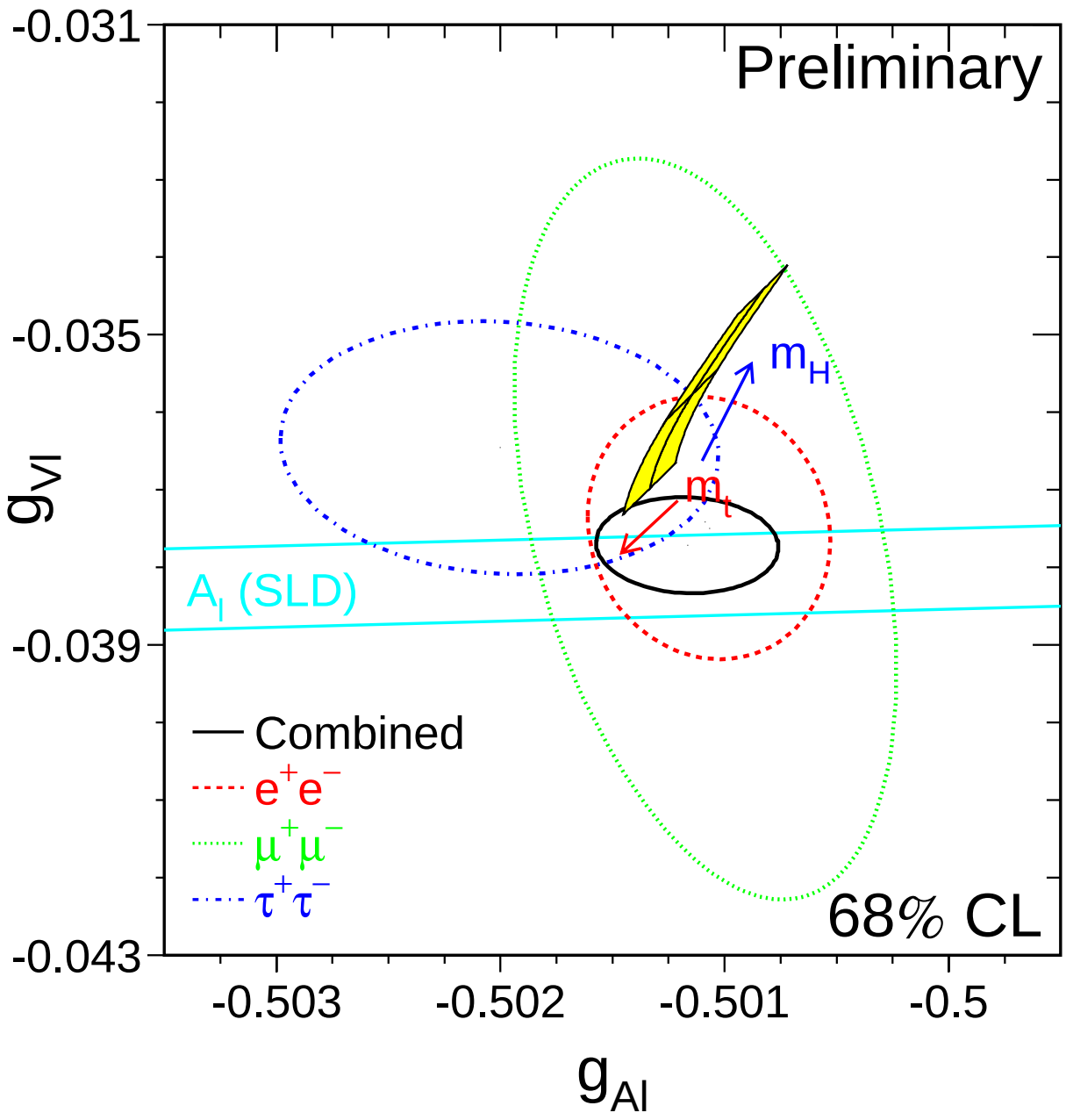

Figure 10: Contours of 68% probability in the $g_{V\ell}$-$g_{A\ell}$ plane from LEP measurements. Also shown is the one standard deviation band resulting from the $\mathcal{A}_\ell$ measurement of SLD. The solid contour results from a fit to the LEP and SLD results assuming lepton universality. The shaded region corresponds to the Standard Model prediction for $m_{\rm t} = 174.3 \pm 5.1$ GeV and $m_{\rm H} = 300^{+700}_{-205}$ GeV. The arrows point in the direction of increasing values of $m_{\rm t}$ and $m_{\rm H}$.

	$\sin^2\theta^{\rm lept}_{\rm eff}$	Average by Group of Observations	Cumulative Average	χ^2/d.o.f.
$A^{0,\ell}_{\rm FB}$	0.23107 ± 0.00053			
$\mathcal{A}_\tau$	0.23210 ± 0.00056			
$\mathcal{A}_{\rm e}$	0.23136 ± 0.00065	0.23151 ± 0.00034	0.23151 ± 0.00034	1.8/2
$A^{0,\rm b}_{\rm FB}$	0.23228 ± 0.00036			
$A^{0,\rm c}_{\rm FB}$	0.23255 ± 0.00086	0.23232 ± 0.00034	0.23191 ± 0.00024	4.7/4
$\langle Q_{\rm FB}\rangle$	0.2321 ± 0.0010	0.2321 ± 0.0010	0.23192 ± 0.00023	4.8/5
$\mathcal{A}_\ell$ (SLD)	0.23099 ± 0.00026	0.23099 ± 0.00026	0.23151 ± 0.00017	11.9/6

Table 31: Determinations of $\sin^2\theta^{\rm lept}_{\rm eff}$ from asymmetries. The second column lists the $\sin^2\theta^{\rm lept}_{\rm eff}$ values derived from the quantities listed in the first column. The third column contains the averages of these numbers by groups of observations, where the groups are separated by the horizontal lines. The fourth column shows the cumulative averages. The χ^2 per degree of freedom for the cumulative averages is also given. The averages have been performed including the small correlation between $A^{0,\rm b}_{\rm FB}$ and $A^{0,\rm c}_{\rm FB}$.

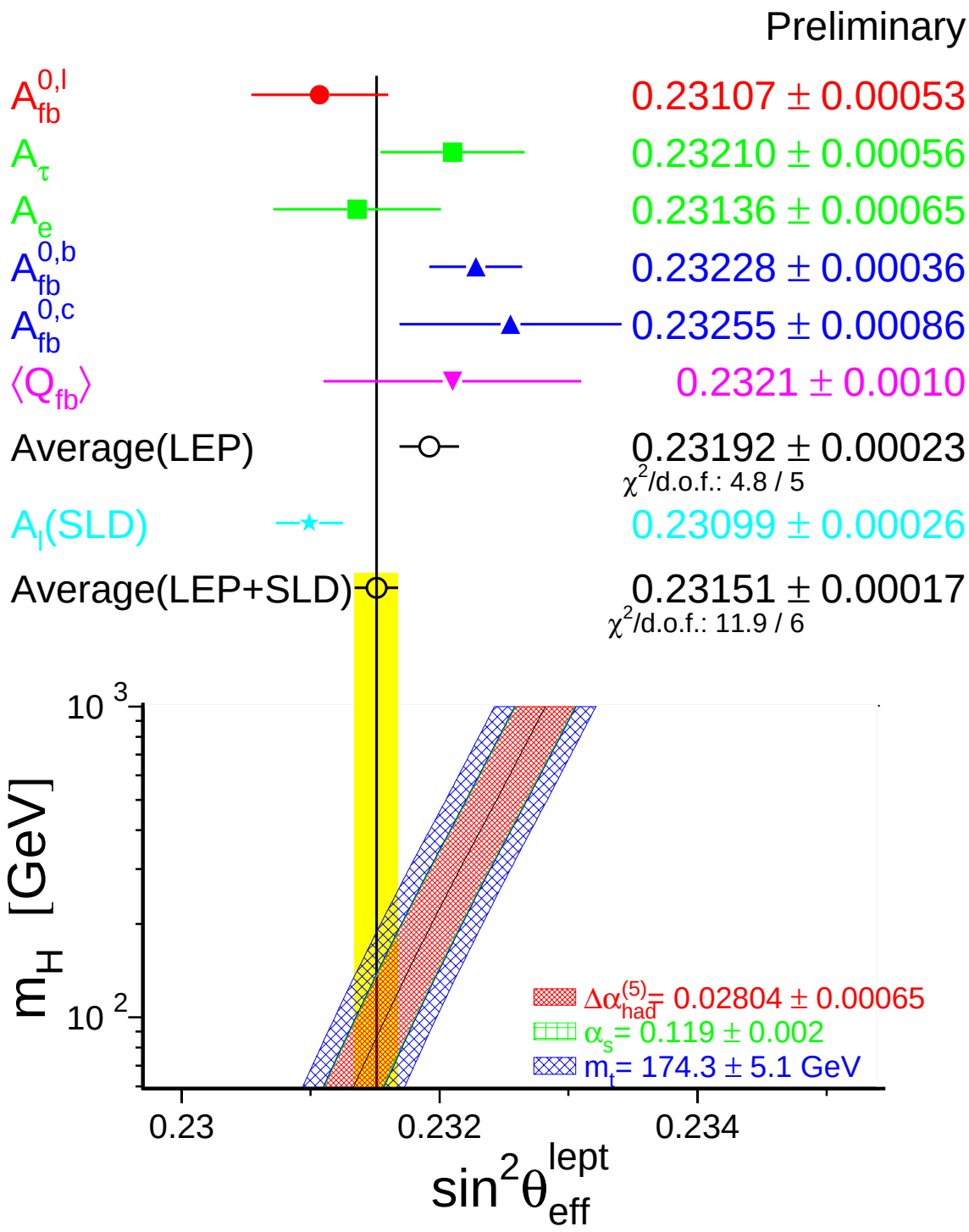

Figure 11: Comparison of several determinations of $\sin^2\theta_{\rm eff}^{\rm lept}$ from asymmetries. In the average, the small correlation between $A_{\rm FB}^{0,\,\rm b}$ and $A_{\rm FB}^{0,\,\rm c}$ has been included. Also shown is the prediction of the Standard Model as a function of $m_{\rm H}$. The width of the Standard Model band is due to the uncertainties in $\Delta\alpha_{\rm had}^{(5)}(m_{\rm Z}^2)$ (see Section 10.5), $\alpha_{\rm s}(m_{\rm Z}^2)$ and $m_{\rm t}$. The total width of the band is the linear sum of these effects.

10.5 Constraints on the Standard Model

The precise electroweak measurements performed at LEP and elsewhere can be used to check the validity of the Standard Model and, within its framework, to infer valuable information about its fundamental parameters. The accuracy of the measurements makes them sensitive to the top quark mass m_{t}, and to the mass of the Higgs boson m_{H} through loop corrections. While the leading m_{t} dependence is quadratic, the leading m_{H} dependence is logarithmic. Therefore, the inferred constraints on m_{H} are not very strong.

The LEP measurements used are summarised in Table 32 together with the results of the Standard Model fit. Also shown are the results from the SLD collaboration [34] as well as measurements of m_{W} from UA2 [129], CDF [130, 131], and DØ [132][3], measurements of the top quark mass by CDF [134] and DØ [135][4], and measurements of the neutrino-nucleon neutral to charged current ratios from CCFR [137] and NuTeV [138]. It should be noted that although these latter results are quoted in terms of $\sin^2\theta_W = 1 - m_{\mathrm{W}}^2/m_{\mathrm{Z}}^2$, radiative corrections result in small m_{t} and m_{H} dependences[5] that are included in the fit. In addition, the value of the electromagnetic coupling constant $\alpha(m_{\mathrm{Z}}^2)$, which is used in the fits, is shown. An additional input parameter, not shown in the table, is the Fermi constant G_F, determined from the μ lifetime, $G_F = (1.16637 \pm 0.00001) \times 10^{-5}\mathrm{GeV}^{-2}$ [139]. The relative error of G_F is comparable to that of m_{Z}; both have neglible effects in the fit results.

Detailed studies of the theoretical uncertainties in the Standard Model predictions due to missing higher-order electroweak corrections and their interplay with QCD corrections have been carried out in the working group on 'Precision calculations for the Z resonance' [142]. Theoretical uncertainties are evaluated by comparing different but, within our present knowledge, equivalent treatments of aspects such as resummation techniques, momentum transfer scales for vertex corrections and factorisation schemes. The effects of these theoretical uncertainties have been reduced by the inclusion of higher-order corrections [143, 144] in the electroweak libraries [145]. The use of the new QCD corrections [144] increases the value of $\alpha_{\mathrm{s}}(m_{\mathrm{Z}}^2)$ by 0.001, as expected. The effects of missing higher-order QCD corrections on $\alpha_{\mathrm{s}}(m_{\mathrm{Z}}^2)$ covers missing higher-order electroweak corrections and uncertainties in the interplay of electroweak and QCD corrections and has been estimated to be about 0.002 [146]. A discussion of theoretical uncertainties in the determination of α_{s} can be found in References 142 and 146. For the moment, the determination of the size of remaining theoretical uncertainties is still under study. All theoretical errors discussed in this paragraph have been neglected for the results presented in Table 33.

At present the impact of theoretical uncertainties on the determination of SM parameters from the precise electroweak measurements is small compared with the error due to the uncertainty in the value of $\alpha(m_{\mathrm{Z}}^2)$. The uncertainty in $\alpha(m_{\mathrm{Z}}^2)$ arises from the contribution of light quarks to the photon vacuum polarisation ($\Delta\alpha_{\mathrm{had}}^{(5)}(m_{\mathrm{Z}}^2)$):

$$\alpha(m_{\mathrm{Z}}^2) = \frac{\alpha(0)}{1 - \Delta\alpha_\ell(m_{\mathrm{Z}}^2) - \Delta\alpha_{\mathrm{had}}^{(5)}(m_{\mathrm{Z}}^2) - \Delta\alpha_{\mathrm{top}}(m_{\mathrm{Z}}^2)}. \tag{37}$$

The top contribution depends on the mass of the top quark, and is therefore determined inside the electroweak libraries [145]. The leptonic contribution has been recently calculated to third order [141] to be 0.031498. For the hadronic contribution, we use the value 0.02804 ± 0.00065 [140], which results in $1/\alpha^{(5)}(m_{\mathrm{Z}}^2) = 128.878 \pm 0.090$. This uncertainty causes an error of 0.00023 on the Standard Model

[3] See Reference 133 for a combination of these m_{W} measurements.

[4] See Reference 136 for a combination of these m_{t} measurements.

[5] The formula used is $\delta \sin^2\theta_W = -0.00142 \frac{m_{\mathrm{t}}^2 - (175\mathrm{GeV})^2}{(100\mathrm{GeV})^2} + 0.00048 \ln(\frac{m_{\mathrm{H}}}{150\mathrm{GeV}})$. See Reference 138 for details.

	Measurement with Total Error	Systematic Error	Standard Model fit	Pull
$\alpha^{(5)}(m_{\rm Z}^2)^{-1}$ [140, 141]	128.878 ± 0.090	0.083	128.878	0.0
a) LEP line-shape and lepton asymmetries:				
$m_{\rm Z}$ [GeV]	91.1871 ± 0.0021	[(a)]0.0017	91.1869	0.1
$\Gamma_{\rm Z}$ [GeV]	2.4944 ± 0.0024	[(a)]0.0013	2.4957	−0.6
$\sigma_{\rm h}^0$ [nb]	41.544 ± 0.037	0.035	41.479	1.7
R_ℓ	20.768 ± 0.024	0.017	20.740	1.2
$A_{\rm FB}^{0,\ell}$	0.01701 ± 0.00095	0.00060	0.01625	0.8
+ correlation matrix Table 8				
τ polarisation:				
$\mathcal{A}_\tau$	0.1425 ± 0.0044	0.0026	0.1472	−1.1
$\mathcal{A}_{\rm e}$	0.1483 ± 0.0051	0.0009	0.1472	0.2
$\rm q\overline{q}$ charge asymmetry:				
$\sin^2\theta_{\rm eff}^{\rm lept}$ ($\langle Q_{\rm FB}\rangle$)	0.2321 ± 0.0010	0.0008	0.23150	0.6
$m_{\rm W}$ [GeV]	80.350 ± 0.056	0.043	80.385	−0.6
b) SLD [34]				
$\sin^2\theta_{\rm eff}^{\rm lept}$ ($\mathcal{A}_\ell$)	0.23099 ± 0.00026	0.00018	0.23150	−2.0
c) LEP and SLD Heavy Flavour				
$R_{\rm b}^0$	0.21642 ± 0.00073	0.00056	0.21583	0.8
$R_{\rm c}^0$	0.1674 ± 0.0038	0.0028	0.1722	−1.3
$A_{\rm FB}^{0,\rm b}$	0.0988 ± 0.0020	0.0010	0.1032	−2.2
$A_{\rm FB}^{0,\rm c}$	0.0692 ± 0.0037	0.0019	0.0738	−1.2
$\mathcal{A}_{\rm b}$	0.911 ± 0.025	0.017	0.935	−0.9
$\mathcal{A}_{\rm c}$	0.630 ± 0.026	0.016	0.668	−1.5
+ correlation matrix Table 18				
d) $\rm p\overline{p}$ and νN				
$m_{\rm W}$ [GeV] ($\rm p\overline{p}$ [133])	80.448 ± 0.062	0.050	80.385	1.0
$1 - m_{\rm W}^2/m_{\rm Z}^2$ (νN [137, 138])	0.2255 ± 0.0021	0.0010	0.2229	1.1
$m_{\rm t}$ [GeV] ($\rm p\overline{p}$ [136])	174.3 ± 5.1	4.0	173.2	0.2

Table 32: Summary of measurements included in the combined analysis of Standard Model parameters. Section a) summarises LEP averages, Section b) SLD results ($\sin^2\theta_{\rm eff}^{\rm lept}$ includes $A_{\rm LR}$ and the polarised lepton asymmetries), Section c) the LEP and SLD heavy flavour results and Section d) electroweak measurements from $\rm p\overline{p}$ colliders and νN scattering. The total errors in column 2 include the systematic errors listed in column 3. Although the systematic errors include both correlated and uncorrelated sources, the determination of the systematic part of each error is approximate. The Standard Model results in column 4 and the pulls (difference between measurement and fit in units of the total measurement error) in column 5 are derived from the Standard Model fit including all data (Table 33, column 5) with the Higgs mass treated as a free parameter.

[(a)]The systematic errors on $m_{\rm Z}$ and $\Gamma_{\rm Z}$ contain the errors arising from the uncertainties in the LEP energy only.

prediction of $\sin^2\theta^{\rm lept}_{\rm eff}$, an error of 1 GeV on $m_{\rm t}$, and 0.2 on $\log(m_{\rm H})$, which are included in the results. The effect on the Standard Model prediction for $\Gamma_{\ell\ell}$ is negligible. The $\alpha_{\rm s}(m^2_{\rm Z})$ values for the Standard Model fits presented in this Section are stable against a variation of $\alpha(m^2_{\rm Z})$ in the interval quoted. There are several evaluations of $\Delta\alpha^{(5)}_{\rm had}(m^2_{\rm Z})$ [140, 147–153]. The most recent of these (References 150–153) are more theory-driven, and result in a smaller error on $\Delta\alpha^{(5)}_{\rm had}(m^2_{\rm Z})$. To show the effects of the uncertainty of $\alpha(m^2_{\rm Z})$, we also use the evaluation of $\Delta\alpha^{(5)}_{\rm had}(m^2_{\rm Z}) = 0.02784 \pm 0.00026$ [151] which results in $1/\alpha^{(5)}(m^2_{\rm Z}) = 128.905 \pm 0.036$.

Figure 12 shows a comparison of the leptonic partial width from LEP (Table 9) and the effective electroweak mixing angle from asymmetries measured at LEP and SLD (Table 31), with the Standard Model. Good agreement with the Standard Model prediction is observed. The point with the arrow shows the prediction if among the electroweak radiative corrections only the photon vacuum polarisation is included, which shows an example of evidence that LEP+SLD data are sensitive to electroweak corrections. Note that the error due to the uncertainty on $\alpha(m^2_{\rm Z})$ (shown as the length of the arrow) is larger than the experimental error on $\sin^2\theta^{\rm lept}_{\rm eff}$ from LEP and SLD. This underlines the growing importance of a precise measurement of $\sigma(\mathrm{e^+e^-} \to \text{hadrons})$ at low centre-of-mass energies.

Of the measurements given in Table 32, R_ℓ is the most sensitive to QCD corrections. Thus, it can be used to determine the value of $\alpha_{\rm s}(m^2_{\rm Z})$. For $m_{\rm Z} = 91.1871$ GeV, and imposing $m_{\rm t} = 174.3 \pm 5.1$ GeV as a constraint, $\alpha_{\rm s} = 0.123 \pm 0.004 \pm 0.001$ is obtained, where the second error accounts for varying $m_{\rm H}$ in the range $m_{\rm H} = 77^{+69}_{-39}$ GeV. This result is in very good agreement with the world average ($\alpha_{\rm s}(m^2_{\rm Z}) = 0.119 \pm 0.002$ [104]).

To test the agreement between the LEP data and the Standard Model, we first perform a fit to the data (including the LEP-II $m_{\rm W}$ determination) leaving the top quark mass and the Higgs mass as free parameters. The result is shown in Table 33, column 2. This fit shows that the LEP data prefer a light top quark and a light Higgs boson, albeit with very large errors. The strongly asymmetric errors on $m_{\rm H}$ are due to the fact that to first order, the radiative corrections in the Standard Model are proportional to $\log(m_{\rm H})$. The correlation between the top quark mass and the Higgs mass is 0.87 (see Figure 13).

The data can also be used within the Standard Model to determine the top quark and W masses indirectly, which can be compared to the direct measurements performed at the Tevatron and LEP. For this, we perform several fits. In the first fit, we use all the results in Table 32, except the LEP-II and Tevatron $m_{\rm W}$ and $m_{\rm t}$ results. The results are shown in column 3 of Table 33. The indirect measurements of $m_{\rm W}$ and $m_{\rm t}$ from this data sample are shown in Figure 14, compared with the direct measurements. Also shown is the Standard Model predictions for Higgs masses between 90 and 1000 GeV. As can be seen in the figure, the indirect and direct measurements of $m_{\rm W}$ and $m_{\rm t}$ are in good agreement, and both sets prefer a low Higgs mass. For the second fit, we include the direct $m_{\rm W}$ measurements from LEP and Tevatron to obtain $m_{\rm t} = 169.7^{+9.8}_{-7.0}$ GeV, in good agreement with the direct measurement of $m_{\rm t} = 174.3 \pm 5.1$ GeV. For the next fit, we use the direct $m_{\rm t}$ measurements to obtain the best indirect determination of $m_{\rm W}$. The result is shown in column 4 of Table 33. Also here, the direct measurements of $m_{\rm W}$ are in excellent agreement with the indirect one.

Finally, the best constraints on $m_{\rm H}$ are obtained when all data are used in the fit. The results of this fit are shown in column 5 of Table 33 and in Figure 13. In Figures 15 and 16 the sensitivity of the LEP and SLD measurements to the Higgs mass is shown. As can be seen, the most sensitive measurements are the asymmetries. A reduced uncertainty for the value of $\alpha(m^2_{\rm Z})$ would therefore result in an improved constraint on $m_{\rm H}$, as shown in Figure 12.

In Figure 17 the observed value of $\Delta\chi^2 \equiv \chi^2 - \chi^2_{\rm min}$ as a function of $m_{\rm H}$ is plotted for the fit

including all data. The solid curve is the result using ZFITTER, and corresponds to the last column of Table 33. The shaded band represents the uncertainty due to uncalculated higher-order corrections, as estimated by ZFITTER and TOPAZ0. The 95% confidence level upper limit on $m_{\rm H}$ (taking the band into account) is 215 GeV. The lower limit on $m_{\rm H}$ of approximately 95 GeV obtained from direct searches [154] has not been used in this limit determination. Also shown is the result (dashed curve) obtained when using $\alpha^{(5)}(m_{\rm Z}^2)$ of Reference 151. The fit results in $\log(m_{\rm H}/{\rm GeV}) = 1.96^{+0.21}_{-0.23}$, a 25% reduction of the error.

	LEP including LEP-II $m_{\rm W}$	all data except $m_{\rm W}$ and $m_{\rm t}$	all data except $m_{\rm W}$	all data
$m_{\rm t}$ [GeV]	172^{+14}_{-11}	167^{+11}_{-8}	172.9 ± 4.7	173.2 ± 4.5
$m_{\rm H}$ [GeV]	134^{+268}_{-81}	55^{+84}_{-27}	81^{+77}_{-42}	77^{+69}_{-39}
$\log(m_{\rm H}/{\rm GeV})$	$2.13^{+0.48}_{-0.40}$	$1.74^{+0.40}_{-0.30}$	$1.91^{+0.29}_{-0.32}$	$1.88^{+0.28}_{-0.30}$
$\alpha_{\rm s}(m_{\rm Z}^2)$	0.120 ± 0.003	0.118 ± 0.003	0.119 ± 0.003	0.118 ± 0.003
χ^2/d.o.f.	11/9	21/12	21/13	23/15
$\sin^2\theta^{\rm lept}_{\rm eff}$	0.23184 ± 0.00021	0.23151 ± 0.00017	0.23152 ± 0.00018	0.23150 ± 0.00016
$1 - m_{\rm W}^2/m_{\rm Z}^2$	0.2237 ± 0.0006	0.2233 ± 0.0007	0.2230 ± 0.0005	0.2229 ± 0.0004
$m_{\rm W}$ [GeV]	80.342 ± 0.032	80.366 ± 0.035	80.381 ± 0.026	80.385 ± 0.022

Table 33: Results of the fits to LEP data alone, to all data except the direct determinations of $m_{\rm t}$ and $m_{\rm W}$ (Tevatron and LEP-II), to all data except direct $m_{\rm W}$ determinations, and to all data. As the sensitivity to $m_{\rm H}$ is logarithmic, both $m_{\rm H}$ as well as $\log(m_{\rm H}/{\rm GeV})$ are quoted. The bottom part of the table lists derived results for $\sin^2\theta^{\rm lept}_{\rm eff}$, $1 - m_{\rm W}^2/m_{\rm Z}^2$ and $m_{\rm W}$. See text for a discussion of theoretical errors not included in the errors above.

11 Prospects for the Future

Most of the measurements from data taken at or near the Z resonance, both at LEP as well as at SLC, that are presented in this report are either final, or are being finalized. The major improvements will therefore take place in the high energy data. The expected increase in statistics at LEP-II to 500 pb^{-1} per experiment will lead to substantially improved measurements of certain electroweak parameters. As a result, the measurements of m_{W} are likely to match the error obtained via the radiative corrections of the Z data, providing a further important test of the Standard Model. In the measurement of the WWγ and WWZ triple-gauge-boson couplings the increase in LEP-II statistics, together with the increased sensitivity at higher beam energies, will lead to an improvement in the current precision by about a factor of 3. The anticipated improvements in the measurements of the hadronic cross section at low energy will reduce the error on the Higgs mass.

12 Conclusions

The combination of the many precise electroweak results yields stringent constraints on the Standard Model. All measurements agree with the predictions. In addition, the results are sensitive to the Higgs mass.

The LEP experiments wish to stress that this report reflects a preliminary status at the time of the 1999 summer conferences. A definitive statement on these results must wait for publication by each collaboration.

Acknowledgements

We would like to thank the CERN accelerator divisions for the efficient operation of the LEP accelerator, the precise information on the absolute energy scale and their close cooperation with the four experiments. We would also like to thank members of the CDF, DØ, NuTeV, and SLD Collaborations for making results available to us in advance of the conferences and for useful discussions concerning their combination. Finally, the results of the section on Standard Model constraints would not have been possible without the close collaboration of many theorists. We especially thank the ZFITTER and TOPAZ0 teams.

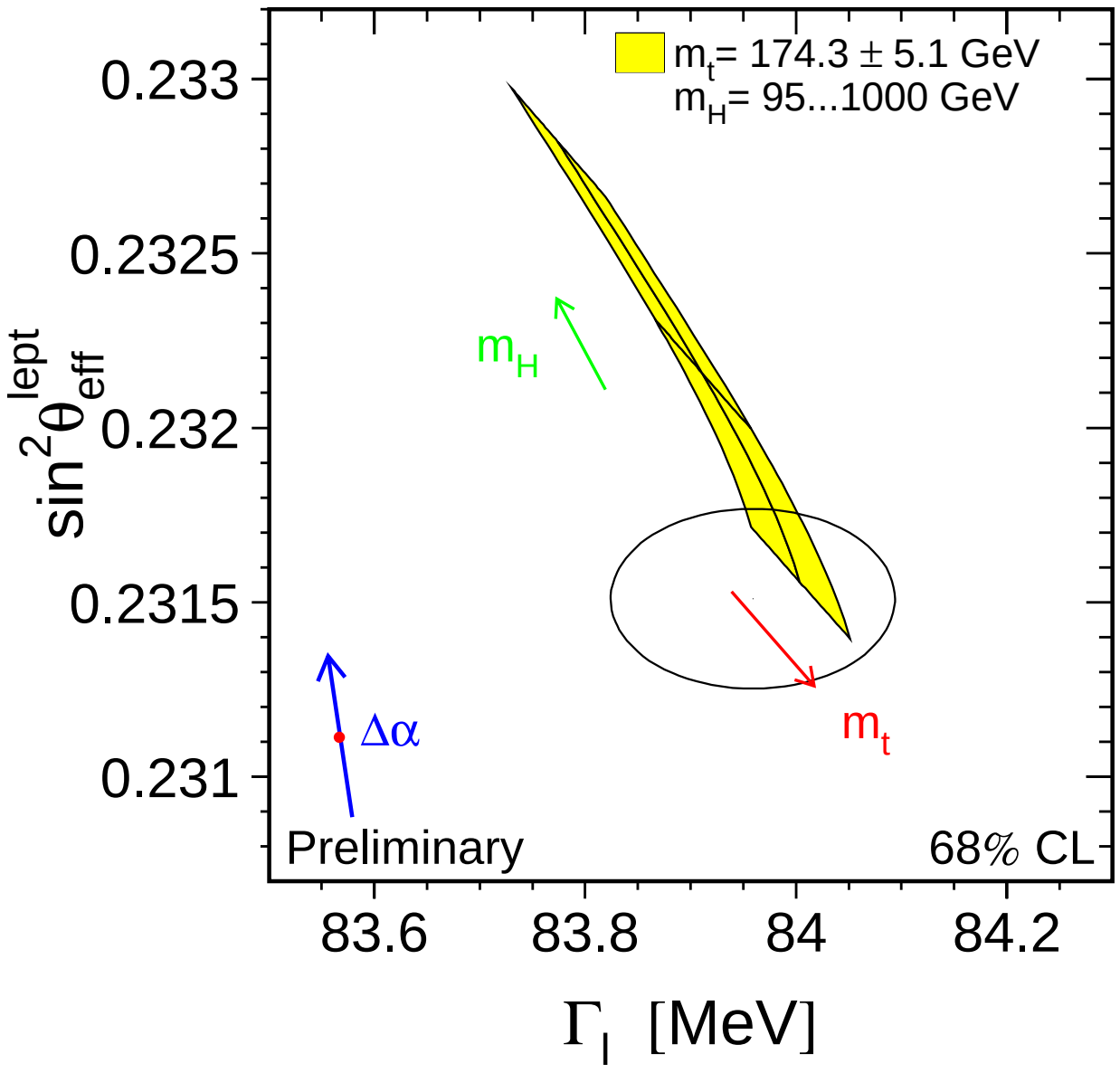

Figure 12: LEP-I+SLD measurements of $\sin^2\theta^{\rm lept}_{\rm eff}$ (Table 31) and $\Gamma_{\ell\ell}$ (Table 9) and the Standard Model prediction. The point shows the predictions if among the electroweak radiative corrections only the photon vacuum polarisation is included. The corresponding arrow shows variation of this prediction if $\alpha(m_{\rm Z}^2)$ is changed by one standard deviation. This variation gives an additional uncertainty to the Standard Model prediction shown in the figure.

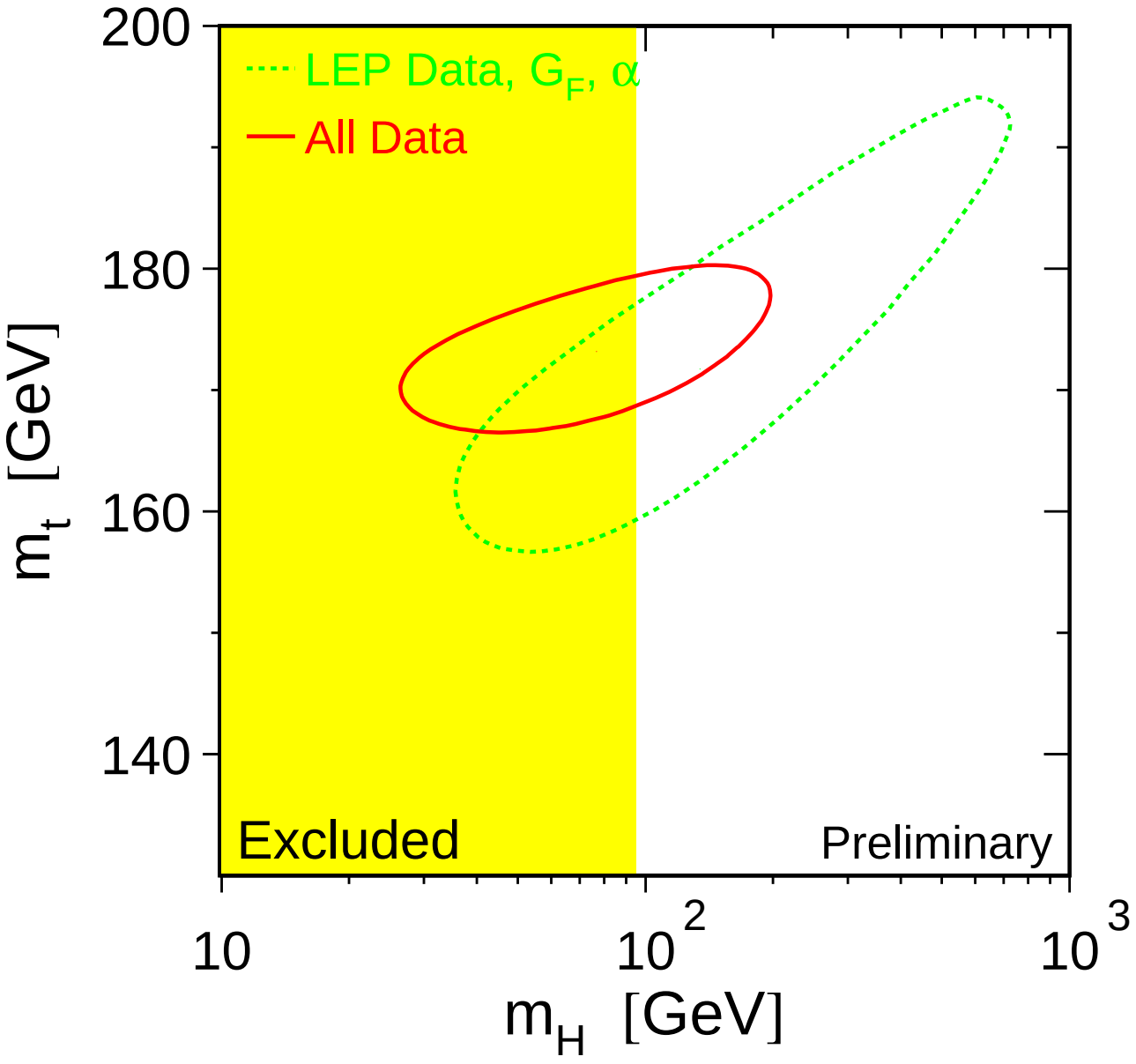

Figure 13: The 68% confidence level contours in $m_{\rm t}$ and $m_{\rm H}$ for the fits to LEP data only (dashed curve) and to all data including the CDF/DØ $m_{\rm t}$ measurement (solid curve). The vertical band shows the 95% CL exclusion limit on $m_{\rm H}$ from the direct search.

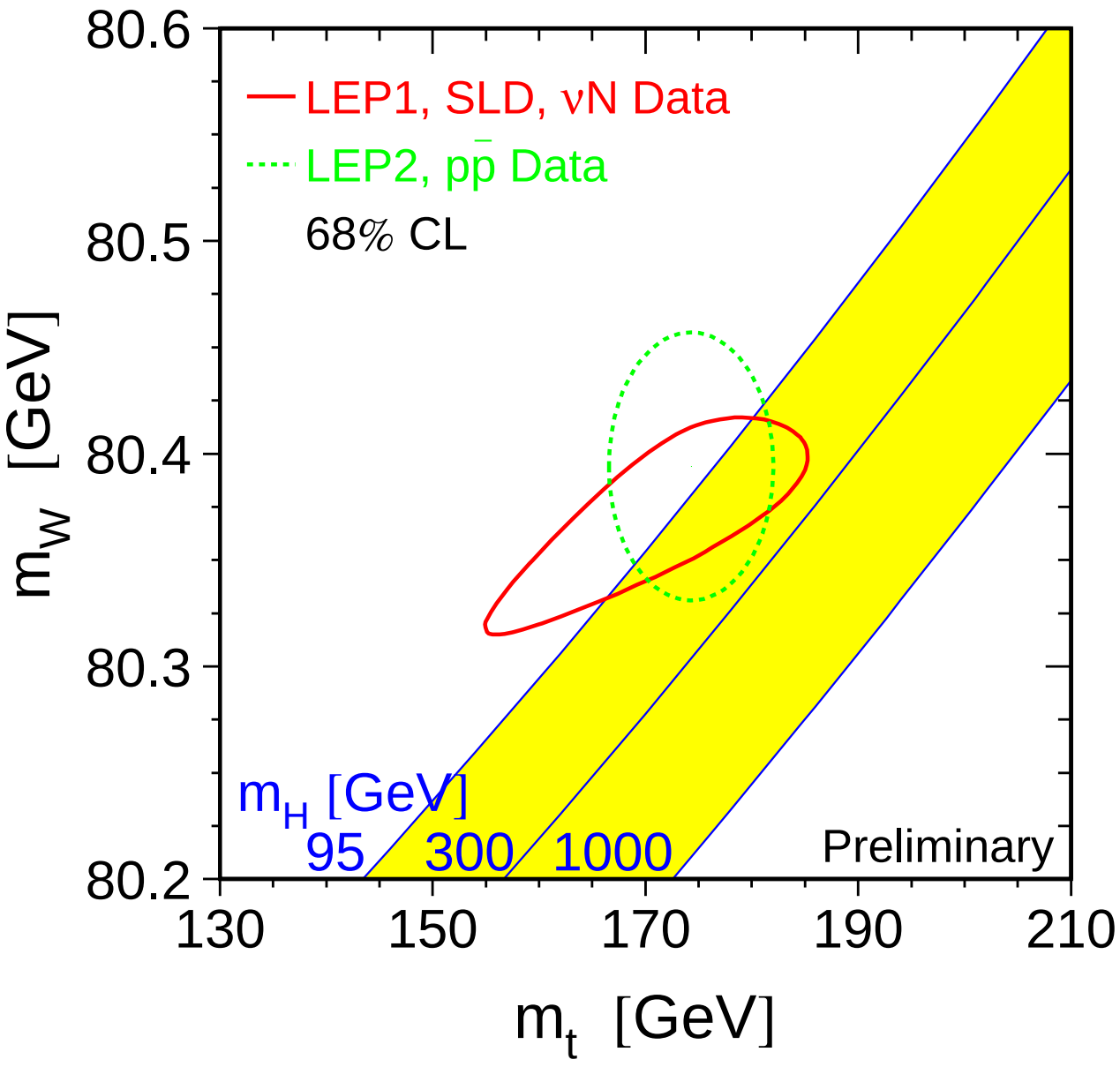

Figure 14: The comparison of the indirect measurements of m_{W} and m_{t} (LEP-I+SLD+νN data) (solid contour) and the direct measurements (Tevatron and LEP-II data) (dashed contour). In both cases the 68% CL contours are plotted. Also shown is the Standard Model relationship for the masses as a function of the Higgs mass.

Figure 15: Comparison of LEP-I measurements with the Standard Model prediction as a function of m_{H}. The measurement with its error is shown as the vertical band. The width of the Standard Model band is due to the uncertainties in $\Delta\alpha^{(5)}_{\mathrm{had}}(m^2_{\mathrm{Z}})$, $\alpha_{\mathrm{s}}(m^2_{\mathrm{Z}})$ and m_{t}. The total width of the band is the linear sum of these effects. See Figure 16 for the definition of these uncertainties.

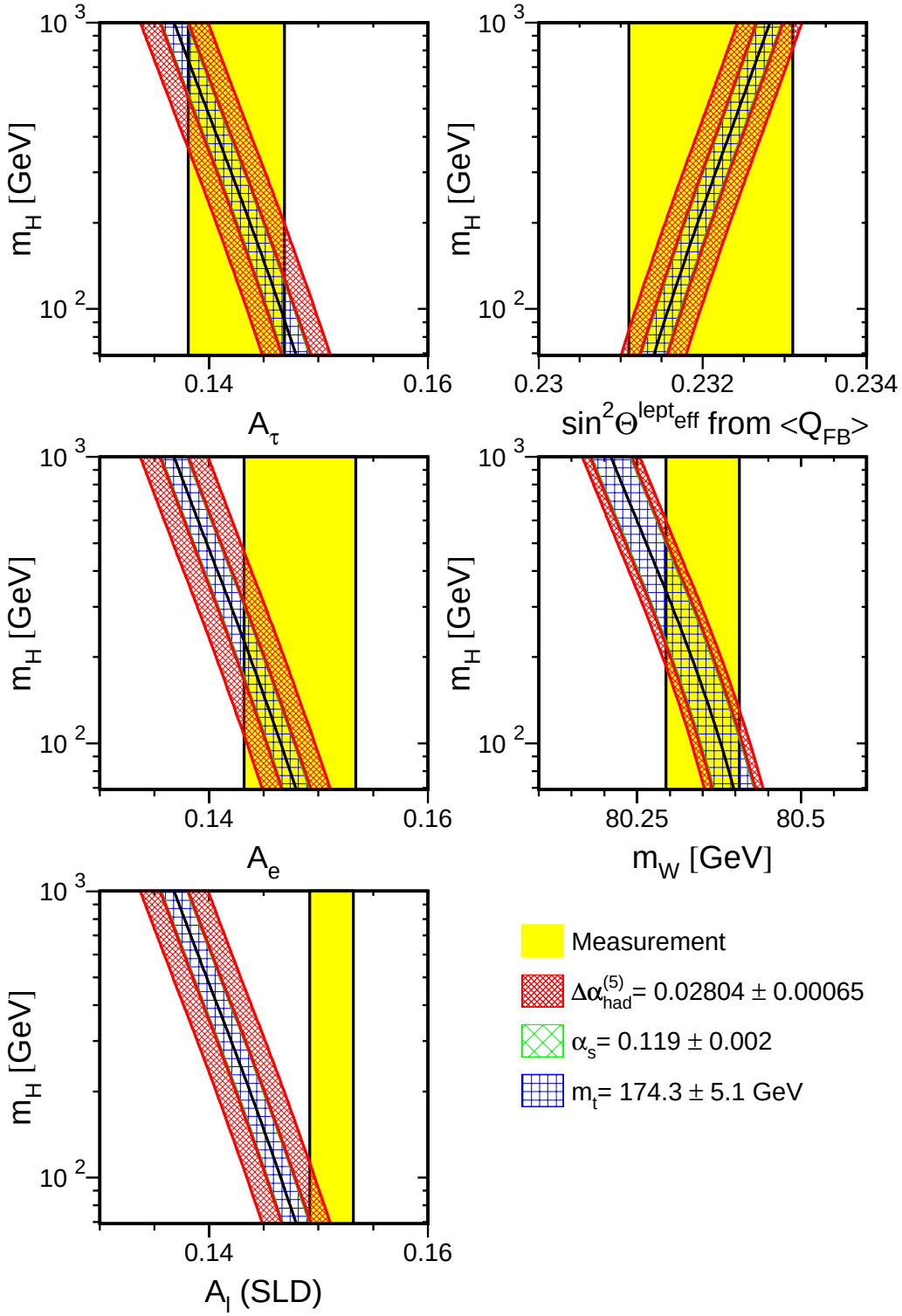

Figure 16: Comparison of LEP-I measurements with the Standard Model prediction as a function of $m_{\rm H}$ (*c.f.* Figure 15). Also shown is the comparison of the SLD measurement of $A^0_{\rm LR}$ with the Standard Model.

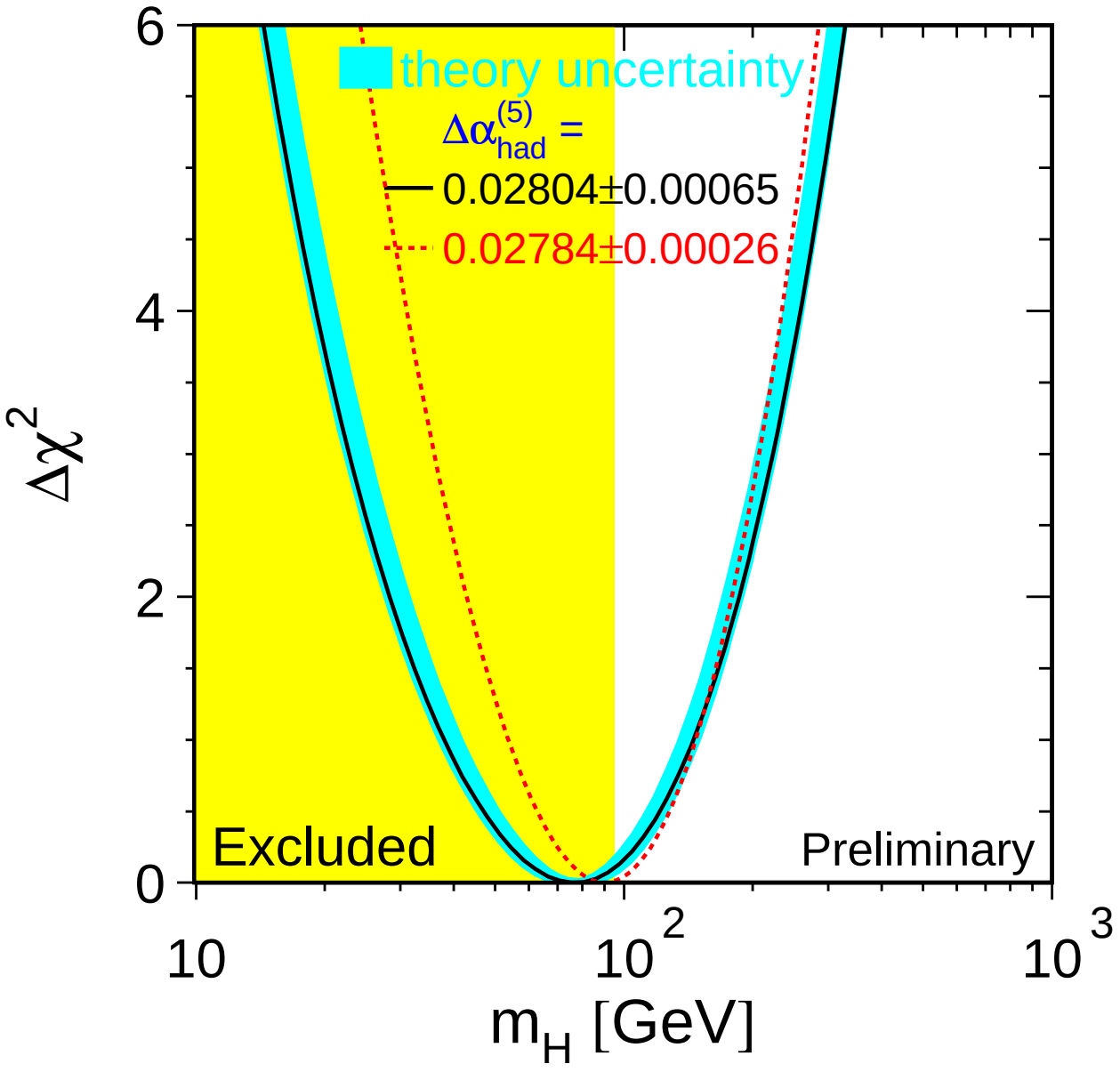

Figure 17: $\Delta\chi^2 = \chi^2 - \chi^2_{min}$ *vs.* $m_{\rm H}$ curve. The line is the result of the fit using all data (last column of Table 33); the band represents an estimate of the theoretical error due to missing higher order corrections. The vertical band shows the 95% CL exclusion limit on $m_{\rm H}$ from the direct search. The dashed curve is the result obtained using the evaluation of $\Delta\alpha^{(5)}_{\rm had}(m^2_{\rm Z})$ from Reference 151.

Appendix

A Heavy-Flavour Fit including Off-Peak Asymmetries

The full 18 parameter fit to the LEP and SLD data gave the following results:

$$
\begin{aligned}
R_{\mathrm{b}}^{0} &= 0.21643 \pm 0.00073 \\
R_{\mathrm{c}}^{0} &= 0.1674 \pm 0.0038 \\
A_{\mathrm{FB}}^{\mathrm{b\bar{b}}}(-2) &= 0.0570 \pm 0.0078 \\
A_{\mathrm{FB}}^{\mathrm{c\bar{c}}}(-2) &= -0.037 \pm 0.017 \\
A_{\mathrm{FB}}^{\mathrm{b\bar{b}}}(\mathrm{pk}) &= 0.0968 \pm 0.0021 \\
A_{\mathrm{FB}}^{\mathrm{c\bar{c}}}(\mathrm{pk}) &= 0.0628 \pm 0.0038 \\
A_{\mathrm{FB}}^{\mathrm{b\bar{b}}}(+2) &= 0.1130 \pm 0.0069 \\
A_{\mathrm{FB}}^{\mathrm{c\bar{c}}}(+2) &= 0.138 \pm 0.015 \\
\mathcal{A}_{\mathrm{b}} &= 0.911 \pm 0.025 \\
\mathcal{A}_{\mathrm{c}} &= 0.630 \pm 0.026 \\
\mathrm{BR}(\mathrm{b} \to \ell) &= 0.1062 \pm 0.0017 \\
\mathrm{BR}(\mathrm{b} \to \mathrm{c} \to \bar{\ell}) &= 0.0807 \pm 0.0025 \\
\mathrm{BR}(\mathrm{c} \to \ell) &= 0.0985 \pm 0.0032 \\
\overline{\chi} &= 0.1186 \pm 0.0043 \\
f(\mathrm{D}^{+}) &= 0.239 \pm 0.016 \\
f(\mathrm{D_s}) &= 0.117 \pm 0.025 \\
f(\mathrm{c_{baryon}}) &= 0.084 \pm 0.023 \\
\mathrm{P}(\mathrm{c} \to \mathrm{D}^{*+}) \times \mathrm{BR}(\mathrm{D}^{*+} \to \pi^{+}\mathrm{D}^{0}) &= 0.1653 \pm 0.0053
\end{aligned}
$$

with a χ^2/d.o.f. of $54/(96-18)$. The corresponding correlation matrix is given in Table 34. The energy for the peak-2, peak and peak$+2$ results are respectively 89.55 GeV, 91.26 GeV and 92.94 GeV. Note that the asymmetry results shown here are not the pole asymmetries shown in Section 6.2.2. The non-electroweak parameters do not depend on the treatment of the asymmetries.

	1) R_b	2) R_c	3) $A_{FB}^{b\bar{b}}$ (−2)	4) $A_{FB}^{c\bar{c}}$ (−2)	5) $A_{FB}^{b\bar{b}}$ (pk)	6) $A_{FB}^{c\bar{c}}$ (pk)	7) $A_{FB}^{b\bar{b}}$ (+2)	8) $A_{FB}^{c\bar{c}}$ (+2)	9) $\mathcal{A}_b$	10) $\mathcal{A}_c$	11) BR (1)	12) BR (2)	13) BR (3)	14) $\overline{\chi}$	15) $f(D^+)$	16) $f(D_s)$	17) $f(c_{bar.})$	18) PcDst
1)	1.00	−0.14	−0.01	−0.01	−0.02	0.01	−0.01	0.01	−0.03	0.02	−0.14	0.03	−0.04	−0.04	−0.16	−0.04	0.12	0.12
2)	−0.14	1.00	0.01	0.01	0.05	−0.05	0.02	−0.02	0.02	−0.03	0.04	−0.02	−0.34	0.03	−0.15	0.22	0.21	−0.54
3)	−0.01	0.01	1.00	0.13	0.04	0.01	0.02	0.00	0.01	0.00	0.02	−0.03	0.01	0.06	0.00	0.00	0.00	0.00
4)	−0.01	0.01	0.13	1.00	0.01	0.01	0.00	0.00	0.00	0.00	0.02	−0.02	0.02	0.02	0.00	0.00	0.00	0.00
5)	−0.02	0.05	0.04	0.01	1.00	0.09	0.11	0.00	0.02	0.00	0.00	−0.07	0.01	0.16	0.01	0.03	0.00	−0.03
6)	0.01	−0.05	0.01	0.01	0.09	1.00	−0.01	0.12	−0.01	0.03	0.22	−0.26	−0.04	0.22	0.01	−0.01	−0.02	0.02
7)	−0.01	0.02	0.02	0.00	0.11	−0.01	1.00	0.11	0.01	0.00	−0.02	−0.01	0.00	0.06	0.01	0.01	0.00	−0.01
8)	0.01	−0.02	0.00	0.00	0.00	0.12	0.11	1.00	0.00	0.01	0.05	−0.07	−0.05	0.04	0.00	−0.01	0.00	0.01
9)	−0.03	0.02	0.01	0.00	0.02	−0.01	0.01	0.00	1.00	0.15	−0.01	0.02	0.04	0.08	−0.01	0.00	0.01	−0.01
10)	0.02	−0.03	0.00	0.00	0.00	0.03	0.00	0.01	0.15	1.00	0.02	−0.04	−0.03	0.01	−0.01	0.00	0.01	0.01
11)	−0.14	0.04	0.02	0.02	0.00	0.22	−0.02	0.05	−0.01	0.02	1.00	−0.37	0.23	0.44	0.05	0.02	−0.02	−0.03
12)	0.03	−0.02	−0.03	−0.02	−0.07	−0.26	−0.01	−0.07	0.02	−0.04	−0.37	1.00	−0.06	−0.43	0.00	−0.01	0.00	0.01
13)	−0.04	−0.34	0.01	0.02	0.01	−0.04	0.00	−0.05	0.04	−0.03	0.23	−0.06	1.00	0.21	0.04	−0.05	−0.06	0.19
14)	−0.04	0.03	0.06	0.02	0.16	0.22	0.06	0.04	0.08	0.01	0.44	−0.43	0.21	1.00	0.02	0.02	−0.01	−0.03
15)	−0.16	−0.15	0.00	0.00	0.01	0.01	0.01	0.00	−0.01	−0.01	0.05	0.00	0.04	0.02	1.00	−0.38	−0.28	0.12
16)	−0.04	0.22	0.00	0.00	0.03	−0.01	0.01	−0.01	0.00	0.00	0.02	−0.01	−0.05	0.02	−0.38	1.00	−0.44	−0.13
17)	0.12	0.21	0.00	0.00	0.00	−0.02	0.00	0.00	0.01	0.01	−0.02	0.00	−0.06	−0.01	−0.28	−0.44	1.00	−0.19
18)	0.12	−0.54	0.00	0.00	−0.03	0.02	−0.01	0.01	−0.01	0.01	−0.03	0.01	0.19	−0.03	0.12	−0.13	−0.19	1.00

Table 34: The correlation matrix for the set of the 18 heavy flavour parameters. BR(1), BR(2) and BR(3) denote BR($b \to \ell$), BR($b \to c \to \bar{\ell}$) and BR($c \to \ell$) respectively, PcDst denotes P($c \to D^{*+}$) × BR($D^{*+} \to \pi^+ D^0$).

The Measurements used in the Heavy Flavour Averages

In the following 20 tables the results used in the combination are listed. In each case an indication of the dataset used and the type of analysis is given. Preliminary results are indicated by the symbol "†". The values of centre-of-mass energy are given where relevant. In each table, the result used as input to the average procedure is given followed by the statistical error, the correlated and uncorrelated systematic errors, the total systematic error, and any dependence on other electroweak parameters. In the case of the asymmetries, the measurement moved to a common energy (89.55 GeV, 91.26 GeV and 92.94 GeV, respectively, for peak−2, peak and peak+2 results) is quoted as *corrected* asymmetry.

Contributions to the correlated systematic error quoted here are from any sources of error shared with one or more other results from different experiments in the same table, and the uncorrelated errors from the remaining sources. In the case of $\mathcal{A}_c$ and $\mathcal{A}_b$ from SLD the quoted correlated systematic error has contributions from any source shared with one or more other measurements from LEP experiments. Constants such as $a(x)$ denote the dependence on the assumed value of $x^{\rm used}$, which is also given.

	ALEPH	DELPHI	L3	OPAL	SLD
	92-95 [37]	92-95 [38]	94-95† [39]	92-95 [40]	93-98† [41]
$R_{\rm b}$	0.2157	0.2163	0.2171	0.2174	0.2159
Statistical	0.0009	0.0007	0.0015	0.0011	0.0014
Uncorrelated	0.0007	0.0004	0.0015	0.0009	0.0013
Correlated	0.0007	0.0004	0.0018	0.0008	0.0006
Total Systematic	0.0009	0.0006	0.0023	0.0012	0.0014
$a(R_{\rm c})$	-0.0033	-0.0041	-0.0376	-0.0122	-0.0074
$R_{\rm c}^{\rm used}$	0.1720	0.1720	0.1734	0.1720	0.1710
$a({\rm BR}({\rm c}\to\ell))$			-0.0133	-0.0067	
${\rm BR}({\rm c}\to\ell)^{\rm used}$			9.80	9.80	
$a(f({\rm D}^+))$	-0.0010	-0.0010	-0.0086	-0.0029	-0.0004
$f({\rm D}^+)^{\rm used}$	0.2330	0.2330	0.2330	0.2380	0.2370
$a(f({\rm D_s}))$	-0.0001	0.0001	-0.0005	-0.0001	-0.0002
$f({\rm D_s})^{\rm used}$	0.1020	0.1030	0.1030	0.1020	0.1140
$a(f(\Lambda_{\rm c}))$	0.0002	0.0003	0.0008	0.0003	-0.0004
$f(\Lambda_{\rm c})^{\rm used}$	0.0650	0.0630	0.0630	0.0650	0.0730

Table 35: The measurements of $R_{\rm b}^0$. All measurements use a lifetime tag enhanced by other features like invariant mass cuts or high p_T leptons.

	ALEPH			DELPHI		OPAL		SLD
	91-95† c-count [46]	91-95 D meson [42]	92-95 lepton [42]	92-95 c-count [44]	92-95 D meson [44]	91-94 c-count [47]	90-95 D meson [45]	93-97† vertex-mass [49]
$R_{\rm c}$	0.1734	0.1679	0.1668	0.1692	0.1610	0.164	0.1760	0.1680
Statistical	0.0049	0.0082	0.0062	0.0047	0.0104	0.011	0.0095	0.0047
Uncorrelated	0.0057	0.0078	0.0059	0.0050	0.0064	0.012	0.0102	0.0044
Correlated	0.0101	0.0026	0.0010	0.0083	0.0060	0.010	0.0062	0.0003
Total Systematic	0.0116	0.0082	0.0059	0.0097	0.0088	0.016	0.0120	0.0044
$a(R_{\rm b})$		-0.0050						-0.0239
$R_{\rm b}^{\rm used}$		0.2159						0.2175
$a({\rm BR}({\rm c}\to\ell))$			-0.1646					
${\rm BR}({\rm c}\to\ell)^{\rm used}$			9.80					

Table 36: The measurements of $R_{\rm c}^0$. "c-count" denotes the determination of $R_{\rm c}^0$ from the sum of production rates of weakly decaying charmed hadrons. "D meson" denotes any single/double tag analysis using exclusive and/or inclusive D meson reconstruction.

	ALEPH				DELPHI			L3	OPAL		
	90-95 lepton [54]	90-95 lepton [54]	90-95 lepton [54]	91-95 jet charge [58]	91-93† lepton [55]	92-95 D meson [63]	92-95 jet charge [59]	90-95 lepton [56]	91-95 jet charge [61]	90-95† lepton [57]	90-95 D meson [64]
$\sqrt{s}$ (GeV)	88.380	89.380	90.210	89.430	89.430	89.434	89.550	89.500	89.440	89.490	89.490
$A_{\rm FB}^{\rm bb}(-2)$	-3.53	5.47	9.11	7.46	6.40	5.65	6.80	6.14	4.10	3.56	-9.30
$A_{\rm FB}^{\rm bb}(-2)$Corrected	5.87			7.75	6.69	5.93	6.80	6.26	4.36	3.70	-9.16
Statistical	1.90			1.78	3.87	7.59	1.80	2.93	2.10	1.73	10.80
Uncorrelated	0.39			0.19	0.16	0.91	0.12	0.37	0.25	0.16	2.62
Correlated	0.70			0.15	0.12	0.08	0.01	0.19	0.02	0.04	1.19
Total Systematic	0.80			0.24	0.20	0.91	0.13	0.41	0.25	0.16	2.88
$a(R_{\rm b})$	-0.3069			-0.2430	-0.7233		-0.1962	-1.4467	-0.7300	-0.1000	
$R_{\rm b}^{\rm used}$	0.2192			0.2155	0.2170		0.2158	0.2170	0.2150	0.2155	
$a(R_{\rm c})$	0.0362			1.4800	0.1221		0.3200	0.3612	0.0700	0.1000	
$R_{\rm c}^{\rm used}$	0.1710			0.1726	0.1710		0.1720	0.1734	0.1730	0.1720	
$a(A_{\rm FB}^{\rm c\bar{c}}(-2))$	-0.2244			-0.2501				-0.1000	-0.3156		
$A_{\rm FB}^{\rm c\bar{c}}(-2)^{\rm used}$	-2.34			-2.70				-2.50	-2.81		
$a({\rm BR}({\rm b}\to\ell))$	-0.2486				-0.9706			-1.0290		0.3406	
${\rm BR}({\rm b}\to\ell)^{\rm used}$	11.34				11.00			10.50		10.90	
$a({\rm BR}({\rm b}\to{\rm c}\to\bar{\ell}))$	-0.1074				0.1580			-0.1440		-0.5298	
${\rm BR}({\rm b}\to{\rm c}\to\bar{\ell})^{\rm used}$	7.86				7.90			8.00		8.30	
$a({\rm BR}({\rm c}\to\ell))$	-0.0474				0.5880			0.5096		0.1960	
${\rm BR}({\rm c}\to\ell)^{\rm used}$	9.80				9.80			9.80		9.80	
$a(\overline{\chi})$	5.259				2.0533						
$\overline{\chi}^{\rm used}$	0.12460				0.12100						
$a(f({\rm D}^+))$						0.5083	0.0949				
$f({\rm D}^+)^{\rm used}$						0.2210	0.2330				
$a(f({\rm D_s}))$						0.1742	0.0035				
$f({\rm D_s})^{\rm used}$						0.1120	0.1020				
$a(f(\Lambda_{\rm c}))$						-0.0191	-0.0225				
$f(\Lambda_{\rm c})^{\rm used}$						0.0840	0.0630				

Table 37: The measurements of $A_{\rm FB}^{\rm b\bar{b}}(-2)$. All numbers are given in %.

	ALEPH	DELPHI	OPAL	
	91-95 D meson [62]	92-95 D meson [63]	90-95† lepton [57]	90-95 D meson [64]
$\sqrt{s}$ (GeV)	89.370	89.434	89.490	89.490
$A_{\rm FB}^{\rm c\bar{c}}(-2)$	-1.10	-5.04	-6.92	3.90
$A_{\rm FB}^{\rm c\bar{c}}(-2)$Corrected	-0.02	-4.35	-6.56	4.26
Statistical	4.30	3.69	2.44	5.10
Uncorrelated	1.00	0.40	0.39	0.86
Correlated	0.09	0.09	0.21	0.02
Total Systematic	1.00	0.41	0.44	0.86
$a(R_{\rm b})$			-3.4000	
$R_{\rm b}^{\rm used}$			0.2155	
$a(R_{\rm c})$			3.2000	
$R_{\rm c}^{\rm used}$			0.1720	
$a(A_{\rm FB}^{\rm b\bar{b}}(-2))$	-1.3365			
$A_{\rm FB}^{\rm b\bar{b}}(-2)^{\rm used}$	6.13			
$a({\rm BR}({\rm b}\to\ell))$			-1.7031	
${\rm BR}({\rm b}\to\ell)^{\rm used}$			10.90	
$a({\rm BR}({\rm b}\to{\rm c}\to\bar{\ell}))$			-1.4128	
${\rm BR}({\rm b}\to{\rm c}\to\bar{\ell})^{\rm used}$			8.30	
$a({\rm BR}({\rm c}\to\ell))$			3.3320	
${\rm BR}({\rm c}\to\ell)^{\rm used}$			9.80	
$a(f({\rm D}^+))$		-0.3868		
$f({\rm D}^+)^{\rm used}$		0.2210		
$a(f({\rm D_s}))$		-0.1742		
$f({\rm D_s})^{\rm used}$		0.1120		
$a(f(\Lambda_{\rm c}))$		-0.0878		
$f(\Lambda_{\rm c})^{\rm used}$		0.0840		

Table 38: The measurements of $A_{\rm FB}^{\rm c\bar{c}}(-2)$. All numbers are given in %

	ALEPH		DELPHI			L3		OPAL		
	91-95† lepton [54]	91-95 jet charge [58]	91-95† lepton [55]	92-95 D meson [63]	92-95 jet charge [59]	91-95 jet charge [60]	90-95 lepton [56]	91-95 jet charge [61]	90-95† lepton [57]	90-95 D meson [64]
$\sqrt{s}$ (GeV)	91.210	91.250	91.26	91.235	91.260	91.240	91.260	91.210	91.240	91.240
$A_{\rm FB}^{\rm bb}$(pk)	9.71	10.40	9.89	7.59	9.83	9.31	9.85	10.06	9.14	8.90
$A_{\rm FB}^{\rm bb}$(pk)Corrected	9.81	10.42	9.99	7.63	9.83	9.35	9.85	10.15	9.18	8.94
Statistical	0.40	0.40	0.65	1.97	0.47	1.01	0.67	0.52	0.44	2.70
Uncorrelated	0.16	0.23	0.18	0.77	0.14	0.51	0.27	0.41	0.14	2.16
Correlated	0.12	0.22	0.19	0.07	0.04	0.21	0.14	0.20	0.15	0.37
Total Systematic	0.20	0.32	0.26	0.77	0.14	0.55	0.31	0.46	0.20	2.20
$a(R_{\rm b})$	-0.9545	-0.2430	-1.773		-0.1962	-9.1622	-2.1700	-7.6300	-0.7000	
$R_{\rm b}^{\rm used}$	0.2172	0.2170	0.2170		0.2158	0.2170	0.2170	0.2150	0.2155	
$a(R_{\rm c})$	0.6450	1.4900	0.9593		0.8400	1.0831	1.3005	0.4600	0.6000	
$R_{\rm c}^{\rm used}$	0.1720	0.1726	0.1733		0.1720	0.1733	0.1734	0.1730	0.1720	
$a(A_{\rm FB}^{\rm c\bar{c}}$(pk))		0.6345				1.1603	0.9262	0.6870		
$A_{\rm FB}^{\rm c\bar{c}}(pk)^{\rm used}$		6.85				6.91	7.41	6.19		
a(BR(b $\to \ell$))	-1.8480		-2.789				-2.0160		-0.3406	
BR(b $\to \ell)^{\rm used}$	10.78		11.12				10.50		10.90	
a(BR(b $\to$ c $\to \bar{\ell}$))	0.4233		0.7321				-0.1280		-0.3532	
BR(b $\to$ c $\to \bar{\ell})^{\rm used}$	8.14		8.03				8.00		8.30	
a(BR(c $\to \ell$))	0.5096		0.3341				1.5288		0.5880	
BR(c $\to \ell)^{\rm used}$	9.80		9.80				9.80		9.80	
$a(\overline{\chi})$	2.9904		3.2259							
$\overline{\chi}^{\rm used}$	0.12460		0.12140							
$a(f(\rm D^+))$				0.0442	0.2761					
$f(\rm D^+)^{\rm used}$				0.2210	0.2330					
$a(f(\rm D_s))$				-0.0788	0.0106					
$f(\rm D_s)^{\rm used}$				0.1120	0.1020					
$a(f(\Lambda_{\rm c}))$				-0.0115	-0.0495					
$f(\Lambda_{\rm c})^{\rm used}$				0.0840	0.0630					

Table 39: The measurements of $A_{\rm FB}^{\rm b\bar{b}}$(pk). All numbers are given in %

	ALEPH		DELPHI		L3	OPAL	
	91-95† lepton [54]	91-95 D meson [62]	91-95† lepton [55]	92-95 D meson [63]	90-95 lepton [56]	90-95† lepton [57]	90-95 D meson [64]
$\sqrt{s}$ (GeV)	91.210	91.220	91.260	91.235	91.240	91.240	91.240
$A_{\rm FB}^{\rm c\bar{c}}$(pk)	5.69	6.20	7.69	6.58	7.94	5.97	6.60
$A_{\rm FB}^{\rm c\bar{c}}$(pk)Corrected	5.94	6.39	7.69	6.70	8.04	6.07	6.70
Statistical	0.53	0.90	1.13	0.97	3.70	0.59	1.20
Uncorrelated	0.24	0.23	0.62	0.25	2.40	0.37	0.51
Correlated	0.36	0.17	0.29	0.04	0.49	0.32	0.19
Total Systematic	0.44	0.28	0.69	0.25	2.45	0.49	0.54
$a(R_{\rm b})$	1.4318		2.702		4.3200	4.1000	
$R_{\rm b}^{\rm used}$	0.2172		0.2170		0.2160	0.2155	
$a(R_{\rm c})$	-2.9383		-5.481		-6.7600	-3.8000	
$R_{\rm c}^{\rm used}$	0.1720		0.1733		0.1690	0.1720	
$a(A_{\rm FB}^{\rm b\bar{b}}$(pk))		-2.1333			6.4274		
$A_{\rm FB}^{\rm b\bar{b}}(pk)^{\rm used}$		9.79			8.84		
a(BR(b $\to \ell$))	1.8993		3.674		3.5007	5.1094	
BR(b $\to \ell$)$^{\rm used}$	10.78		11.12		10.50	10.90	
a(BR(b $\to$ c $\to \bar{\ell}$))	-1.0745		-2.964		-3.2917	-1.7660	
BR(b $\to$ c $\to \bar{\ell}$)$^{\rm used}$	8.14		8.03		7.90	8.30	
a(BR(c $\to \ell$))	-3.2732		-1.864		-6.5327	-3.9200	
BR(c $\to \ell$)$^{\rm used}$	9.80		9.80		9.80	9.80	
$a(\overline{\chi})$	0.0453		-0.0784				
$\overline{\chi}^{\rm used}$	0.12460		0.12140				
$a(f(\rm D^+))$				-0.0221			
$f(\rm D^+)^{\rm used}$				0.2210			
$a(f(\rm D_s))$				0.0788			
$f(\rm D_s)^{\rm used}$				0.1120			
$a(f(\Lambda_{\rm c}))$				0.0115			
$f(\Lambda_{\rm c})^{\rm used}$				0.0840			

Table 40: The measurements of $A_{\rm FB}^{\rm c\bar{c}}$(pk). All numbers are given in %

	ALEPH				DELPHI			L3	OPAL		
	90-95 lepton [54]	90-95 lepton [54]	90-95 lepton [54]	91-95 jet charge [58]	91-93† lepton [55]	92-95 D meson [63]	92-95 jet charge [59]	90-95 lepton [56]	91-95 jet charge [61]	90-95† lepton [57]	90-95 D meson [64]
$\sqrt{s}$ (GeV)	92.050	92.940	93.900	92.970	93.017	92.990	92.940	93.100	92.910	92.950	92.950
$A_{\rm FB}^{\rm bb}(+2)$	3.93	10.60	9.03	9.24	15.50	8.78	12.30	13.78	14.60	10.75	-3.40
$A_{\rm FB}^{\rm bb}(+2)$Corrected	10.03			9.21	15.42	8.73	12.30	13.62	14.63	10.74	-3.41
Statistical	1.51			1.79	3.67	6.37	1.60	2.40	1.70	1.43	9.00
Uncorrelated	0.14			0.45	0.50	0.97	0.25	0.34	0.64	0.25	2.16
Correlated	0.24			0.26	0.41	0.13	0.05	0.20	0.34	0.28	1.59
Total Systematic	0.28			0.52	0.65	0.98	0.26	0.40	0.73	0.37	2.68
$a(R_{\rm b})$	-1.964			-0.2430	-2.8933		-0.1962	-3.3756	-12.9000	-0.8000	
$R_{\rm b}^{\rm used}$	0.2192			0.2155	0.2170		0.2158	0.2170	0.2150	0.2155	
$a(R_{\rm c})$	1.575			1.4900	-0.9771		1.2000	1.9869	0.6900	0.8000	
$R_{\rm c}^{\rm used}$	0.1710			0.1726	0.1710		0.1720	0.1734	0.1730	0.1720	
$a(A_{\rm FB}^{\rm c\bar{c}}(+2))$	1.081			1.2018				0.5206	1.3287		
$A_{\rm FB}^{\rm c\bar{c}}(+2)^{\rm used}$	12.51			12.96				12.39	12.08		
$a({\rm BR}({\rm b}\to\ell))$	-1.762				-3.2353			-2.0790		-1.3625	
${\rm BR}({\rm b}\to\ell)^{\rm used}$	11.34				11.00			10.50		10.90	
$a({\rm BR}({\rm b}\to{\rm c}\to\bar{\ell}))$	-0.2478				0.4740			-1.1200		0.7064	
${\rm BR}({\rm b}\to{\rm c}\to\bar{\ell})^{\rm used}$	7.86				7.90			8.00		8.30	
$a({\rm BR}({\rm c}\to\ell))$	1.524				-1.3720			1.9796		0.7840	
${\rm BR}({\rm c}\to\ell)^{\rm used}$	9.80				9.80			9.80		9.80	
$a(\overline{\chi})$	6.584				4.8400						
$\overline{\chi}^{\rm used}$	0.12460				0.12100						
$a(f({\rm D}^+))$						0.3978	0.4229				
$f({\rm D}^+)^{\rm used}$						0.2210	0.2330				
$a(f({\rm D_s}))$						-0.0788	0.0211				
$f({\rm D_s})^{\rm used}$						0.1120	0.1020				
$a(f(\Lambda_{\rm c}))$						0.0573	-0.0855				
$f(\Lambda_{\rm c})^{\rm used}$						0.0840	0.0630				

Table 41: The measurements of $A_{\rm FB}^{\rm b\bar{b}}(+2)$. All numbers are given in %

	ALEPH	DELPHI	OPAL	
	91-95 D meson [62]	92-95 D meson [63]	90-95† lepton [57]	90-95 D meson [64]
$\sqrt{s}$ (GeV)	92.960	92.990	92.950	92.950
$A_{\rm FB}^{\rm c\bar{c}}(+2)$	10.94	11.78	15.65	16.70
$A_{\rm FB}^{\rm c\bar{c}}(+2)$Corrected	10.89	11.65	15.62	16.67
Statistical	3.30	3.20	2.02	4.10
Uncorrelated	0.79	0.52	0.75	0.95
Correlated	0.18	0.07	0.37	0.46
Total Systematic	0.81	0.52	0.84	1.05
$a(R_{\rm b})$			9.6000	
$R_{\rm b}^{\rm used}$			0.2155	
$a(R_{\rm c})$			-8.9000	
$R_{\rm c}^{\rm used}$			0.1720	
$a(A_{\rm FB}^{\rm b\bar{b}}(+2))$	-2.6333			
$A_{\rm FB}^{\rm b\bar{b}}(+2)^{\rm used}$	12.08			
$a({\rm BR}({\rm b}\to\ell))$			9.5375	
${\rm BR}({\rm b}\to\ell)^{\rm used}$			10.90	
$a({\rm BR}({\rm b}\to{\rm c}\to\bar{\ell}))$			-1.5894	
${\rm BR}({\rm b}\to{\rm c}\to\bar{\ell})^{\rm used}$			8.30	
$a({\rm BR}({\rm c}\to\ell))$			-9.2120	
${\rm BR}({\rm c}\to\ell)^{\rm used}$			9.80	
$a(f({\rm D}^+))$		-0.2984		
$f({\rm D}^+)^{\rm used}$		0.2210		
$a(f({\rm D_s}))$		0.0539		
$f({\rm D_s})^{\rm used}$		0.1120		
$a(f(\Lambda_{\rm c}))$		0.0764		
$f(\Lambda_{\rm c})^{\rm used}$		0.0840		

Table 42: The measurements of $A_{\rm FB}^{\rm c\bar{c}}(+2)$. All numbers are given in %

	SLD			
	93-98† lepton [155]	93-98† jet charge [66]	94-98† $K^{\pm}$ [67]	97-98† multi [69]
$\sqrt{s}$ (GeV)	91.280	91.280	91.280	91.280
$\mathcal{A}_{\rm b}$	0.924	0.882	0.960	0.897
Statistical	0.032	0.020	0.040	0.027
Uncorrelated	0.020	0.029	0.056	0.034
Correlated	0.007	0.001	0.002	0.002
Total Systematic	0.022	0.029	0.056	0.034
$a(R_{\rm b})$	-0.0483			
$R_{\rm b}^{\rm used}$	0.2173			
$a(R_{\rm c})$	0.0472			
$R_{\rm c}^{\rm used}$	0.1730			
$a(\mathcal{A}_{\rm c})$	0.0578	0.0134	-0.0112	
$\mathcal{A}_{\rm c}{}^{\rm used}$	0.667	0.670	0.666	
$a(\mathrm{BR}(\mathrm{b}\to\ell))$	-0.2037			
$\mathrm{BR}(\mathrm{b}\to\ell)^{\rm used}$	11.06			
$a(\mathrm{BR}(\mathrm{b}\to\mathrm{c}\to\bar{\ell}))$	0.1103			
$\mathrm{BR}(\mathrm{b}\to\mathrm{c}\to\bar{\ell})^{\rm used}$	8.02			
$a(\mathrm{BR}(\mathrm{c}\to\ell))$	0.0529			
$\mathrm{BR}(\mathrm{c}\to\ell)^{\rm used}$	9.80			
$a(\overline{\chi})$	0.2884			
$\overline{\chi}^{\rm used}$	0.12170			

Table 43: The measurements of $\mathcal{A}_{\rm b}$.

	SLD		
	93-98† lepton [155]	93-97† D meson [156]	93-98† K+vertex [68]
$\sqrt{s}$ (GeV)	91.280	91.280	91.280
$\mathcal{A}_c$	0.567	0.688	0.603
Statistical	0.051	0.035	0.028
Uncorrelated	0.056	0.022	0.023
Correlated	0.018	0.003	0.001
Total Systematic	0.059	0.022	0.023
$a(R_b)$	0.2173		
R_b^{used}	0.2173		
$a(R_c)$	-0.4089		
R_c^{used}	0.1730		
$a(\mathcal{A}_b)$	0.2151	-0.0617	-0.0306
$\mathcal{A}_b{}^{used}$	0.935	0.935	0.900
$a(BR(b \to \ell))$	0.2328		
$BR(b \to \ell)^{used}$	11.06		
$a(BR(b \to c \to \bar{\ell}))$	-0.1178		
$BR(b \to c \to \bar{\ell})^{used}$	8.02		
$a(BR(c \to \ell))$	-0.4077		
$BR(c \to \ell)^{used}$	9.80		
$a(\overline{\chi})$	0.1138		
$\overline{\chi}^{used}$	0.12170		
$a(f(D^+))$			-0.0140
$f(D^+)^{used}$			0.2300
$a(f(D_s))$			-0.0028
$f(D_s)^{used}$			0.1150
$a(f(\Lambda_c))$			0.0005
$f(\Lambda_c)^{used}$			0.0740

Table 44: The measurements of $\mathcal{A}_c$.

	ALEPH	DELPHI	L3		OPAL
	92-93† multi [70]	94-95† multi [71]	92 lepton [72]	94-95† multi [39]	92-95 multi [73]
BR(b $\to \ell$)	11.01	10.65	10.68	10.18	10.83
Statistical	0.10	0.07	0.11	0.13	0.10
Uncorrelated	0.20	0.23	0.36	0.21	0.20
Correlated	0.17	0.42	0.22	0.12	0.21
Total Systematic	0.26	0.48	0.42	0.24	0.29
$a(R_{\mathrm{b}})$			-9.2571		-0.1808
$R_{\mathrm{b}}^{\mathrm{used}}$			0.2160		0.2169
$a(R_{\mathrm{c}})$				1.4450	0.4867
$R_{\mathrm{c}}^{\mathrm{used}}$				0.1734	0.1770
$a(\mathrm{BR}(\mathrm{b} \to \mathrm{c} \to \bar{\ell}))$			-1.1700	0.1618	
$\mathrm{BR}(\mathrm{b} \to \mathrm{c} \to \bar{\ell})^{\mathrm{used}}$			9.00	8.09	
$a(\mathrm{BR}(\mathrm{c} \to \ell))$	0.1960	-0.1960	-2.5480	0.9212	
$\mathrm{BR}(\mathrm{c} \to \ell)^{\mathrm{used}}$	9.80	9.80	9.80	9.80	
$a(\overline{\chi})$	0.2075				
$\overline{\chi}^{\mathrm{used}}$	0.12610				
$a(f(\mathrm{D}^+))$				0.5523	0.1445
$f(\mathrm{D}^+)^{\mathrm{used}}$				0.2330	0.2380
$a(f(\mathrm{D_s}))$				0.0213	0.0055
$f(\mathrm{D_s})^{\mathrm{used}}$				0.1030	0.1020
$a(f(\Lambda_{\mathrm{c}}))$				-0.0427	-0.0157
$f(\Lambda_{\mathrm{c}})^{\mathrm{used}}$				0.0630	0.0650

Table 45: The measurements of BR(b $\to \ell$). All numbers are given in %

	ALEPH	DELPHI	OPAL
	92-93† multi [70]	94-95† multi [71]	90-95 multi [73]
$BR(b \to c \to \bar{\ell})$	7.68	7.88	8.40
Statistical	0.18	0.13	0.16
Uncorrelated	0.26	0.26	0.19
Correlated	0.38	0.36	0.34
Total Systematic	0.46	0.45	0.39
$a(R_b)$			-0.1808
R_b^{used}			0.2169
$a(R_c)$			0.3761
R_c^{used}			0.1770
$a(BR(c \to \ell))$	-0.5880	-0.1960	
$BR(c \to \ell)^{used}$	9.80	9.80	
$a(\overline{\chi})$	-0.5108		
$\overline{\chi}^{used}$	0.12610		
$a(f(D^+))$			0.1190
$f(D^+)^{used}$			0.2380
$a(f(D_s))$			0.0028
$f(D_s)^{used}$			0.1020
$a(f(\Lambda_c))$			-0.0110
$f(\Lambda_c)^{used}$			0.0660

Table 46: The measurements of $BR(b \to c \to \bar{\ell})$. All numbers are given in %

	DELPHI	OPAL
	92-95 D+lepton [43]	90-95 D+lepton [74]
$BR(c \to \ell)$	9.59	9.60
Statistical	0.42	0.60
Uncorrelated	0.24	0.49
Correlated	0.14	0.43
Total Systematic	0.27	0.65
$a(BR(b \to \ell))$	-0.5600	-1.4335
$BR(b \to \ell)^{used}$	11.20	10.99
$a(BR(b \to c \to \bar{\ell}))$	-0.4100	-0.7800
$BR(b \to c \to \bar{\ell})^{used}$	8.20	7.80

Table 47: The measurements of $BR(c \to \ell)$. All numbers are given in %

	ALEPH	DELPHI	L3	OPAL
	90-95 multi [54]	dbl multi [71]	90-95 lepton [56]	90-95† lepton [57]
$\overline{\chi}$	0.12461	0.12700	0.11920	0.11390
Statistical	0.00515	0.01300	0.00680	0.00540
Uncorrelated	0.00252	0.00566	0.00214	0.00306
Correlated	0.00397	0.00554	0.00252	0.00324
Total Systematic	0.00470	0.00792	0.00330	0.00446
$a(R_{\mathrm{b}})$	0.0341		0.0000	
$R_{\mathrm{b}}^{\mathrm{used}}$	0.2192		0.2170	
$a(R_{\mathrm{c}})$	0.0009		0.0004	
$R_{\mathrm{c}}^{\mathrm{used}}$	0.1710		0.1734	
$a(\mathrm{BR}(\mathrm{b} \to \ell))$	0.0524		0.0550	0.0170
$\mathrm{BR}(\mathrm{b} \to \ell)^{\mathrm{used}}$	11.34		10.50	10.90
$a(\mathrm{BR}(\mathrm{b} \to \mathrm{c} \to \bar{\ell}))$	-0.0440		-0.0466	-0.0318
$\mathrm{BR}(\mathrm{b} \to \mathrm{c} \to \bar{\ell})^{\mathrm{used}}$	7.86		8.00	8.30
$a(\mathrm{BR}(\mathrm{c} \to \ell))$	0.0035	-0.0020	0.0006	0.0039
$\mathrm{BR}(\mathrm{c} \to \ell)^{\mathrm{used}}$	9.80	9.80	9.80	9.80

Table 48: The measurements of $\overline{\chi}$.

	DELPHI	OPAL
	92-95 D meson [43]	90-95 D meson [45]
$\mathrm{P}(\mathrm{c} \to \mathrm{D}^{*+}) \times \mathrm{BR}(\mathrm{D}^{*+} \to \pi^{+}\mathrm{D}^{0})$	0.1740	0.1513
Statistical	0.0100	0.0096
Uncorrelated	0.0040	0.0088
Correlated	0.0007	0.0011
Total Systematic	0.0041	0.0089
$a(R_{\mathrm{b}})$	0.0293	
$R_{\mathrm{b}}^{\mathrm{used}}$	0.2166	
$a(R_{\mathrm{c}})$	-0.0158	
$R_{\mathrm{c}}^{\mathrm{used}}$	0.1735	

Table 49: The measurements of $\mathrm{P}(\mathrm{c} \to \mathrm{D}^{*+}) \times \mathrm{BR}(\mathrm{D}^{*+} \to \pi^{+}\mathrm{D}^{0})$.

	ALEPH	DELPHI	OPAL
	91-95† D meson [46]	92-95 D meson [44]	91-94 D meson [47]
$R_c f_{D^+}$	0.0406	0.0384	0.0390
Statistical	0.0013	0.0013	0.0050
Uncorrelated	0.0014	0.0015	0.0042
Correlated	0.0032	0.0025	0.0031
Total Systematic	0.0035	0.0030	0.0052
$a(f(D^+))$		0.0008	
$f(D^+)^{used}$		0.2210	
$a(f(D_s))$		-0.0002	
$f(D_s)^{used}$		0.1120	
$a(f(\Lambda_c))$		0.0000	
$f(\Lambda_c)^{used}$		0.0840	

Table 50: The measurements of $R_c f_{D^+}$.

	ALEPH	DELPHI	OPAL
	91-95† D meson [46]	92-95 D meson [44]	91-94 D meson [47]
$R_c f_{D_s}$	0.0207	0.0213	0.0160
Statistical	0.0033	0.0017	0.0042
Uncorrelated	0.0011	0.0010	0.0016
Correlated	0.0053	0.0054	0.0043
Total Systematic	0.0054	0.0055	0.0046
$a(f(D^+))$		0.0007	
$f(D^+)^{used}$		0.2210	
$a(f(D_s))$		-0.0009	
$f(D_s)^{used}$		0.1120	
$a(f(\Lambda_c))$		-0.0001	
$f(\Lambda_c)^{used}$		0.0840	

Table 51: The measurements of $R_c f_{D_s}$.

	ALEPH	DELPHI	OPAL
	91-95† D meson [46]	92-95 D meson [44]	91-94 D meson [47]
$R_c f_{\Lambda_c}$	0.0157	0.0169	0.0091
Statistical	0.0018	0.0035	0.0050
Uncorrelated	0.0007	0.0016	0.0015
Correlated	0.0044	0.0045	0.0035
Total Systematic	0.0045	0.0048	0.0038
$a(f(D^+))$		0.0002	
$f(D^+)^{\text{used}}$		0.2210	
$a(f(D_s))$		-0.0001	
$f(D_s)^{\text{used}}$		0.1120	
$a(f(\Lambda_c))$		-0.0002	
$f(\Lambda_c)^{\text{used}}$		0.0840	

Table 52: The measurements of $R_c f_{\Lambda_c}$.

	ALEPH	DELPHI	OPAL
	91-95† D meson [46]	92-95 D meson [44]	91-94 D meson [47]
$R_c f_{D^0}$	0.0964	0.0926	0.0997
Statistical	0.0029	0.0026	0.0070
Uncorrelated	0.0040	0.0038	0.0057
Correlated	0.0045	0.0023	0.0041
Total Systematic	0.0060	0.0044	0.0070
$a(f(D^+))$		0.0020	
$f(D^+)^{\text{used}}$		0.2210	
$a(f(D_s))$		-0.0004	
$f(D_s)^{\text{used}}$		0.1120	
$a(f(\Lambda_c))$		-0.0004	
$f(\Lambda_c)^{\text{used}}$		0.0840	

Table 53: The measurements of $R_c f_{D^0}$.

	DELPHI	OPAL
	92-95 D meson [44]	90-95 D meson [45]
$R_c P(c \to D^{*+}) \times BR(D^{*+} \to \pi^+ D^0)$	0.0282	0.0266
Statistical	0.0007	0.0005
Uncorrelated	0.0010	0.0010
Correlated	0.0007	0.0009
Total Systematic	0.0012	0.0014
$a(f(D^+))$	0.0006	
$f(D^+)^{\text{used}}$	0.2210	
$a(f(D_s))$	-0.0001	
$f(D_s)^{\text{used}}$	0.1120	
$a(f(\Lambda_c))$	-0.0004	
$f(\Lambda_c)^{\text{used}}$	0.0840	

Table 54: The measurements of $R_c P(c \to D^{*+}) \times BR(D^{*+} \to \pi^+ D^0)$.

References

[1] The LEP Collaborations ALEPH, DELPHI, L3, OPAL and the LEP Electroweak Working Group, and the SLD Heavy Flavour and Electroweak Groups, *A Combination of Preliminary Electroweak Measurements and Constraints on the Standard Model*, CERN-EP/99-15.

[2] The LEP Collaborations ALEPH, DELPHI, L3, OPAL and the LEP Electroweak Working Group, *Combined Preliminary Data on* Z *Parameters from the LEP Experiments and Constraints on the Standard Model*, CERN-PPE/94-187.

[3] The LEP Experiments: ALEPH, DELPHI, L3 and OPAL, Nucl. Inst. Meth. **A378** (1996) 101.

[4] ALEPH Collaboration, D. Decamp *et al.*, Z. Phys. **C48** (1990) 365;
ALEPH Collaboration, D. Decamp *et al.*, Z. Phys. **C53** (1992) 1;
ALEPH Collaboration, D. Buskulic *et al.*, Z. Phys. **C60** (1993) 71;
ALEPH Collaboration, D. Buskulic *et al.*, Z. Phys. **C62** (1994) 539;
ALEPH Collaboration, R. Barate *et al.*, *Measurement of the Z Resonance Parameters at LEP*, CERN-EP/99-104, submitted to Eur. Phys. Jour. C.
The very small differences between the results of this reference and those of Tables 3 and 6 are due to special fits, which are based on a common energy matrix and explicitely include the t-channel dependence on m_{Z} in the $\mathrm{e^+e^-}$ final state.

[5] DELPHI Collaboration, P. Aarnio *et al.*, Nucl. Phys. **B367** (1991) 511;
DELPHI Collaboration, P. Abreu *et al.*, Nucl. Phys. **B417** (1994) 3;
DELPHI Collaboration, P. Abreu *et al.*, Nucl. Phys. **B418** (1994) 403;
DELPHI Collaboration, DELPHI Note 98-113 CONF 175, June 1998;
DELPHI Collaboration, *Update of Z parameters for EPS-HEP99*, contributed paper to EPS-HEP 99, Tampere, **6_361**.

[6] L3 Collaboration, B. Adeva *et al.*, Z. Phys. **C51** (1991) 179;
L3 Collaboration, O. Adriani *et al.*, Phys. Rep. **236** (1993) 1;
L3 Collaboration, M. Acciarri *et al.*, Z. Phys. **C62** (1994) 551;
L3 Collaboration, *Precise Determination of Z Parameters*, L3 Note 2436, contributed paper to EPS-HEP 99, Tampere, **6_259**.

[7] OPAL Collaboration, G. Alexander *et al.*, Z. Phys. **C52** (1991) 175;
OPAL Collaboration, P.D. Acton *et al.*, Z. Phys. **C58** (1993) 219;
OPAL Collaboration, R. Akers *et al.*, Z. Phys. **C61** (1994) 19;
OPAL Collaboration, *Precision Measurements of the Z^0 Lineshape and Lepton Asymmetry*, OPAL Physics Note PN358, July 1998;
OPAL Collaboration, *Precision Luminosity for Z^0 Lineshape Measurements with a Silicon-Tungsten Calorimeter*, CERN-EP/99-136, submitted to Eur. Phys. Jour. C;
OPAL Collaboration, *Update to Precision Measurements of the Z^0 Lineshape and Lepton Asymmetry*, OPAL Physics Note PN404, July 1999.

[8] G. Montagna *et al.*, Nucl. Phys. **B547** (1999) 39;
G. Montagna *et al.*, *Light Pair Corrections to Small-Angle Bhabha Scattering in Realistic Set-up at LEP*, FNT/T-99/06, to be submitted to Phys Lett. B.

[9] B.F.L Ward *et al.*, Phys. Lett. **B450** (1999) 262.

[10] The LEP Collaborations ALEPH, DELPHI, L3, OPAL and the LEP Electroweak Working Group, *Updated Parameters of the* Z *Resonance from Combined Preliminary Data of the LEP Experiments*, CERN-PPE/93-157.

[11] F.A. Berends et al., in *Z Physics at LEP 1, Vol. 1*, ed. G. Altarelli, R. Kleiss and C. Verzegnassi, (CERN Report: CERN 89-08, 1989), p. 89.
M. Böhm et al., in *Z Physics at LEP 1, Vol. 1*, ed. G. Altarelli, R. Kleiss and C. Verzegnassi, (CERN Report: CERN 89-08, 1989), p. 203.

[12] See, for example, M. Consoli *et al.*, in "Z Physics at LEP 1", CERN Report CERN 89-08 (1989), eds G. Altarelli, R. Kleiss and C. Verzegnassi, Vol. 1, p. 7.

[13] S. Jadach, *et al.*, Phys. Lett. **B257** (1991) 173.

[14] M. Skrzypek, Acta Phys. Pol. **B23** (1992) 135.

[15] G. Montagna, *et al.*, Phys. Lett. **B406** (1997) 243.

[16] LEP Electroweak Working Group, *Precise Determination of Z-Boson Parameters from Combined Results of LEP Experiments*, LEP EWWG/LS 99-01.

[17] LEP Energy Working Group, R. Assmann *et al.*, Eur. Phys. Jour. **C6** (1999) 187.

[18] LEP Energy Working Group note 96-07, E. Lancon and A. Blondel, *Determination of the LEP Energy Spread Using Experimental Constraints.*

[19] D. Bardin, M. Grünewald and G. Passarino, *Precision Calculation Project Report*, hep-ph/9902452.

[20] Combination of the LEP2 $f\bar{f}$ Results, LEPEWWG $f\bar{f}$ subgroup note, LEP2FF/99-01.

[21] ALEPH Collab., *"A study of Fermion Pair Production in* e^+e^- *Collisions at 130-183 GeV"*, CERN-EP/99-042 (submitted to Eur. Phys Jour. **C**); ALEPH Collab., *"Fermion Pair Production in* e^+e^- *Collisions at 189 GeV and Limits on Physics beyond the Standard Model"*, ALEPH-CONF/99-013, contribution #6_694 to EPS-HEP conference, Tampere, Finland (1999);
DELPHI Collab., *"Results on Fermion-Pair Production at LEP running near 183 and 189 GeV"*, DELPHI-MORIO-CONF-247, contribution #6_362 to EPS-HEP conference, Tampere, Finland (1999);
L3 Collab., *"Measurement of Hadron and Lepton-Pair Production above the Z resonance"*, L3 note 2398, contribution #6_262 to EPS-HEP conference, Tampere, Finland (1999);
OPAL Collab., *"Tests of the Standard Model and Constraints on New Physics from Measurements of Fermion Pair Production at 183 GeV at LEP"*, Eur. Phys. Jour. **C6** (1999) 1; *"Tests of the Standard Model and Constraints on New Physics from Measurements of Fermion Pair Production at LEP2"*, contribution #20 to EPS-HEP conference, Tampere, Finland (1999).

[22] D. Bardin *et al.*, Z. Phys. **C44** (1989) 493; Comp. Phys. Comm. **59** (1990) 303; Nucl. Phys. **B351**(1991) 1; Phys. Lett. **B255** (1991) 290 and CERN-TH 6443/92 (May 1992); the most recent version of Zfitter (6.21) is described in hep-ph/9908433 and DESY 99-070 (Aug 1999).

[23] G. Montagna *et al.*, Comput. Phys. Commun. **117** (1999) 278;
http://www.to.infn.it/∼giampier/topaz0.html .

[24] S. Jadach *et al.*, http://home.cern.ch/∼jadach/KKindex.html .

[25] LEP2 Monte Carlo Workshop: http://www.to.infn.it/∼giampier/lep2.html .

[26] Private communication: D. Bardin, G. Passarino, S. Jadach.

[27] LEP EWWG $f\bar{f}$ subgroup: http://www.cern.ch/LEPEWWG/lep2/ .

[28] E. Eichten, K. Lane and M. Peskin, Phys. Rev. Lett. **50** (1983) 811.

[29] H. Kroha, Phys. Rev. **D46** (1992) 58.

[30] ALEPH Collaboration, D. Buskulic *et al.*, Zeit. Phys. **C69** (1996) 183;
ALEPH Collaboration, *Measurement of the tau polarisation by ALEPH with the full LEP I data sample*, ALEPH 96-067 CONF 98-037, contributed paper to ICHEP 98 Vancouver **ICHEP'98 #939**.

[31] DELPHI Collaboration, *A Precise Measurement of τ Polarisation at LEP-I*, DELPHI 99-130 CONF 317, contributed paper to EPS-HEP 99, Tampere, 15-21 July 1999.

[32] L3 Collaboration, M. Acciarri *et al.*, Phys. Lett. **B429** (1998) 387.

[33] OPAL Collaboration, G.Alexander *et al.*, Z. Phys. **C75** (1996) 365.

[34] SLD Collaboration, J. Brau, *Electroweak Precision Measurements with Leptons*, talk presented at EPS-HEP-99, Tampere, Finland, 15-21 July 1999.

[35] The LEP Heavy Flavour Group, *Input Parameters for the LEP/SLD Electroweak Heavy Flavour Results for Summer 1998 Conferences* , LEPHF/98-01,
http://www.cern.ch/LEPEWWG/heavy/lephf9801.ps.gz.

[36] OPAL Collaboration, G. Abbiendi *et al.*, *Measurement of the Production Rate of Charm Quark Pairs from Gluons in Hadronic Z0 Decays* CERN EP/99-089 subm. to Eur. Phys. J. C.

[37] ALEPH Collaboration, R. Barate *et al.*, Physics Letters **B 401** (1997) 150;
ALEPH Collaboration, R. Barate *et al.*, Physics Letters **B 401** (1997) 163.

[38] DELPHI Collaboration, P.Abreu *et al.*, *A precise measurement of the partial decay width ratio* $R_b^0 = \Gamma_{b\bar{b}}/\Gamma_{had}$ CERN EP/98-180, subm. to Eur. Phys. Jour.

[39] L3 Collaboration, *Measurement R_b and Br($b \to \ell\nu X$) at LEP Using Double Tag Methods,* L3 Note 2420 contributed paper to the EPS-HEP-99, Tampere, **5_282**.

[40] OPAL Collaboration, G. Abbiendi *et al.*, Eur. Phys. J. **C8** (1999) 217.

[41] SLD Collaboration, SLAC-PUB-7585, contributed paper to EPS-HEP-97, Jerusalem, **EPS-118**;
V.Serbo, *Electroweak measurements with heavy quarks at SLD*, III International conference on Hyperons, Charm and Beauty Hadrons, Genova, Italy, June/30–July/3/1998.

[42] ALEPH Collaboration, R. Barate *et al.*, Eur. Phys. J. **C4** (1998) 557.

[43] DELPHI Collaboration, *Determination of $P(c \to D^{*+})$ and $BR(c \to l^+)$ at LEP I* CERN EP/99-67, subm. to Eur. Phys. Jour.

[44] DELPHI Collaboration, *Measurement of the Z Partial Decay Width into $c\bar{c}$ and Multiplicity of Charm Quarks per b Decay* CERN EP/99-66, subm. to Eur. Phys. Jour.

[45] OPAL Collaboration, K. Ackerstaff *et al.*, Eur. Phys. J. **C1** (1998) 439.

[46] ALEPH Collaboration, *Study of Charmed Hadron Production in Z Decays,* contributed paper to the EPS-HEP-97, Jerusalem, **EPS-623**.

[47] OPAL Collaboration, G. Alexander *et al.*, Z. Phys. **C72** (1996) 1.

[48] DELPHI Collaboration, *Summary of R_c measurements in DELPHI,* DELPHI 96-110 CONF 37 contributed paper to ICHEP96, Warsaw, 25-31 July 1996 **PA01-060**.

[49] SLD Collaboration, *A Measurement of R_c with the SLD Detector* SLAC–PUB–7880, contributed paper to ICHEP 98 Vancouver **ICHEP'98 #174** ;
N. de Groot, *Electroweak results from SLD*, talk prsented at XXXIVth Rencontres de Moriond, Electroweak Interactions and Unified Theories, Les Arcs, March 13-20 1999.

[50] D. Abbaneo *et al.*, Eur. Phys. J. **C4** (1998) 2, 185.

[51] V. Ravindran, W.L. van Neerven, Phys. Lett. **B445** (1998) 206.

[52] S. Catani, M. Seymour, *Corrections of $\mathcal{O}(\alpha_s^2)$ to the forward backward asymmetry*, hep-ph/9905424.

[53] G. Altarelli, B. Lampe, Nucl. Phys. **B 391** (1993) 3.

[54] ALEPH Collaboration, D. Buskulic *et al.*, Phys. Lett. **B384** (1996)414;
ALEPH Collaboration, *Measurement of the b and c forward-backward asymmetries using leptons* ALEPH 99-076 CONF 99-048, contributed paper to EPS 99 Tampere **HEP'99 #6-65**.

[55] DELPHI Collaboration, P.Abreu *et al.*, Z. Phys **C65** (1995) 569;
DELPHI Collaboration, *Measurement of the Forward-Backward Asymmetries of $e^+e^- \to Z \to b\overline{b}$ and $e^+e^- \to Z \to c\overline{c}$ using prompt leptons* DELPHI 98-143 CONF 204, contributed paper to ICHEP 98 Vancouver **ICHEP'98 #124** .
Delphi notes are available at http://wwwcn.cern.ch/~pubxx/www/delsec/delnote/.

[56] L3 Collaboration, O. Adriani *et al.*, Phys. Lett. **B292** (1992) 454;
L3 Collaboration, *L3 Results on $A_{\rm FB}^{\rm b\bar{b}}$, $A_{\rm FB}^{\rm c\bar{c}}$ and χ for the Glasgow Conference,* L3 Note 1624;
L3 Collaboration, M. Acciarri *et al.*, Phys. Lett. **B448** (1999) 152.

[57] OPAL Collaboration, G. Alexander *et al.*, Z. Phys. **C70** (1996) 357;
OPAL Collaboration, *Updated Measurement of the Heavy Quark Forward-Backward Asymmetries and Average B Mixing Using Leptons in Multihadronic Events*, OPAL Physics Note PN226 contributed paper to ICHEP96, Warsaw, 25-31 July 1996 **PA05-007**
OPAL Collaboration, *QCD corrections to the bottom and charm forward-backward asymmetries* OPAL Physics Note PN284.

[58] ALEPH Collaboration, R. Barate *et al.*, Phys. Lett. **B426**, (1998) 217.

[59] DELPHI Collaboration, P.Abreu *et al.*, Eur. Phys. Jour. **C9** (1999) 367.

[60] L3 Collaboration, M. Acciarri *et al.*, Phys. Lett. **B439** (1998) 225.

[61] OPAL Collaboration, K.Ackerstaff *et al.*, Z. Phys. **C75** (1997) 385.

[62] ALEPH Collaboration, R. Barate *et al.*, Phys. Lett. **B434** (1999) 415.

[63] DELPHI Collaboration, P.Abreu *et al.*, *Measurement of the forward backward asymmetry of c and b quarks at the Z pole using reconstructed D mesons* CERN EP/99-07, subm. to Eur. Phys. Jour.

[64] OPAL Collaboration, G. Alexander *et al.*, Z. Phys. **C73** (1996) 379.

[65] N. de Groot, *Electroweak results from SLD*, talk prsented at XXXIVth Rencontres de Moriond, Electroweak Interactions and Unified Theories, Les Arcs, March 13-20 1999.

[66] SLD Collaboration, *Measurement of $\mathcal{A}_b$ at the Z resonance using a Jet-Charge Technique* SLAC–PUB–7886, contributed paper to ICHEP 98 Vancouver **ICHEP'98 #179** ;
N. de Groot, *Electroweak results from SLD*, talk prsented at XXXIVth Rencontres de Moriond, Electroweak Interactions and Unified Theories, Les Arcs, March 13-20 1999.

[67] SLD Collaboration, K. Abe *et al.*, Phys. Rev. Lett. **83** (1999) 1902;
SLD Collaboration, K. Abe *et al.*, *Direct measurement of* $\mathcal{A}_b$ *using charged kaons at the SLD detector*, SLAC-PUB-8200, contributed paper to EPS-HEP-99, Tampere, **6-473**.

[68] SLD Collaboration, K. Abe *et al.*, *Direct measurement of* $\mathcal{A}_c$ *using inclusive charm tagging at the SLD detector*, SLAC-PUB-8199, contributed paper to EPS-HEP-99, Tampere, **6-474**.

[69] SLD Collaboration, K. Abe *et al.*, *New measurement of* $\mathcal{A}_b$ *at the* Z^0 *resonance using a vertex-charge technique*, SLAC-PUB-8201, contributed paper to EPS-HEP-99, Tampere, **6-473**.

[70] ALEPH Collaboration., D. Buskulic *et al.*, *Measurement of the semileptonic b branching ratios from inclusive leptons in Z decays*, Contributed Paper to EPS-HEP-95 Brussels, **eps0404**.
This note may be found at http://alephwww.cern.ch/ALPUB/oldconf/HEP95/HEP95.html.

[71] DELPHI Collaboration, *Measurement of the semileptonic b branching ratios in Z decays* DELPHI 99-111 CONF 298, contributed paper to EPS 99 Tampere **HEP'99 #5_522** .

[72] L3 Collaboration, M. Acciarri *et al.*, Z Phys. **C71** 379 (1996).

[73] OPAL Collaboration, G. Abbiendi *et al.*, *Measurements of inclusive semileptonic branching fractions of b hadrons in* Z^0 *decays*, CERN-EP/99-078, Submitted to Eur. Phys. Jour. C.

[74] OPAL Collaboration, G. Abbiendi *et al.*, Eur. Phys. J. **C8** (1999) 573.

[75] ALEPH Collaboration, D. Decamp *et al.*, Phys. Lett. **B259** (1991) 377.

[76] ALEPH Collaboration, ALEPH-Note 93-041 PHYSIC 93-032 (1993);
ALEPH Collaboration, ALEPH-Note 93-042 PHYSIC 93-033 (1993);
ALEPH Collaboration, ALEPH-Note 93-044 PHYSIC 93-035 (1993).

[77] ALEPH Collaboration, D. Buskulic *et al.*, Z. Phys. **C71** (1996) 357.

[78] DELPHI Collaboration, P. Abreu *et al.*, Phys. Lett. **B277** (1992) 371.

[79] DELPHI Collaboration, *Measurement of the Inclusive Charge Flow in Hadronic Z Decays,* DELPHI 96-19 PHYS 594.

[80] OPAL Collaboration, P. D. Acton *et al.*, Phys. Lett. **B294** (1992) 436.

[81] OPAL Collaboration, *A determination of* $\sin^2\theta_W$ *from an inclusive sample of multihadronic events,* OPAL Physics Note PN195 (1995).

[82] T. Sjöstrand, Comp. Phys. Comm. **82** (1994) 74.

[83] G. Marchesini *et al.*, Comp. Phys. Comm. **67** (1992) 465.

[84] Calibration Working Group, contributed paper Conference on High-Energy Physics (ICHEP 98), LEP Energy Note 98/02. LEP Energy Calibration Working Group, *Evaluation of the LEP centre-of-mass energy for data taken in 1998*, LEP Energy Note 99/01.

[85] ALEPH Collaboration, R. Barate, *et al.*, Phys. Lett. **B453** (1999) 107.

[86] DELPHI Collaboration, *W-pair Production cross-section and W branching ratios in* e^+e^- *interactions at 183 GeV*, CERN-EP/99–47.

[87] L3 Collaboration, M. Acciarri, *et al.*, Phys. Lett. **B436** (1998) 437.

[88] OPAL Collaboration, *W^+W^- production and triple gauge boson couplings at LEP energies up to 183 GeV*, G. Abbiendi, *et al.*, Eur. Phys. Jour. **C8** (1999) 191.

[89] ALEPH Collaboration, *Measurement of W-pair production in e^+e^- collisions at 189 GeV*, ALEPH note 99-064 CONF-99-038.

[90] DELPHI Collaboration, *Results on WW and ZZ production in e^+e^- collisions at $\sqrt{s}$ = 189 GeV*, DELPHI note 98-146 CONF 206.

[91] L3 Collaboration, *Preliminary Results on the Measurement of W-pair Cross Sections in e^+e^- Interactions at $\sqrt{s}$ = 189 GeVand W-Decay Branching Fractions*, L3 note 2376, contributed paper to EPS-HEP 99, Tampere, **6_253**.

[92] OPAL Collaboration, *W^+W^- production in e^+e^- collisions at $\sqrt{s}$ = 189 GeV*, OPAL Physics note PN378.

[93] ALEPH Collaboration, R. Barate, *et al.*, Phys. Lett. **B453** (1999) 121.

[94] DELPHI Collaboration, *Measurement of the mass W boson using direct reconstruction at $\sqrt{s}$ = 183 GeV*, CERN-EP/99–79.

[95] L3 Collaboration, M. Acciarri, *et al.*, Phys. Lett. **B454** (1999) 386.

[96] OPAL Collaboration, *Measurement of the W Mass and Width in $e^+e^- \to W^+W^-$ at 183 GeV*, G. Abbiendi, *et al.*, Phys. Lett. **B453** (1999) 138.

[97] ALEPH Collaboration, *Measurement of the W mass from $W \to lnu$ decays at 183 GeV* ALEPH note 99-015 CONF-99-010.

[98] ALEPH Collaboration, *Measurement of the W Mass in e^+e^- Collisions from 161 to 189 GeV*, ALEPH note 99-017 CONF-99-12.

[99] DELPHI Collaboration, *Direct measurement m_{W}*, DELPHI note 99-64 CONF 251
The W mass extracted from the τ semileptonic channel has not been used in the LEP average.

[100] L3 Collaboration, *Preliminary Results on the Measurement of Mass and Width of the W Boson at LEP*, L3 note 2377, contributed paper to EPS-HEP 99, Tampere, **6_255**.

[101] OPAL Collaboration, *Measurement of the W boson mass in e^+e^- collisions at 189 GeV*, OPAL Physics note PN385.

[102] LEP Energy Calibration Working Group, *Evaluation of the LEP centre-of-mass energy above w-pair production threshold*, CERN-EP/98-191, CERN-SL/98-073, submitted to Eur. Phys. Jour. C.

[103] D. Bardin, *et al.*, Comp. Phys. Comm. **104** (1997) 161.

[104] The Particle Data Group, C. Caso et al., Eur. Phys. Jour. **C3** (1998) 1.

[105] ALEPH Collaboration, *A direct measurement of $|V_{cs}|$ in hadronic W decays using a charm tag*, ALEPH note 99-062 CONF-99-037.

[106] DELPHI Collaboration, *Measurement of $|V_{cs}|$ using W-decays at LEP 2*, P. Abreu, *et al.*, Phys. Lett. bf B439 (1998) 209.

[107] L3 Collaboration, *Measurement of $W \to cs$ and direct determination of $|V_{cs}|$* , L3 note 2232.

[108] OPAL Collaboration, *A measurement of Charm Production in* $e^+e^- \to W^+W^-$ *at LEP2*, OPAL Physics Note PN402.

[109] The LEP Collaborations ALEPH, DELPHI, L3, OPAL and the LEP Electroweak Working Group, and the SLD Heavy Flavour Group, *A Combination of Preliminary LEP Electroweak Measurements and Constraints on the Standard Model*, CERN-PPE/97-154.

[110] The LEP-TGC Combination group, LEPEWWG/TGC/98-02 and references therein.

[111] The ALEPH Collaboration, R. Barate *et al.*, Phys. Lett. **B 422** (1998) 369;
The ALEPH Collaboration, ALEPH 99-072 CONF 99-046;
The ALEPH Collaboration, ALEPH 98-052 CONF 99-028.

[112] The DELPHI Collaboration, P. Abreu *et al.*, Phys. Lett. **B 423** (1998) 194;
The DELPHI Collaboration, DELPHI 99-63/CONF 250.

[113] The L3 Collaboration, M. Acciari *et al.*, Phys. Lett. **B 413** (1998) 176;
The L3 Collaboration, L3 Note 2378, March 1999;
The L3 Collaboration, L3 Note 2367, July 1999.

[114] The OPAL Collaboration, G. Abbiendi *et al.*, Eur. Phys. Jour. **C 8** (1999) 191;
The OPAL Collaboration, OPAL physics note PN375, March 1999.

[115] The DØ Collaboration, S. Abachi *et al.*, Phys. Rev. **D 58** (1998) 3102.

[116] K. Gaemers and G. Gounaris, Z. Phys. **C 1** (1979) 259.

[117] K. Hagiwara, S. Ishihara, R. Szlapski, and D. Zeppenfeld, Phys. Lett. **B 283** (1992) 353;
K. Hagiwara, S. Ishihara, R. Szlapski, and D. Zeppenfeld, Phys. Rev. **D 48** (1993) 2182.

[118] M. Bilenky, J. L. Kneur, F. M. Renard and D. Schildknecht, Nucl. Phys. **B 409** (1993) 22;
M. Bilenky, J. L. Kneur, F. M. Renard and D. Schildknecht, Nucl. Phys. **B 419** (1994) 240.

[119] I. Kuss and D. Schildknecht, Phys. Lett. **B 383** (1996) 470.

[120] G. Gounaris and C. G. Papadopoulos, Eur. Phys. Jour. **C2** (1998) 365.

[121] G. Gounaris *et al.*, in *Physics at LEP 2*, Report CERN 96-01 (1996), eds G. Altarelli, T. Sjöstrand, F. Zwirner, Vol. 1, p. 525.

[122] L3 Collaboration, M. Acciarri, *et al.*, Phys. Lett. **B450** (1999) 281.

[123] ALEPH Collaboration, *Measurement of the* $e^+e^- \to ZZ$ *Production Cross Section at Centre-of-mass Energies of 183 and 189 GeV*, ALEPH note 99-060 CONF-99-035.

[124] DELPHI Collaboration, *Measurement of the* Z^0Z^0 *cross-section in* e^+e^- *interactions at 189 GeV*, DELPHI note 99-69 CONF 256.

[125] L3 Collaboration, *ZZ Production in* e^+e^- *interactions at* $\sqrt{s}$*=189 GeV*, L3 note 2413, contributed paper to EPS-HEP 99, Tampere, **7_249**.

[126] OPAL Collaboration, *Study of Z Boson Pair Production in* e^+e^- *Collisions at* $\sqrt{s}$*=183 and 189 GeV*, OPAL Physics Note PN408.

[127] S. Jadach, W. Placzek and B.F.L. Ward, Phys. Rev. **D56** (1997) 74.

[128] CHARM II Collaboration, P. Vilain *et al.*, Phys. Lett. **B335** (1994) 246.

[129] UA2 Collaboration, J. Alitti *et al.*, Phys. Lett. **B276** (1992) 354.

[130] CDF Collaboration, F. Abe *et al.*, Phys. Rev. Lett. **65** (1990) 2243;
CDF Collaboration, F. Abe *et al.*, Phys. Rev. **D43** (1991) 2070.

[131] CDF Collaboration, F. Abe *et al.*, Phys. Rev. Lett. **75** (1995) 11;
CDF Collaboration, F. Abe *et al.*, Phys. Rev. **D52** (1995) 4784.
A. Gordon, talk presented at XXXIInd Rencontres de Moriond, Les Arcs, 16-22 March 1997, to appear in the proceedings.

[132] DØ Collaboration, S. Abachi *et al.*, Phys. Rev. Lett. **77** (1996), 3309;
K. Streets, talk presented at Hadron Collider Physics 97, Stony Brook, to appear in the proceedings.

[133] Y.K. Kim, talk presented at the Lepton-Photon Symposium 1997, Hamburg, 28 July - 1 Aug, 1997, to appear in the proceedings.

[134] CDF Collaboration, W. Yao, *t Mass at CDF*, talk presented at ICHEP 98, Vancouver, B.C., Canada, 23-29 July, 1998.

[135] DØ Collaboration, B. Abbott *et al.*, Phys. Rev. **D58** (1998) 052001.

[136] R. Partridge, *Heavy Quark Production and Decay (t and b Onia)*, talk presented at ICHEP 98, Vancouver, B.C., Canada, 23-29 July, 1998.

[137] CCFR/NuTeV Collaboration, K. McFarland *et al.*, Eur. Phys. Jour. **C1** (1998) 509.

[138] NuTeV Collaboration, K. McFarland, talk presented at the XXXIIIth Rencontres de Moriond, Les Arcs, France, 15-21 March, 1998, hep-ex/9806013. The result quoted is a combination of the NuTeV and CCFR results.

[139] T. van Ritbergen and R.G. Stuart, Phys. Rev. Lett. **82** (1999) 488.

[140] S. Eidelmann and F. Jegerlehner, Z. Phys. **C67** (1995) 585.

[141] M. Steinhauser, Phys. Lett. **B429** (1998) 158.

[142] *Reports of the working group on precision calculations for the Z resonance*, eds. D. Bardin, W. Hollik and G. Passarino, CERN Yellow Report 95-03, Geneva, 31 March 1995.

[143] G. Degrassi, S. Fanchiotti and A. Sirlin, Nucl. Phys. **B351** (1991) 49;
G. Degrassi and A. Sirlin, Nucl. Phys. **B352** (1991) 342;
G. Degrassi, P. Gambino and A. Vicini, Phys. Lett. **B383** (1996) 219;
G. Degrassi, P. Gambino and A. Sirlin, Phys. Lett. **B394** (1997) 188.

[144] A. Czarnecki and J. Kühn, Phys. Rev. Lett. **77** (1996) 3955;
R. Harlander, T. Seidensticker and M. Steinhauser, Phys. Lett. **B426** (1998) 125.

[145] Electroweak libraries:
ZFITTER: see Reference 22;
BHM (G. Burgers, W. Hollik and M. Martinez): W. Hollik, Fortschr. Phys. **38** (1990) 3, 165; M. Consoli, W. Hollik and F. Jegerlehner: Proceedings of the Workshop on Z physics at LEP I, CERN Report 89-08 Vol.I,7 and G. Burgers, F. Jegerlehner, B. Kniehl and J. Kühn: the same proceedings, CERN Report 89-08 Vol.I, 55;
TOPAZ0 Version 4.0i: G. Montagna, O. Nicrosini, G. Passarino, F. Piccinni and R. Pittau, Nucl. Phys. **B401** (1993) 3; Comp. Phys. Comm. **76** (1993) 328.

These computer codes have upgraded by including the results of [142] and references therein. ZFITTER and TOPAZ0 have been further updated using the results of references 143 and 144. See, D. Bardin and G. Passarino, *Upgrading of Precision Calculations for Electroweak Observables*, CERN-TH/98-92, hep-ph/9803425.

[146] T. Hebbeker, M. Martinez, G. Passarino and G. Quast, Phys. Lett. **B331** (1994) 165;
P.A. Raczka and A. Szymacha, Phys. Rev. **D54** (1996) 3073;
D.E. Soper and L.R. Surguladze, Phys. Rev. **D54** (1996) 4566.

[147] M. L. Swartz, Phys. Rev. **D53** (1996) 5268.

[148] A.D. Martin and D. Zeppenfeld, Phys. Lett. **B345** (1994) 558.

[149] H. Burkhardt and B. Pietrzyk, Phys. Lett. **B356** (1995) 398.

[150] R. Alemany, *et al.*, Eur. Phys. J. **C2** (1998) 123.

[151] M. Davier and A. Höcker, Phys. Lett. **B419** (1998) 419.

[152] J.H. Kühn and M. Steinhauser, Phys. Lett. **B437** (1998) 425.

[153] J. Erler, Phys. Rev. **D59**, (1999) 054008.

[154] A.Read, *Search for the Standard Model Higgs at LEP"*, talk presented at EPS-HEP 99, Tampere, Finland, 15-21 July, 1999.

[155] SLD Collaboration, SLAC–PUB–7637, contributed paper to EPS-HEP-97, Jerusalem, **EPS-124**;
S. Fahey, *Measurements of Quark Coupling Asymmetries on the Z*, talk presented at EPS-HEP-99, Tampere, Finland, July 15-21, 1999.

[156] SLD Collaboration, K. Abe, *et al.*, *Measurement of $\mathcal{A}_c$ with charmed mesons at SLD*, SLAC-PUB-8195, contributed paper to EPS-HEP-99, Tampere, **6-474**.